Fall 12-20-2021

Identifying MicroRNAs Panel Associated With Hepatocellular Carcinoma in Serum of Chronic Hepatitis C Patients

Areeg Dabbish
The American University in Cairo AUC, adabbish@aucegypt.edu

Identifying microRNAs panel associated with hepatocellular carcinoma in serum of chronic hepatitis C patients

A Thesis Submitted to

The Biotechnology Graduate Program

In partial fulfillment of the requirements for

The degree of Master of Science

By:

Areeg Mohammad Medhat Abdelrahman Dabbish

Under the supervision of:

Dr. Anwar Abd Elnaser (Advisor)

Assistant Professor,
Institute of Global Health and Human Ecology (IGHHE)
The American University of Cairo

Prof. Dr. Hassan Azzazy (Co-advisor)

Professor and Chairman, Department of Chemistry
The American University of Cairo

Spring 2021

The American University in Cairo

School of Science and Engineering

Identifying microRNAs panel associated with hepatocellular carcinoma in serum of chronic hepatitis C patients

Thesis Submitted by

Areeg Mohammad Medhat Abdelrahman Dabbish

To the Biotechnology Graduate Program

Spring 2021

In partial fulfillment of the requirements for

The degree of Master of Science in Biotechnology

Has been approved by

_____ _____ _____

Dept. Chair/ Director Date Dean Date

DEDICATION

This thesis work is dedicated to
my father, Medhat Abdelrahman
my mother, Hayam Hassan
and my beloved husband, Mohamed Khaled
for their love and support

ACKNOWLEDGEMENTS

I cannot begin to express my thanks without showing my greatest gratitude towards GOD for allowing me to have such a fruitful experience, and for giving me the ability and strength to continue this path.

I would like to express my sincere gratitude to my advisor, Assistant prof. Anwar Abdelnaser, for his continuous support, guidance, patience and encouragement throughout my thesis. His expertise was invaluable in formulating the research question and methodology, and his insightful comments helped sharpening my thinking and bringing my work to a higher level. I would like also to thank him for dedicating time to his students. Indeed, it is an honor to be one of his students. I would like to extend my special thanks to Professor Hassan El-Fawal, Dean of the school of science and engineering at AUC, who opened his lab for me to perform my practical experiments and financially supported my project for the samples' analysis. His valuable feedbacks definitely enriched my knowledge, in addition to his encouragement that aided me in choosing the right direction and successfully completing my master's degree. I wish to show my appreciation to my co-advisor, Professor Hassan Azzazy, Chairman of Chemistry Department at AUC, for his valuable guidance and support throughout my thesis. He supplied me with the equipment and tools that I needed to start my practical work. Furthermore, I would like to express my sincere gratitude to my AUC professors, who taught me the academic skills and the basics of scientific research.

I'm deeply indebted to Professor Nashwa El-Khazragy, at Clinical Pathology-Hematology Department, Faculty of Medicine, Ain Shams University, for providing me with the proper training and giving me the opportunity to have hands-on-experience in her lab. I would like thank her for donating the healthy control samples necessary for my research.

I wish also to thank the hepatology Consultant Professor Mohamed Hassany, head of the scientific research department and head of the thermal and radio frequency unit at the National Hepatology and Tropical Medicine Research Institute (NHTMRI) for allowing me to collect the required clinical samples for my project. Special thank is provided to Dr. Mohamed Manna, Dr. Amr Maged, Dr. Yosra Hosny, all the physicians and nurses in the thermal and radio frequency unit at NHTMRI for supporting the sampling procedures.

I'm immensely grateful to my friend and lab-mate Hana Abdelzaher for teaching me the basic laboratory skills and for redirecting my steps and keeping a close eye on me in every single detail

of this project. Besides, I would like to acknowledge the assistance of Mousafa Abo-Hawya in performing the bioinformatic analysis of the project. I would like also to thank Mr. Samir Nabhan for performing the liver biomarkers testing. I wish to extend my special thanks to all my colleagues and friend at AUC generally and the biology department specifically. I wish also to show appreciation to my friend Alaa Youssef for her support. The assistance provided by the technical and support staff in the biology department is highly appreciated. Moreover, I would like to thank AUC for providing research grant which financially supported this project.

Finally, I couldn't have achieved any progress without the support and motivation of my dear husband (Mohamed Khaled), and no words can express my forever gratitude to my father (Medhat Abdelrahman) and mother (Hayam Hassan) for their wise counsel, sympathetic ear and support. All of you are always there for me. I would like to express my deepest thanks to my sisters (Yasmin and Sana), my brother (Abdelrahman), my kids (Judy, Yunus and Fayrouz), my parents-in-law (Khaled Mostafa and Fatma Abdullatif), my brothers and sisters-in-law for their infinite encouragement and prayers, and that this work wouldn't have been possible without them.

ABSTRACT

Introduction: early detection of hepatocellular carcinoma (HCC) will reduce morbidity and mortality rates of this poorly diagnosed widely-spread disease. Dysregulation in microRNA (miRNAs) expression is associated with HCC progression. ***Objective:*** Is to identify a panel of differentially expressed miRNAs (DE-miRNAs) to enhance HCC early prediction in hepatitis C virus (HCV) infected patients. ***Methodology:*** Candidate miRNAs were selected using bioinformatic analysis of microarray and RNA-sequencing datasets, resulting in nine DE- miRNAs (miR-142, miR-150, miR-183, miR-199a, miR-215, miR-217, miR-224, miR-424 and miR-3607). Their expressions were validated in the serum of 44 healthy individuals, 62 non-cirrhotic HCV patients, 67 cirrhotic-HCV and 72 HCV-associated HCC patients using real time PCR (qPCR). ***Results:*** There was a significant increase in serum concentrations of the nine-candidate miRNAs in HCC and HCV patients relative to healthy individuals. MiR-424, miR-199a, miR-142, and miR-224 expressions were significantly altered in HCC compared to non-cirrhotic patients. While miR-199a and miR-183 showed differential expression in cirrhotic relative to non-cirrhotic patients. A panel of 5 miRNAs improved sensitivity and specificity of HCC detection to 100% and 95.12% relative to healthy controls. Distinguishing HCC from HCV-treated patients was achieved by 70.8% sensitivity and 61.9% specificity using the combined panel, compared to alpha-fetoprotein (51.4% sensitivity and 60.67% specificity). ***Conclusion:*** MiR-142, miR-183, miR-199a, miR-224 and miR-424 novel panel could serve as non-invasive biomarker for HCC early prediction in chronic HCV patients.

TABLE OF CONTENTS

LIST OF TABLES

LIST OF FIGURES

LIST OF ABBREVIATIONS

A1ATD	α1-Antitrypsin deficiency
AAR	AST to ALT ratio
Abs	Absorbance
AFB1	Aflatoxin B 1
AFP	Alpha fetoprotein
ALT	Alanine aminotransferase
AASLD	American Association for the Study of Liver Disease
ANOVA	Analysis of variance
APRI	Aspartate aminotransferase to platelet ratio index
AST	Aspartate aminotransferase
AUC	Area under the curve
AIH	Autoimmune hepatitis
BCLC	Barcelona clinic liver cancer
BMI	Body mass index
cDNA	Complementary deoxyribonucleic acid
CEUS	Contrast-enhanced ultrasound
CHB	Chronic hepatitis B
CHC	Chronic hepatitis C
CPEB3	Cytoplasmic polyadenylation element-binding protein 3
CT	Computed Tomography
Ct	Cycle threshold
CTP	Child-Turcotte-Pugh score
DAA	Direct acting antiviral
D. Bil	Direct bilirubin
DE-miRNAs	Differentially expressed miRNAs
DM	Diabetes Mellitus
DMSO	Dimethyl sulfoxide
ds	Double stranded

EASL	European Association for the Study of the Liver
EMT	Epithelial to mesenchymal transition
FIB-4	Fibrosis-4
FL	Focal lesion
FPKM	Fragments Per Kilobase Million
GEO	Gene expression omnibus
GO	Gene Ontology
HBV	Hepatitis B virus
HCC	Hepatocellular carcinoma
HCV	Hepatitis C virus
IFN	Interferon
IRB	Institutional Review Board
LC	Liver cirrhosis
MDCT	Multidetector computed tomography
miRNA	Micro ribonucleic acid
MRI	Magnetic resonance imaging
mRNA	Messenger ribonucleic acid
MWA	Microwave ablation
NADH	Nicotinamide adenine dinucleotide hydride
NAFLD	Non-alcoholic fatty liver disease
NASH	Non-alcoholic steatohepatitis
NCBI	National center for biotechnology information
NHTMRI	National Hepatology and Tropical Medicine Research Institute
NS	Non-structural
NPV	Negative predictive value
ORF	Open reading frame
OS	Overall survival
pAKT	Phosphorylated serine/threonine protein kinase
PCI	Percutaneous injection
PCR	Polymerase chain reaction

Peg-IFN	Pegylated interferon
pre-miRNA	precursor miRNAs
pri-miRNA	Primary microRNA
PS	Performance status
PPV	Positive predictive value
qRT-PCR	Quantitative real time polymerase chain reaction
RAS	Resistance-associated substitutions
RBCs	Red blood cells
RFA	Radiofrequency ablation
RISC	RNA induced silencing complex
RNA	Ribonucleic acid
ROC	Receiver operating characteristic
RPM	Rotation per minute
RQ	Relative quantification
RT	Reverse transcription
SNORD	Small nucleolar RNA
ss	Single stranded
SVR	Sustained virological response
T. Bil	Total bilirubin
TCGA	The cancer genome atlas
TGFβ	Tumor growth factor β
TLC	Total leukocytes count
TNM	Tumor, nodes and metastasis
TRBP	Transactivation-responsive RNA-binding protein
TRIS	Tris Hydroxymethyl aminomethane
T2DM	Type 2 diabetes mellitus
US	Ultra sound
UTR	Untranslated region
WHO	World health organization

1. CHAPTER 1: LITERATURE REVIEW

1.1. Hepatocellular carcinoma (HCC) epidemiology

Chronic hepatic diseases account for 1.4 million death cases ever year, and they are commonly associated with inflammatory disorders [1]. In healthy livers, inflammation triggers growth and repair mechanisms which guarantee restoration of normal hepatocytes structure and function. While persistent inflammation destroys the regeneration machinery resulting in the origination of extravagant scar tissues named fibrosis. Prolonged fibrosis is progressed to cirrhosis that negatively influences the liver normal function and architecture, predisposing irreversible liver damage. Liver cirrhosis (LC) is usually exacerbated to liver failure and/or liver cancer (Fig. 1.1) [2]. Primary liver cancer is classified into hepatocellular carcinoma (HCC), intrahepatic cholangiocarcinoma (cancer that originates in the bile duct), in addition to other rare types. HCC is the most predominant type of liver malignancies, encompasses 75% - 85% of hepatic carcinogenic cases [3]. HCC pathogenesis is a complex multistep process associated with sustained inflammatory destruction, resulting in fibrotic deposition, necrotic liver damage and hepatic regeneration. The risk of HCC progression increases when cirrhosis is manifested, which is usually accompanied by deterioration in liver functions and perturbation in cellular functions [4, 5]. A cascade of cellular impairments occurs during liver carcinogenesis development, including cell cycle control disturbances, abnormal cell growth, senescence, apoptosis, migration and deregulation in energy production [6, 7].

HCC is classified the sixth most prevalent cause of cancer [8, 9] and the third major cause of global cancer mortality cases [10, 11]. An estimate of 905,577 (4.7%) newly diagnosed HCC patients, and around 830,130 death cases (8.3%) were recorded in 2020 by the world health organization (WHO) - International Agency for Research on Cancer office (Fig. 1.2) [12–15]. Whereas, Egypt was ranked the third in Africa and the fifteenth globally in HCC prevalence and newly recorded cases were doubled over a decade, resulting in more challenging health problem [16]. HCC is the fourth in incidence and the first in mortality related cancers among Egyptian patients [17].

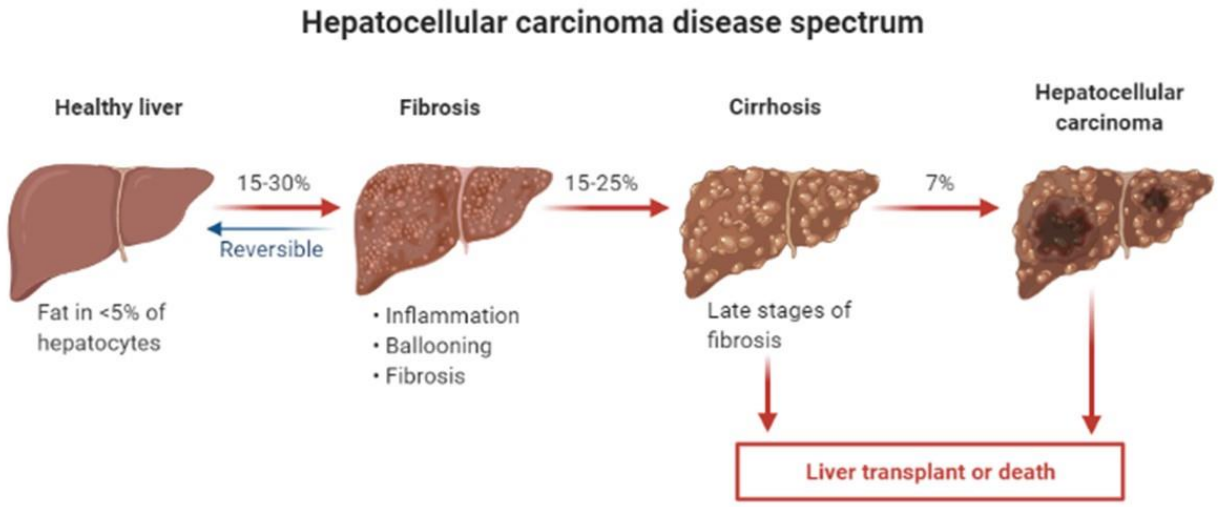

Figure 1.1. Progression of liver disease. Healthy liver is turned into fatty liver with fat deposition in the hepatocytes, followed by fibrotic liver in which the nature of the liver cells begins to change into connective tissues, then cirrhotic liver during that the liver starts restructurings and vascular systems are formed with the development of necrotic area. Finally, the liver carcinogenesis is formed and the hepatocytes are transformed into the malignant state. *Reprinted from "Non-Alcoholic Fatty Liver Disease (NAFLD) Spectrum", by BioRender, July 2020, retrieved from* [18] *Copyright 2021 by BioRender.*

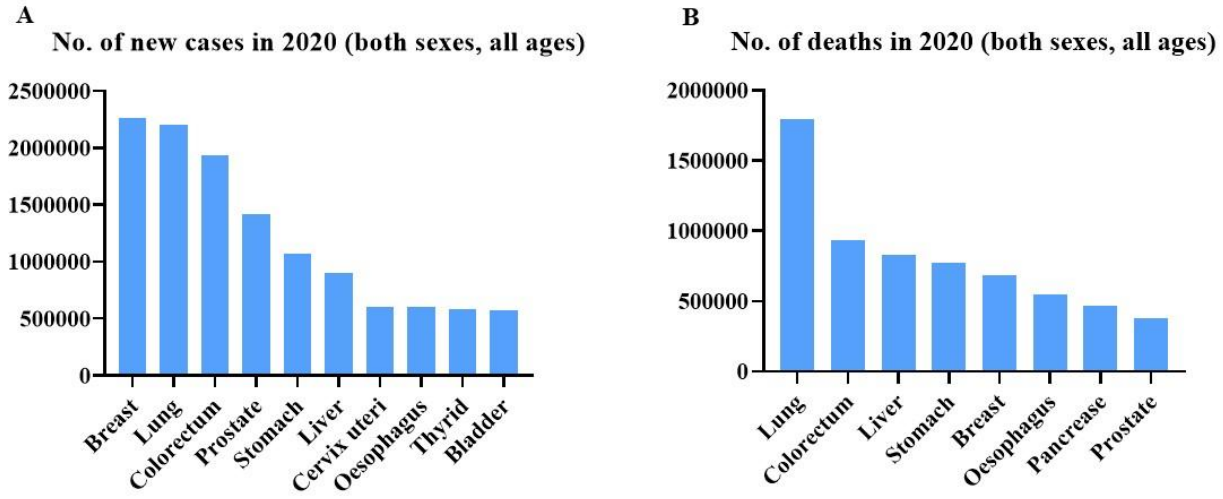

Figure 1.2. Estimated cancer new cases and death cases statistics. Statistical estimated obtained from the World health organization (WHO) - International Agency for Research on Cancer in 2020. (A) Number of newly discovered cases in different cancers in 2020, in both sexes and among all age groups. Liver cancer is ranked the sixth in new cancer cases. (B) Number of death cases from different cancers in 2020, in both sexes and among all age groups. Liver cancer is the third among mortality rates worldwide.

1.2. HCC risk factors

Several risk factors account for HCC development and progression; which are categorized in to three major classes: environmental, genetic, and non-genetic host-related factors.

1.2.1. Environmental risk factors

1.2.1.1.Infectious agents (Viral hepatitis)

Chronic infection with a viral contagious agent (such as hepatitis B virus (HBV), hepatitis C virus (HCV), and hepatitis D virus (HDV)); termed viral hepatitis, develops cirrhotic liver that usually progresses to HCC. The disease severity in viral infected patients is 20 folds higher relative to those who haven't been exposed to the virus [19]. Around 75% of cirrhosis-associated HCC cases are consequences of either chronic hepatitis B (CHB) or chronic hepatitis C (CHC) infections [2]. HBV can be transmitted either through sexual routes or during delivery from the mother to her newborn child [20]. If kept without treatment, HBV is capable of integrating its genome into the host's genetic material leading to activation of oncogenes and suppression of tumor suppressors [21]. However, the spread of HBV infection has dynamically decreased in the previous two decades because of the widespread vaccination strategies in some countries including Egypt [22, 23]. Similarly, LC is manifested in 93% of HCV infected patients, which is a leading cause to HCC in these cases [24]. HCV stimulates protein expression leading to mutations and carcinogenesis of the HCV infected hepatocytes [25–27]. Owing to the increased prevalence of HCV not only worldwide, but also in Egypt, this research is focused on studying the HCV induced HCC in Egyptian population.

1.2.1.2.Non-infectious agents

Chemical compounds

Exposure to some chemical components was found to be a predisposing factor for HCC. Examples of these products are organic compounds as vinyl chloride compounds, in addition to organic solvents like perchloroethylene, dioxin-like compounds, N-nitrosamine, polybrominated biphenyls, polychlorinated biphenyls [28, 29], and heavy metals such as arsenic and cadmium [30]. Moreover, heavy exposure to some pesticides and insecticides in some countries relying on agricultural resources such as in Egypt, resulted in adverse effects on the liver condition. Studies

on the occupational risk factors reported that the chemical ingredients as chloral hydrate in pesticides and ortho-toluidine in some herbicides are leading factors in HCC progression [31].

Alcohol

Excessive alcohol consumption is a potential risk factor associated with different malignancies owing to the carcinogenic effect induced by alcohol ingestion [32, 33]. Nearly 90% of the persons regularly consuming 40-60 grams of alcohol daily are diagnosed with steatosis (fatty liver disease). Steatosis is accompanied by hepatic inflammation and fibrosis in 20-40% of the alcohol consumers, and it progresses to LC in 10-20% of the dependent drinkers [34]. HCC is developed in 2-3% of the alcoholic cirrhotic patients [35, 36]. Moreover, regular consumption of 80 g/day of alcohol stimulates HCC onset, especially in conjunction with other comorbid conditions like diabetes (increased from 2.4% to 9.9%), and HCV-infected patients (increased from 19.1% to 53.9%) [37]. The possible therapeutic treatments for alcohol-induced HCC are liver transplantation, resection or percutaneous ablation [38].

Smoking

Chemical components of tobacco smoke as 4-aminobiphenyl, N-nitroso-dimethylamine, arsenic, and vinyl chloride proved to have hepatic carcinogenic effect [21]. Recent research studies reported that tobacco smoking accounts for 13% of gross cases of HCC worldwide [39]. Additionally, the risk of HCC development increases 1.5 folds in smokers when compared to control individuals who have never smoked before. Even when smoking is stopped, the severity of HCC development is retained in former smokers. A recent study reported that while current smokers showed higher risk by 1.51 folds, former smokers have increased risk by 1.12 folds to develop HCC when compared to healthy non-smokers [40].

1.2.2. Non-genetic host related risk factors

1.2.2.1. Gender

HCC incidence, pathogenesis and progression expressed gender-related differences. Males are more susceptible to liver cancer development 2-4 times higher than females [41, 42]. Incidence of HCC is ranked as the fifth and the ninth most common cancer in males and females respectively [43]. In Egypt, HCC is classified as the second in incidence among men and the sixth in incidence

among women [44]. Divergence in sex hormones levels is the main reasons for the HCC incidence variation between both sexes. Interleukin 6 (IL-6) is one of the cytokines that plays major role in the liver response to systemic inflammation and infection. Estrogen hormone is partially responsible for suppressing IL-6 and inhibiting IL-6-mediated inflammation [45]. Thus, physiological levels of estrogen can decrease liver injury and compensatory proliferation [46], in addition to inhibiting HCC metastasis to act as a protective agent for females before menopause [47]. On the other hand, testosterone can potentiate signaling of androgen receptors [48, 49]. Stimulated androgen receptor suppresses IL-12A expression, which inhibits the activity of natural killer cells, thus depresses the cytotoxic mechanism against malignant liver cancer cell [50]. This mechanism could provide an explanation to the enhanced liver cell proliferation in men. Furthermore, environmental factors could also affect the onset of HCC in men. This could be illustrated by the higher exposure rates to liver carcinogens, including alcohol, smoking and occupational hazardous chemicals [51, 52].

1.2.2.2. Obesity

Obesity is a metabolic disorder characterized by a body mass index (BMI) ≥ 30 kg/m^2, whereas, BMI >25 and <30 kg/m^2 is categorized as an overweight. Both of these metabolic defects are correlated with the development of many cancers, including liver cancer [53]. Higher obesity rates are recorded lately to reach epidemic levels. According to WHO statistical estimates in 2008, 22.5% of adult Egyptian males are suffering from obesity, where the percentage is doubled in the Egyptian females to reach 46.3% [44]. When compared to normal individuals, the relative risks for HCC development are 1.17 folds and 1.89 folds for overweight and obese patients respectively [53]. Moreover, there is significant association between BMI and HCC mortality rates in both sexes. In obese patients, the probability of death from liver cancer is ranked the highest among mortality rates of other cancer types [54]. Thus, continuous monitoring of liver condition among these patients is highly recommended for early diagnosis of silent asymptomatic HCC.

1.2.2.3. Diabetes Mellitus (DM)

Several hypotheses were proposed to explain the prevalence of HCC in type 2 diabetes mellitus (T2DM) patients, since diabetes is considered a metabolic disorder disease that may result in non-alcoholic steatohepatitis (NASH) and thus HCC [55, 56]. Also, hyperinsulinemia which is usually

associated with T2DM results in insulin resistance in addition to marked elevation in insulin-like growth factor-1 levels, releasing proinflammatory cytokines, promoting inflammation and affecting cell proliferation. Insulin or insulin precursors may affect the liver inducing mitogenesis and carcinogenesis [57, 58]. While persistent hyperglycemia may induce oxidative stress and hepatocytes damage [59]. Another hypothesis explaining this association is a molecular mechanism, in which a mutation in the apoptotic *p53* gene was observed in diabetic HCC patients compared to others with no history of DM [60]. The severity for HCC onset; in the co-existence of other cofounding factors as alcohol consumption, smoking and elevated BMI, was elevated in diabetic patients. Additionally, the relative risk of HCC incidence was 1.86 for chronic liver disease with DM, 1.93 for diabetic patients with cirrhotic liver, 1.9 for diabetic CHC patients, and 1.69 for diabetic CHB patients [61]. In Egypt, WHO estimated statistics in 2008 declared that 7.4% of adult females and 7% of adult males were manifested with elevated blood glucose levels. The association between T2DM and HCC was also observed among Egyptian patients, and several studies reported 2-3 folds increase in HCC incidence upon type 2 diabetic patients in comparison to non-diabetic individuals [62, 63]. The association between T1DM and HCC is still debatable however [64–66].

1.2.2.4. Non-alcoholic fatty liver disease (NAFLD)

Nonalcoholic fatty liver disease (NAFLD) is indicated by abnormal elevated levels of hepatic triglycerides and accumulation of fats within the liver, in the absence of any hazardous effects from alcohol ingestion [67, 68]. Recently, the proportion of cases diagnosed with NAFLD is increasing, as the result of several predisposing factors such as obesity, DM and metabolic syndromes [69]. The severity of NAFLD is manifested when the liver progresses to NASH [70], which is characterized by liver inflammation, metabolic stress, insulin resistance and hepatocytic damage [71]. Genetic polymorphisms were also discovered to be closely correlated with the incidence of NASH. It is estimated that 30-40% of NAFLD patients develop NASH, and around 40-50% of patients diagnosed with NASH are manifested with hepatic fibrosis [72]. Subsequently, the liver condition became at higher risk to develop cirrhosis and finally HCC [73]. In an Egyptian epidemiological study that was conducted in the period between January 1996 and December 2010 including 1759 HCC patients, reported NASH etiology was the leading factor in 5.3% of total HCC cases [74]. Other studies explained the correlation between NAFLD and HCC, where obese

and T2DM patients who suffer from metabolic disorders, possess higher risk to develop HCC two folds more than non-obese non-diabetic persons [54, 75]. The pathophysiology of NAFLD-NASH could be illustrated by the excessive fats accumulation and hepatic steatosis that stimulate fatty acid oxidation and promote reactive oxidative stress [76, 77]. Consequently, the production of proinflammatory cytokines is stimulated, the release of pro-oncogenic signals and epigenetic modification are enhanced. The seriousness of these manifestations is that they may occur without any signs of cirrhosis. Some case studies reported that HCC was diagnosed in NASH patients without any signs of cirrhosis [78], which makes it more challenging for the health practitioners to track the disease progression.

1.2.2.5. Autoimmune hepatitis (AIH)

Autoimmune hepatitis (AIH) is an unspecified inflammation of liver occurring more frequently in females [79]. It is manifested when immune cells mark normal hepatocytes as harmful foreign bodies and attack them. Progression of AIH leads to cirrhotic liver, and become a risk factor for HCC development with a rate of 1.9% per year [80]. Such high risk is comparable to the risk from other confounding factors including HBV and HCV induced LC, and alcohol-associated hepatic disorders. The incidence of HCC within patients with AIH induced LC is reported to be 1% [79]. An Egyptian epidemiological study conducted on HCC patients over a period of 15 years reported that 0.5% population study were HCC patients suffered from AIH etiology [74]. Liver transplantation is the recommended therapeutic option for AIH-HCC cases [81].

1.2.3. Genetic risk factors

1.2.3.1. Monogenic risk factors

α1-Antitrypsin deficiency (A1ATD)

α1-Antitrypsin deficiency (A1ATD) is a autosomal recessive disorder [82], occuring as the result of mutation in serpine family A member 1 (*SERPINA1*) gene causing abnormal deposition of α1-Antitrypsin (A1AT) protein/SERPINA1 in the liver's endoplasmic reticulum, thus enhancing the hepatic cellular damage, cirrhosis and subsequently HCC [83, 84]. The prevalence of HCC secondary to A1ATD is more in men and in obese individuals [85]. Several epidemiological studies reported the remarkable correlation between the incidence of LC and HCC in severe cases

of A1ATD, while there is no strong evidence of the suitability of HCC progression in moderate cases of A1ATD, the HCC risk increases only in the presence of another predisposing factor such as HCV or HBV infections [85, 86]. An Egyptian molecular analysis study revealed that the coexistence of A1ATD allele with *HFE* mutant allele in patients with HCV-induced cirrhosis, highlighting the importance of explaining their relevance as risk factors for HCC progression among individuals of the affected families [87].

Hereditary hemochromatosis and iron overload

Deposition of iron inside the liver is attributed to either hemochromatosis or to excess dietary iron [88]. Hereditary hemochromatosis is a genetic disorder that takes palce following a homozygous mutation in the Human homeostatic iron regulator (*HFE)* gene at position 282, where tyrosine is substituted by cysteine (C282Y) or due to an alteration in iron metabolism machinery [89]. Subsequently, iron overload is observed in the liver and can cause necro-inflammatory hepatitis, resulting in fibrosis, then cirrhosis and eventually hepatic cellular damage and HCC [90]. The relative risk for HCC development in hereditary hemochromatosis patients is 20 folds higher, whereas during a long period of 10 years, the cumulative risk for liver cancer incidence is estimated to be 6% and 1.5% among males and females with hereditary hemochromatosis respectively [91]. Previous researches have correlated the higher incidence of HCC development in those diagnosed with hemochromatosis with or without marked cirrhosis [92, 93]. A possible explanation is that ionic iron exerts direct hepatocarcinogenic effect. The incidence of hemochromatosis in Egypt is approximately 0.5% [94]. Moreover, elevated total body iron as the result of iron overload in some populations such as people with African origin or any other etiology as β thalassemia have also showed increased risk for HCC development, even with no evidence to genetic hemochromatosis [95, 96]. Thus, in the presence of iron overload, continuous monitoring to HCC occurrence is recommended [97].

1.2.3.2. Polygenic risk factors

Family history of HCC

Several studies revealed the correlation between familial history of liver cancers and the incidence of HCC [98]. This could be attributed to the heritable factors and the shared environmental risk factors among the members of the same family such as metabolic disorders

(NAFLD, T2DM, obesity), and life style (smoking, excess alcohol consumption) [99, 100]. Furthermore, HBV infection could be easily transmitted from the patient to the family members and vertically from the mother to her newborn infant at birth. Cirrhosis induced by some hereditary disorders such as A1ATD, hemochromatosis and Wilson's disease could be categorized as familial HCC predisposing factors [101, 102]. It was reported that individuals with first degree relatives suffering from HCC or have history of liver cancer are more susceptible to develop HCC two folds higher than those with no family history of hepatic disorders [91], whereas, the hazard ratio increased to 5.35 if the mother suffered from liver disorder. In Egypt, it is estimated that 21.4% of HCC patients are descendants of families with history of HCC (first- or second-degree relatives) [103].

Aflatoxin

Aflatoxin B 1 (AFB1) is a mycotoxin originated from Aspergillus family. It is more abundant in warm and humid regions like Africa and Asia [104]. AFB1 is a widespread food contaminant of some agricultural crops such as cottonseed, maize, peanuts, and some vegetables in these areas [105, 106]. WHO categorized AFB1 as group 1 carcinogen [107], and the International Agency of Research on Cancer sorted it as a potent hepatocarcinogenic agent. The increased HCC risk upon AFB1 exposure occurs as the result of a genetic mutation in the *TP53* (tumor suppressor) gene [108–111]. AFBI is metabolically activated via cytochrome P450 enzymes in the liver to form AFB1-8,9-exo-epoxide reactive form, which can easily bind to the DNA producing AFB1-N7-guanine; a pro-mutagenic adduct [112]. Additionally, some studies reported the impact of AFB1 on the genome causing chromosomal instability [113]. The carcinogenic impact of aflatoxin is synergized with a concomitant infection with HBV. This explains the high HCC incidence rates in geographical region with endemic to hepatitis B infection and highly contaminated by AFB1 [114–116]. In a Chinese prospective study, it was determined that the relative risk for HCC incidence in patients with increased urinary levels of AFB1 is 6.2 compared to healthy individuals. While the risk dramatically increased to 59.4 in patients with chronic HBV infection, whose urine samples showed elevated levels of AFB1 [117, 118]. The global burden of HCC induced by AFB1 ingestion extends from 4.6% to 28.2% [119]. Several Egyptian studies assured the existence of AFB1-albumin adducts in patients' blood in areas having AFB1 contaminants in food [120–122].

1.3. HCC diagnosis

The gold standard techniques for HCC diagnosis are the histopathology and the radiology. However, diagnosis of HCC has switched recently from invasive techniques as angiography and tissue biopsy to non-invasive imaging procedures as ultrasound (US), computed tomography (CT) and magnetic resonance imaging (MRI), in addition to serological testing using AFP [123–125]. The imaging procedures are usually used for diagnosis, choosing the appropriate treatment plan and surveillance [126].

In small hepatic focal lesions (FL) 1 - 2 cm in size, neo-angiogenesis usually evolves, resulting in lesion arterial vascularization stronger than the vascularization in the adjacent liver parenchymal cells, such process is termed wash-in. Concomitantly, the portal blood flow within the lesion decreases when compared to the adjacent parenchymal cells in the venous phase, this condition is called wash-out [127]. Diagnosis of HCC is explained by strong contrast uptake during the arterial phase, pursued by contrast wash-out in the extracellular matrix during the delayed or venous phases [127]. So, hallmark for HCC diagnosis is the appearance of arterial enhancement pursed by washout [128].

1.3.1. Alpha-fetoprotein (AFP)

The history of AFP introduction as a serological marker in HCC diagnosis returns back to the 1960s [129]. Although it is considered the most extensively chosen circulatory biomarker for HCC, it is characterized by inconvenient sensitivity and specificity in the determination of HCC lesions even at low-level cutoffs (10-20 ng/mL) [130]. It has 25% sensitivity for the identification of small-sized lesions (< 3 cm), and the sensitivity could reach 50% for FL larger than 3 cm [131]. AFP level increases in some benign hepatic disorder such as LC and hepatitis [132], and normal AFP serum level is detected in 15-30% of advanced HCC cases [133]. Therefore, the Practice Guideline Committee of the American Association for the Study of Liver Disease (AASLD) are no longer depending on the measurement of AFP in the early detection of HCC [134]. Currently, there is no sole serum biomarker; including IgM immunocomplexes, that could provide accurate diagnosis for HCC. Therefore, a combination of multiple biomarkers has been forecasted to improve the efficiency and the sensitivity of detection [135].

1.3.2. Imaging techniques

1.3.2.1. Ultrasound (US) and Contrast-enhanced Ultrasound (CEUS)

Ultrasound (US) is considered the primary screening tool for liver patients at risk. Any nodule or abnormal mass identified in the cirrhotic liver is treated as suspicious. Small HCC FL less than 3 cm usually appears as hypoechoic mass in the US screening [136]. US can determine HCC lesions with 60% sensitivity and 97% specificity [137]. Contrast-enhanced ultrasound (CEUS) could provide a complementary method for determination of HCC nodules. CEUS uses microbubble contrast agent to have a microflow imaging of the lesion [138]. CEUS can provide an overview to the tissue blood flow, thus explains the vascular pattern of HCC. Strong intra-tumoral improvement is displayed in the HCC during the arterial phase, which is pursued by delayed phase or portal venous phases characterized by rapid washout and isoechoic or hypoechoic manifestations [139]. CEUS has provided positive predicative values for over 90% of HCC cases with high sensitivity and specificity [140].

1.3.2.2. Computed Tomography (CT)

CT is the most frequent imaging tool for HCC diagnosis because of the short examination time and the widespread accessibility. Multidetector computed tomography (MDCT) can improve imaging performance via enhancing the temporal and the spatial resolution during HCC imaging [141]. HCC lesions are manifested as hyper-attenuated nodule in the arterial phase, pursued by a washout and iso-attenuated or hypo-attenuated lesion in the portal venous or delayed phase [142]. When compare to pathological examination, MDCT showed 68% sensitivity and 93% specificity in determination of HCC FLs [137]. A Recent improvement of this imaging technique is a perfusion CT, which presents quantitative estimate to the perfusion behavior. This could facilitate the differentiation between several tumor tissues depending on the perfusion parameters, resulting in advanced tumor grading and better therapeutic monitoring. HCC is manifested with high perfusion rates including increased blood volume, blood flow, permeability and decreased mean transient time, when compared to normal liver tissues [143].

1.3.2.3. Magnetic Resonance Imaging (MRI)

Recently, Magnetic Resonance Imaging **(**MRI) is considered one of the most preferable imaging techniques in HCC diagnosis. It provides images with a better lesion-to-liver contrast compared to

CT [144]. MRI succeeded in revealing the malignant characteristics of HCC including tumor architecture and intracellular structure, as well as the tumor grade [145]. Dynamic MRI presents arterial hyperenhancement in addition to the washout during portal venous or delayed phase, which confirms the classical features of HCC with 90% sensitivity and 95% specificity [146]. MRI possesses an advantage over CT in the enhanced ability of detecting small lesions (1- 2 cm) [147]. However, relatively low sensitivity is still attributed to the diagnosis of small FLs. Diagnosis efficiency of hepatic nodules greater than 2 cm could reach 90%, compared to 33% for detection of lesions smaller than 2 cm [148].

1.4. Drawbacks of current screening techniques

Although the improvements in the diagnostic criteria have presented the imaging techniques in the forefront rank for HCC diagnosis, these techniques are still having some limitations in the early diagnosis of HCC lesions [149]. The possibility of differentiating malignant nodules from benign ones remains one of the drawbacks of US screening [150]. Also, the sensitivity of US in identifying small FLs ranges from 65% - 80%, depending on operator's proficiency, degree of cirrhosis and patient's liver condition [151]. Although CEUS diagnosis relies on arterial phase hypervascularity, only 50% of the patients could show portal venous phase washout [152]. CEUS also has short imaging interval, therefore the overall scanning of the liver is difficult, resulting in less than 50% sensitivity in the identification of small lesions [153]. Owing to the similar vascular profiles, CEUS can't distinguish between different types of malignant lesions as HCC and intrahepatic cholangiocarcinoma [154–156].

Furthermore, CT can only provide relatively low sensitivity; ranging from 33% - 45% in diagnosing small lesions less than 1 cm [157], with a positive predictive value of 59% - 88% [145, 158]. Benign hepatic FLs such as hemangioma, peliosis, benign regenerative nodule and focal confluent fibrosis could be misdiagnosed to HCC during the CT scan [144]. Moreover, HCC surveillance using advanced CT or MRI techniques has some constraints such as the risk of radiation, the increased probability of false positive results, and the high cost if applied on regular bases [159, 160]. Surveillance using the serological marker AFP is characterized by lower efficiency in the early detection of hepatic FL and for HCC diagnosis, in addition to lower

sensitivity in identification of small lesions. Elevated level of AFP usually indicates advanced stage HCC with poor prognosis [161].

1.5. HCC staging

Accurate staging of HCC is an essential step to provide precise prognostic assessment to the liver condition and to select the best therapeutic choice (Fig. 1.3). HCC staging and the overall outcome of HCC rely on some clinical characteristics as size and number of FLs, local extent and metastasis, disease aggressiveness, and patient's performance status (PS) [136, 162]. Several staging criteria have been suggested for HCC staging including, Barcelona Clinic Liver Cancer (BCLC), the modified tumor, nodes metastasis (TNM), the model for end-stage liver disease (MELD) score, Okuda, Cancer of the Liver Italian Program (CLIP), Child-Turcotte-Pugh (CTP) score. The most widely used is the BCLC model, a precise predictive tool that combines information about tumor characteristics and liver disease severity with the patient's performance status, thus provides perfect correlation with the patient's overall survival (OS) rates [163, 164]. HCC patients are classified in to patients with single nodule < 2 cm, in which liver functions are preserved, and performance status PS = zero (BCLC stage 0 (very early stage)), patients with single or multiple nodules ≤ 3 cm, retain the preserved liver functions, and PS = zero (BCLC stage A (early stage)), patients with multiple nodules, unresectable, preserved liver functions and with PS = zero (BCLC stage B (intermediate stage)), patients with extrahepatic metastatic spread, portal invasion, liver functions are preserved and PS = 1 or 2 (BCLC stage C (advanced stage)) and non-transplantable HCC patients, with end-stage liver functions and PS > 2 (BCLC stage D (terminal stage)) [165, 166]. Patients classified as BCLC 0 and A are perfect candidates for curative approaches, such as surgical resection, ablative electrochemical therapies (radiofrequency ablation (RFA), microwave ablation (MWA) or percutaneous injection (PCI)), in addition to liver transplantation [167]. The estimates of the patient's overall survival (OS) after applying these curative strategies could reach to 5 years in 50% to 75% of patients. However, trans-arterial chemoembolization could provide an alternative therapy for BCLC stage B patients, with OS up to 4 years [168]. BCLC stage C patients might suffer from HCC related symptoms, and the systemic treatment would be the recommended non-curative therapeutic approach in such advanced stage to reach OS more than 10 months [169–171]. The second commonly applied therapeutic approach is the tumor, nodes, metastasis, which was evolved by the American Joint Committee on Cancer and the International

Union for Cancer Control. The classification criterion is based on studying the tumor characteristics, the lymph node involvement and the possibilities of metastasis [172]. TNM staging system examines the tumor's histopathology while considering the local growth of the tumor on the local nodules and the surrounding organs. Applying TNM is beneficial in anticipating the OS of patients after surgical removal of HCC lesions [173, 174]. CTP score provides an estimate to the mortality rates in the cirrhotic patients and for the assessment of the liver functions. Accordingly, patients are classified into three groups: "A" with good hepatic functions, "B" for impairment in the liver functions, and "C" in cases with advanced hepatic dysfunction. The system scores the patients using five criteria: serum total bilirubin, serum albumin, prothrombin time, ascites and hepatic encephalopathy [175, 176].

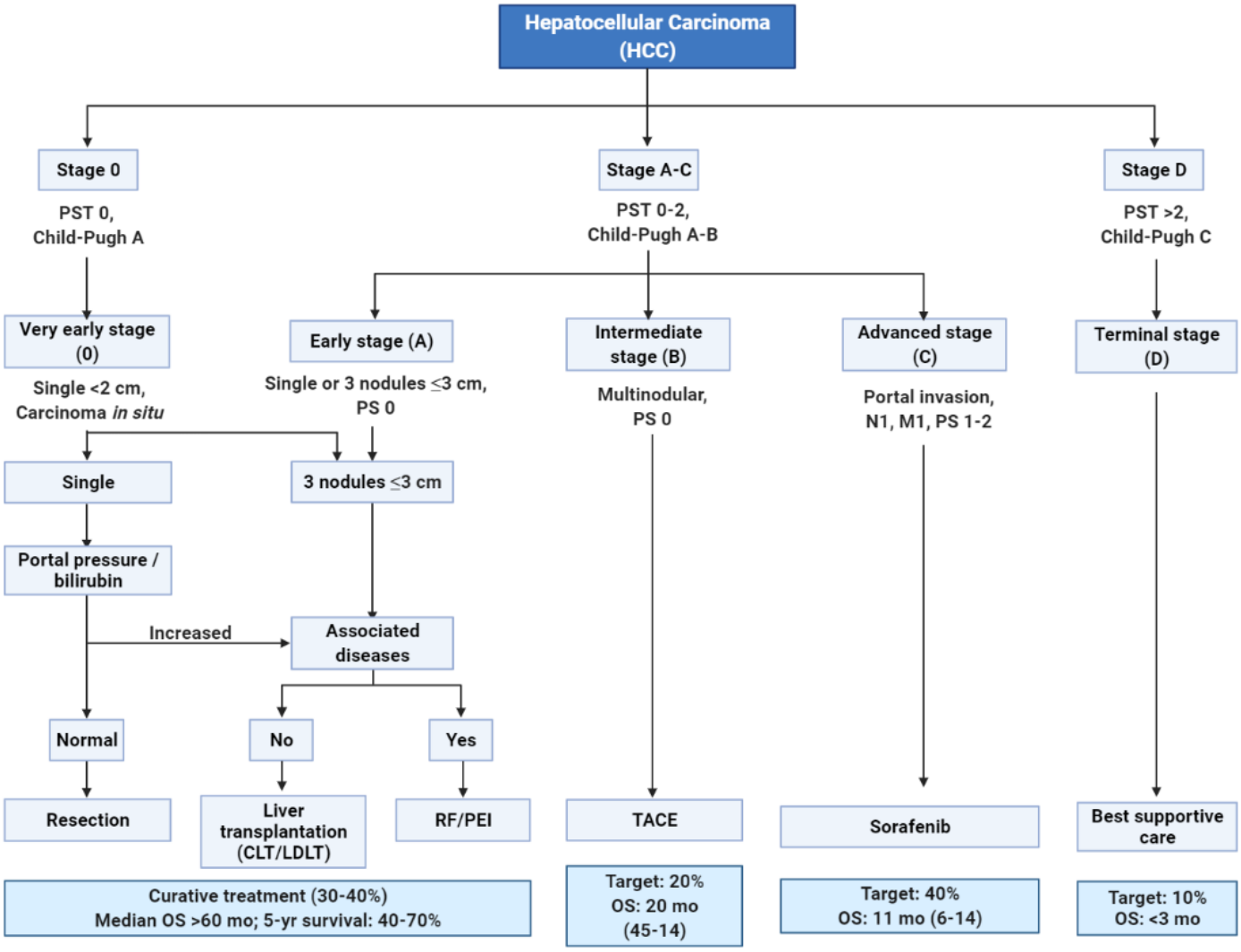

Figure 1.3. BCLC staging systems and therapeutic approaches. Classification of patients based on BCLC and CTP scoring systems for the optimum choice of the therapeutic option and the overall survival rates in each strategy. (BCLC: Barcelona clinic liver cancer, CLT: Cadaveric liver transplantation, LDLT: living donor liver transplantation, OS: Overall survival, PEI: Percutaneous ethanol injection, PS: Performance status, PST: Performance status test, RF: Radiofrequency ablation, TACE: trans-arterial chemoembolization). *Reprinted from "Barcelona Clinic Liver Cancer (BCLC) Staging System", by BioRender, July 2020, retrieved from* [177] *Copyright 2021 by BioRender.*

1.6. HCC surveillance

LC is mostly predominant in HCC patients [178], the severity of the case may hinder the effectiveness of HCC treatment even with the availability of highly efficient anticancer medications and treatment strategies [171, 179, 180]. Conflict information was raised about the

impact of early detection of HCC on the recovery rates and the overall survival rates [181]. Many guidelines were reported for the screening and surveillance of high-risk individuals, most importantly cirrhotic patients and people with acute or chronic infection with HBV or HCV (either cirrhotic or non-cirrhotic). The main differences across these guidelines are in the choice of the appropriate screening technique and the surveillance intervals. The poor commitment to these screening protocols is the main reason for the sustained elevated mortality levels from HCC all over the globe [19]. Moreover, LC and early stages of HCC are characterized by asymptomatic nature and silent hepatic complications, thus in most cases of HCC patients aren't diagnosed until the disease reaches an advanced stage [182, 183].

High-risk category is defined by hepatologists if a nodule more than 1 cm is discovered in the liver, thus regular monitoring to the nodule and to the liver condition is usually recommended. Clinical guidelines formulated by National Comprehensive Cancer Network (NCCN) advise patients with cirrhotic liver; whose risk to develop HCC is high, to measure serum AFP and perform ultrasound screening twice a year for monitoring [184–186]. Additionally, the latest guideline announced by the AASLD favors the reliance on non-invasive techniques for the detection beside regular follow up for small HCC lesions. They recommended the use of single dynamic imaging procedure for FL more than 2 cm that appears with typical vascular enhancement pattern, while two dynamic imaging procedures are recommended every year for FL measuring 1-2 cm with the same features [187]. While European Association for the Study of the Liver (EASL) recommends verification of the typical vascular pattern using two imaging procedures (CT and MRI) for the follow up of lesions between 1 - 2 cm in size [188]. EASL also suggests diagnosis of FL larger than 2 cm; and AFP higher than 400 ng/mL or AFP increasing sequentially via MRI or CT scan, without any need to perform histological biopsies. Moreover, histopathology is not considered for patients with suspicious lesion and no history of chronic liver disease [189]. If the results of the biopsy ruled out HCC in the histological pattern of the FL, the nodule should be monitored every 3 – 6 months until the nodule sizes increases or the imaging features changes. Asia-Pacific Association for the Study of the Liver guideline in 2010 recommended applying another imaging examination as endoscopic ultrasonography for FL with irregular vascular pattern [190].

1.7. Hepatitis C virus

1.7.1. Hepatitis C virus (HCV) infection epidemiology

Hepatitis C virus infection is a contagious hepatic disease, causing persistent liver inflammation. HCV has relatively long incubation period that extends from 15 to 150 days [191]. At acute phase of infection, clinical symptoms aren't manifested in 70-90% of the patients [192]. However, 10-30% of people at acute phase suffer from non-specific symptoms as flu-like signs, muscular pain, and loss of appetite. Spontaneous HCV clearance is detected in 20% of the infected individuals, while in 80% of the cases, CHC infection is evolved without marked signs of the disease [193]. HCV slowly progresses over years forming fibrotic wound scars, cirrhosis and eventually HCC [194]. Nearly 2.5% of the world's populations (approximately 180 million people) are suffering from HCV infection, and approximately 350,000 – 500,000 annual death cases are recorded from HCV associated liver complications [195–197]. Extensive research and huge efforts are exerted to overcome the viral spread, through national eradication programs and to explore novel anti-HCV therapies. Despite these facts, the annual incidence rates of CHC infection or co-CHC/CHB infections are increasing, as the result of blood transfusion, hemodialysis, the use of unsterilized tools and reused injections [198, 199].

The geographic distribution of HCV genotypes hugely differs across the globe [200]. Genotype 1 is the most frequent among the globe (49.1%), the second most frequent is genotype 3, followed by genotype 4 and 2 with prevalence rates 17.9%, 16.8% and 11% respectively. The rare genotypes 5 and 6 account for the remaining 5% of the world's distribution. However, genotype 4 and 5 are the most prevalent in low socioeconomic countries [195]. Egypt has an exceptional high prevalence of HCV worldwide [201]. According to the Egyptian demographic health survey in 2015, 4% of the Egyptian population had active HCV infection (age between 1-59) and almost 6 million Egyptians in the age group of 15-59 were chronically infected with HCV [202], with nearly 2.09% yearly incidence of new diagnosed cases [203]. The chronic infection rate is directly correlated with age, and its estimated incidence in patients with age group 50-60 years is 25% [202, 204]. The most predominant HCV genotype across the Egyptian population is genotype 4. Historically, the HCV epidemic through to have originated in Egypt from the insufficiently sterilized anti-schistosomiasis parental injections, administered during the nationwide treatment campaign that was conducted in 1960s-1980s, highlighting one of the world's huge iatrogenic

transmission of a blood-borne microorganism [205, 206]. Recently, a governmental screening campaign was implemented in 2018 by the Egyptian Ministry of Health (MOH), to restrain the incredibly high incidence of HCV among the Egyptian population by 2020. All the examined candidates with active HCV infection had joined a government-subsidized treatment agenda using sofosbuvir-based regimen; a direct acting antiviral (DAA) [207]. However, a mass surveillance campaign targeting HCC patients and high-risk patients with hepatic disorders is highly recommended [208].

1.7.2. Hepatitis C virus structure

HCV is an enveloped virus, small sized with single stranded (ss) linear positively polarized RNA ((+) ssRNA), family *Flaviridiae*. Its major components are nucleocapsid which encloses the RNA genome, wrapped by icosahedral protective protein shell and a lipid bilayer envelope. The genome is formed of one open reading frame (ORF) contains 9027-9111 nucleotides. The number of nucleotides varies based on the HCV genotype [209]. The single ORF is translated into a sole protein product, that undergo further processing into smaller active proteins. Three structural proteins are encoded by HCV ORF (core C protein and envelope E1 and E2 proteins), in addition to ion channel protein (P7), and six non-structural (NS) proteins (NS2, NS3, NS4A, NS4B, NS5A and NS5B). C, E1 and E2 are mature structural proteins, obtained from proteolytic activities on the viral single polyprotein via host signal peptidases. On the contrary, mature non-structural protein production requires the activity of the viral proteases [210]. 5’ and 3’ untranslated regions (UTR) are fundamental domains in the viral RNA translation and replication. The 5’ UTR contains the ribosome binding site at which initiation of translation occurs [211, 212].

1.7.3. Hepatitis C virus proteins

HCV core protein is a multifunctional protein which participates in the synthesis of the viral nucleocapsid to protect the viral genome, participates in RNA binding. Core protein is also essential in the regulation of various cellular proteins and controls host cell functions including lipid metabolism, gene transcription, cell signaling and apoptosis [213, 214]. However, envelope glycoproteins (E1 and E2) facilitate viral entry through involvement in the receptor binding and the viral fusion with the cell surface [215, 216]. The P7 hexamer is an vital membrane protein,

composed of two transmembrane domains structured in α-helices, it serves as a cation channel which participates in the viral maturation and release [217].

The NS2/3 protein is a hydrophobic protease, two amino acid regions are responsible for its encoding; NS2 and the NS3 terminal, and it is known to participate in HCV life cycle. NS2/3 catalyzes the splitting of the polypeptide linkage formed between NS2 and NS3 [218]. Recent studies highlighted the importance of the cleaved non-structural transmembrane protein NS2 in the modulation of host cell gene expression, apoptosis, and contributes to the viral replication process [219, 220]. Moreover, the protease domain on the N-terminal of NS3, the C-terminal also possesses RNA helicase domain. NS3 protein can also form heterodimeric complex with NS4A to create membrane protein, known to be important protease cofactor. NS3/4A is capable of antagonizing interferon regulatory factor 3, that is known to be an essential mediator of interferon inducement during the HCV infection [221]. NS4B participates in the replication and assembly of HCV viral particles, in addition to its potential action in HCV carcinogenesis [222]. However, RNA-dependent RNA polymerase activity has been manifested for NS5B protein, whereas NS5A is a cytoplasmic phosphoprotein, proved to regulate HCV resistance to interferon [222, 223].

1.7.4. Hepatitis C virus treatment

Estimation of the patient's case is required prior to the start of the treatment protocol for the optimum choice of therapeutic approach. Examination is done through testing anti-HCV antibodies, antimitochondrial antibody (AMA), anti-smooth muscle antibody (ASMA), antinuclear antibody (ANA), and anti-liver kidney microsome (LKM). In addition to HCV genetic material in the patient's blood, genotype of the virus, HCV viral load baseline, degree of liver fibrosis, assessing the thyroid stimulating hormone (TSH), thyroxine (T4) and triiodothyronine (T3) levels to determine thyroid activity, and finally the co-existence of other diseases including autoimmune diseases, epilepsy and recurring depression. Success of the treatment protocol is guaranteed when the patient achieved sustained virological response (SVR), which is measured by the disappearance of viral particles in the blood 12 or 24 weeks after the discontinuation of the therapy [224].

1.7.4.1. Pegylated-interferon and ribavirin combination therapy

Before 2011, the basic HCV treatment protocol included combination therapy of pegylated interferon (Peg-IFN) subcutaneous injection with ribavirin orally administered for a period of 6 – 12 months depending on the viral genotype [225]. The Peg-IFN is more stable and less frequently administered compared to IFN-α (once per week for the former and three times per week for the later) [226]. Binding of polyethylene glycol chain to IFN-α-2b molecule resulted in a protection from degradation, thus increased action half-life, better bioavailability and reduced immunogenicity were achieved [227]. The antiviral potency of IFN relied on its ability to inhibit HCV replication, induce apoptosis of HCV-infected cells and modulation of the immune response [228]. However, ribavirin exerts its antiviral action via multiple molecular processes. The first mechanism is though blocking HCV replication, secondly via mutagenic effect that increases the possibilities and frequencies of vial mutations resulting in replication errors, thus hastens HCV extinction. The third mechanism is achieved by ribavirin monophosphate, that stimulates the competitive inhibition of inosine-5- monophosphate dehydrogenase enzyme. This enzyme participates in the formation of guanine nucleotides, resulting in a significant decrease in guanosine triphosphate intracellular content. The fourth mechanism is due to the immunomodulatory action of ribavirin, by stimulating T-helper cell (Th1) cytokine response and inhibition of Th2 cytokine phenotype [229–232].

Administration of Peg-INF-ribavirin combined therapy basically improved the treatment efficacy, expressed as increased SVR from 13% (using IFN-α alone) to 40% (after using the combination therapy). Similarly, SVR rate in relapsed cases increased from 5% to 49% after receiving Peg-INF-ribavirin [233, 234]. Furthermore, such combination therapy proved more success compared to Peg-INF monotherapy alone, in which SVR was 56% in the former and 29% in the latter [234]. Although ribavirin alone didn’t show positive results in reducing HCV viremia [235]. The therapeutic effectiveness of this combination therapy substantially varied across different HCV genotypes, 70% for genotype 2, 80% for genotype 3, and 45-70% for genotypes 1 and 4. Whereas, inadequate antiviral efficacy and lower SVR rates were recorded 6 months after completing the treatment protocol, especially in HCV patients of genotype 1, or those with elevated HCV baseline viral load, or patients with deteriorated hepatic condition, or who were co-infected with other viral disease as HIV, and in some ethnics as African Americans [236].

Furthermore, this combination therapy was associated with frequent adverse effects as hemolytic anemia, cough, insomnia, pruritis and rash [237].

1.7.4.2. Direct acting antivirals (DDAs)

The first direct antiviral (DAA) drugs approved by the Food and Drug administration (FDA) in 2011 were boceprevir and telaprevir, to be used in combination with Peg-IFN plus ribavirin combination therapy. Marked increase in patients' SVR rates were recorded for HCV treated patients after DAAs administration, although the safety and efficacy were below the optimum targets. DAAs are classified into three categories targeting several steps in HCV life cycle [238].

NS3/4A protease inhibitors

NS3/4A protease inhibitors interfere with the intracellular life cycle via inhibition of viral polyprotein maturation. Protease inhibitors were the first approved class by the FDA as a medication for HCV patients. NS3/4A inhibitors are divided into several categories: first-generation ketoamide peptidomimetics (e.g., boceprevir and telaprevir), which form reversible covalent bond with the serine 139 residue at the N-terminus of NS3 causing inhibition of the protease enzyme, although they are no longer available in the market. Modification of the first-generation drugs gave rise to the second-generation macrocyclic inhibitors, that encounter higher affinity and selectivity towards protein targets. They are considered reversible, non-covalent, competitive inhibitors (e.g., simeprevir) [209, 239]. Simeprevir mechanism of action is through non-covalent binding to HCV proteases, followed by fast association and slow dissociation [240]. The macrocyclic reversible non-covalent inhibitors are classified into three subclasses: P1-P3 macrocyclic inhibitor (e.g., ciluprevir, faldprevir and danoprevir), acyclic inhibitors (e.g., BMS-605339 and asunaprevir), and P2-P4 macocyclic compounds (e.g., grazoprevir and vaniprevir). Third generation drugs include P2-P4 macrocyclic acylsulfonamides (e.g., glecaprevir, voxilaprevir and grazoprevir) and P1-P3 macrocyclic acylsulfomanides (e.g., paritaprevir) [241].

NS5A serine protease inhibitors

NS5A inhibitors block HCV RNA replication through disruption of membranous web, which is heterogenous meshwork found in the cytoplasmic membrane and is essential for HCV replication.

Despite the exact mechanism of action is still unclear, NS5A inhibitors possess inhibitory effect on dimerization, structural stability and subcellular distribution of NS5A protein. Studies also reported their inhibitory action on viral assembly and release, consequently suppression of the HCV replication process. Examples of drugs that belongs to this class are daclatasvir, ombitasvir, elbasvir and ledipasvir [242, 243].

NS5B inhibitors

This category of drugs targets HCV replication by two mechanisms: first, through nucleoside polymerase inhibitors (e.g., sofosbuvir), RNA dependent RNA polymerase inhibitors that are capable of termination of the RNA chain owing to their nucleotide analogues structure, thus inhibition of replication. Second, through non-nucleoside polymerase inhibitors (e.g., dasabuvir), which bind to enzyme's allosteric sites, turning it non-functional [244].

DAAs combination therapies

Resistance-associated substitutions (RASs) are modifications in the viral amino acid sequence generated during replication, that took place either naturally occurring or selected [245]. It negatively affects the efficacy of DAAs, resulting in viral resistance to the drugs, which is known as resistance associated variants (RAVs) [244]. A monotherapy of DAAs is not recommended to avoid the risk of developing RASs. Consequently, interferon-free therapies are usually composed of more than two DAAs belonging to different classes (NS3/4A, NS5B and NS5A inhibitors), with the addition of ribavirin if necessary. DAAs combination therapies improves the effectiveness of the therapeutic protocol compared to DAAs monotherapy. Examples of these combination therapies are: sovaldi (sofosbuvir + Peg-IFNα/RBV), olysio (simeprevir + sofosbuvir) both prescribed for genotype 1 and 4 and harvoni (ledipasvir + sofosbuvir) [246].

1.7.4.3. Hepatitis C virus entry inhibitors

A recent mechanism for HCV antiviral drugs is via blocking the viral entry to the cell. This approach provides higher probabilities to excise HCV infection from the beginning even before the viral genome is released and might also stop cell-to-cell communication that is essential for the viral spread. Moreover, such novel approach may overcome drug resistance acquired for DAAs, as it targets host structural components as key enzymes and receptors utilized for HCV

entry, thus lower the chances of resistance towards cell's conserved nature [247]. Different techniques might be followed for repurposing of some medications to be sued as entry inhibitors, including decrease the affinity of viral attachment and binding to the cell surface. Example of candidate drugs is lectin cyanovirin, which is a carbohydrate-binding agent, it weakens the viral binding by the reaction with the viral envelope glycoproteins that is rich in mannose oligosaccharide [248]. Also, heparin is considered a structural analog for heparan sulfate; one of the host's cell attachment factors, can be used as competitive inhibitor for viral attachment to the host's cell [249]. The second technique could be achieved through inhibition of post-binding interaction with cellular entry factors [250]. HCV requires the availability of several host factors as CD81 for complete entry. CD81 is identified as an important HCV entry agent, and it is a transmembrane protein with small and large extracellular loops [251]. CD81 large extracellular loop interaction with E2 protein on HCV surface is essential for HCV infection. Therefore, the use of imidazole-based compound would induce D-helix of CD81 and void CD81 function during HCV entry [252]. Similarly, using CD81 monoclonal antibodies might interfere with HCV entry and abrogate HCV infection in vivo [253, 254]. Another mechanism for blocking the viral entry is through inhibition of HCV fusion with cell membrane [255]. One approach to achieve this technique is the acidification triggering mechanisms of the viral-cell membrane fusion. Example of these repurposed drugs are chloroquine and ammonium chloride, which disrupt the endosome acidification and inhibit membrane fusion [256].

1.8. MicroRNAs (miRNAs)

Various small RNAs have developed inside eukaryotic cells to regulate undesired transcripts and genetic materials. Small RNAs (less than 200 nucleotides) are classified into small interfering RNA (siRNA), microRNA (miRNA) and Piwi-interacting RNA (piRNA) [257, 258]. MiRNAs are single stranded, short (around 22 nucleotides in length), non-coding RNAs, which are associated with argonaute family protein. The first miRNA was identified in *Caenorhabditis elegans* back in 1993, after that a huge number of miRNAs has been reported in various species [259]. Post-transcriptionally, miRNAs control gene expression resulting in gene silencing [260].

1.8.1. MicroRNA biogenesis

The onset of miRNA biogenesis (Fig. 1.4) occurs when the RNA polymerase II (Pol II) is transcribed into capped, spliced and polyadenylated primary miRNAs (pri-miRNAs) [261]. One pri-miRNA can be proceeded into single miRNA or into cluster of two or more miRNAs. A microprocessor RNase enzymes, called DROSHA with its cofactors; binding protein DiGeorge syndrome critical region 8 (DGCR8), are essential for cleaving the long pri-miRNAs [262, 263]. The cleavage occurs across the base of the stem-loop structure of the pri-miRNA with the aid of two RNase III domains of DROSHA, producing hairpin structured precursor miRNAs (pre-miRNAs) nearly 60-70 nucleotides in length [264, 265]. Furthermore, the microprocessor splits 11 nucleotides dsRNA from the stem junction with ssRNA overhang, resulting in hairpin-shaped pre-miRNA with 1 or 2 flanking nucleotides at 3' end [266, 267]. The following step is the exportation of the pre-miRNA out of the nucleus to the cytoplasm, facilitated by exportin 5 (XPO5), where it undergoes further processing by DICER1 enzyme. An RNase III enzyme composed of two catalytic RNase III domains, that binds to the dsRNA causing its cleavage and the production of 22 nucleotides mature miRNA duplex having 2 nucleotides 3' overhangs [268–271]. Moreover, DICER1 is accompanied by transactivation-responsive RNA-binding protein (TARBP2 or TRBP) which links DICER1 with Argonaute proteins to contribute in RNA induced silencing complex (RISC) assembly [272]. The RISC complex consists of the guide strand which base pairs with the mRNA at the 3' UTR end [273] and Argonaute proteins that recruits several factors to stimulate gene silencing via suppression of translation, mRNA de-adenylation or mRNA decay [274, 275]. The structure of the miRNA is composed of an important domain at the 5' end extending from nucleotide 2 to 7; called 'miRNA seed', is essential for target recognition. Nonetheless, the downstream nucleotides may also participate in the target base pairing. Moreover, single conserved miRNA-binding site is found in at least 2/3 of the coding genes in addition to several non-conserved sites [276]. Generally, the majority of the protein-coding genes are controlled by miRNAs, also miRNAs biogenesis and functions are highly controlled [276, 277]. Thus, deregulation in miRNAs expression is directly corelated with many physiological disorders such as cancer [278, 279]

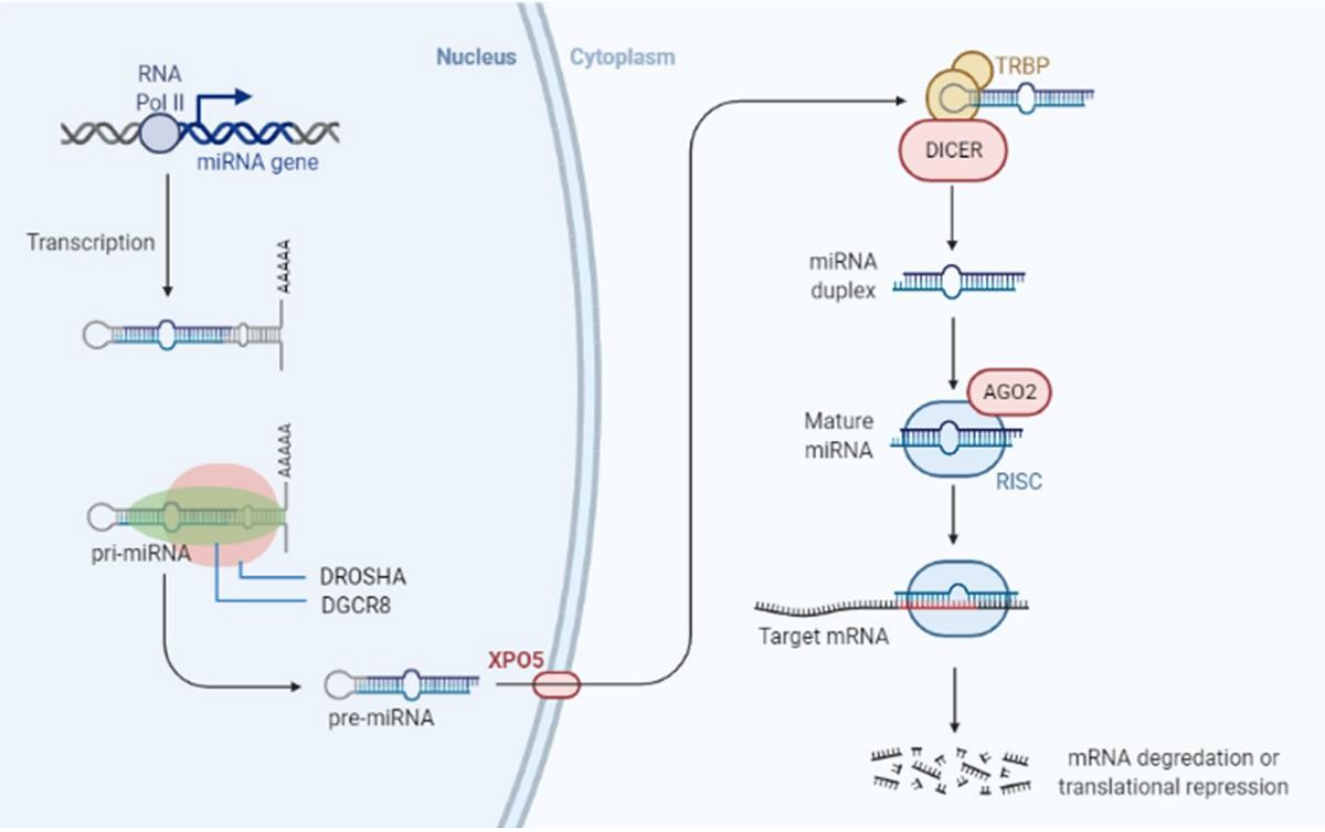

Figure 1.4. A schematic diagram of miRNA biogenesis pathway. MiRNA biogenesis starts within the nucleus, transcription of the miRNA gene occurs by RNA-polymerase II to produce capped, polyadenylated pri-miRNA. Processing of pri-miRNA is done by Drosha and DGCR8 to result in shorter stem-looped pre-miRNA, which is then exported out of the nucleus with the aid of exportin 5. Once inside the cytoplasm, further processing occurs to the pre-miRNA by DICER enzyme to generate ds-mature miRNA. The mature miRNA is linked to RISC complex, which guide the miRNA to the complementary mRNA resulting in post-transcription inhibition and gene silencing. (DGCR8: DiGeorge syndrome biorender.com critical region 8, ds: double stranded, mi-RNA: microRNA, pre-miRNA: precursor microRNA, pri-miRNA: primary microRNA, RISC: RNA-induced silencing complex). *Reprinted from "microRNA in Cancer", by BioRender, February 2021, retrieved from* [280] *Copyright 2021 by BioRender.*

1.8.2. MicroRNAs in hepatocellular carcinoma

Numerous profiling studies have addressed miRNAs expression in HCC, marked changes in miRNAs expression were recorded in HCC tissues relative to neighboring non-tumorous heptaic tissues [281, 282]. Some miRNAs are predominant in the liver cells such as miR-21, miR-221, miR-222. The overexpression of these miRNAs in the liver is explained by oncogenic role through inhibition of tumor suppressor genes related to HCC [283–285]. The term ‘oncomiRs’ was given

to the miRNAs with oncogenic function. On the contrary, miR-101, miR-122, miR-125b, miR-139 and let-7 are down regulated in HCC cells, which can be demonstrated by the stimulation of tumor suppressor gene or inhibition of an oncogene [286–289]. Deregulation in miRNAs expression was detected not only in liver carcinogenesis, but also in pre-malignant dysplastic nodules [290]. Marked reduction in miRNA expression was also determined in HCV venous thrombi relative to their primary HCC nodules [291]. Therefore, it is suggested that disordered miRNAs biogenesis triggers miRNAs deregulation to further increase HCC and metastasis [292–295].

Evidences also showed the abundance of stable miRNAs in the circulation, in addition to other body fluids of both healthy persons and HCC patients with different expression patterns, suggests a promising function for these miRNAs in the diagnosis and prognosis of hepatic carcinogenesis [296–298]. Moreover, circulatory miRNAs differential expression provides a tool for differentiating HCC patients of different etiologies (HCV, HBV, alcohol- associated HCC) with marked sensitivity and specificity. Additionally, circulating miRNAs high prognostic power to track the progression of the disease and in segregating patients with HCC from cirrhotic or fibrotic patients. The non-coding RNA expression levels are also representative to the size and stage of tumor, cirrhotic state, and patients' overall survival [299–304].

1.8.3. MicroRNAs in HCV and HCV-induced HCC

The molecular mechanisms regulating HCV-associated HCC might diverge from that controlling HBV-induced HCC. Transcriptome profiling of liver tissues isolated from HCV-HCC patients resulted in dissimilar subset of miRNAs obtained from HCC patients under HBV etiology. Furthermore, pathway analysis proposed that in HCV-induced HCC, miRNAs were enriched in pathways related to cell cycle, metabolic and immune responses [305]. Whereas, HCV infection basically changes the host's miRNAs expression patters to serve the viral own purposes as facilitating HCV replication., e.g. miRNA-122 expression is necessary for HCV replication [306–308]. Is s suggested that miR-122 binds to the viral RNA 5' end and stabilizes the viral genome. Additionally, HCV RNA facilitates segregation of miRNA-122 from its complementary mRNA target, and inhibits its normal targets resulting in downregulation of miR-122 during HCV infection. Such suppression promotes liver carcinogenesis progression [309–311]. In contrast,

miR-199 main objective is the ribosomal entry site of HCV RNA. MiRNA-199a-3p overexpression inhibits HCV viral replication targeting RISC-dependent mechanism [312].

Moreover, IFN-β antiviral therapy exerts regulatory effect on host's miRNA expression. Previous studies showed that INF- β suppresses miR-122 expression and stimulates several miRNAs (miR-196, miR-351, miR-431, miR-296 and miR-448), those miRNAs directly suppress HCV replication [313]. Furthermore, miRNAs were considered reliable prognostic biomarker for determination of disease stage. The dysregulation of miR-484, miR-524-5p, miR-615-5p and miR-628-39 in the plasma of Egyptian HCV patients, promotes the segregation between fibrosis, cirrhosis, and early stages of HCC [314]. Additionally, one mechanism by which HCV induces HCC is through upregulation of host's miRNA and dysregulation of cellular signaling pathways. Increased miR-155 expression was reported in CHC patients compared to patients with non-alcoholic steatohepatitis and healthy individuals [315]. MiR-155 expression is substantially influenced by HCV infection [316], its upregulation occurs as the result of stimulation of upstream transcription factors and nuclear factor-κB, leading to stimulation of cell cycle progression and suppression of cell apoptosis [317].

1.8.4. MicroRNAs as biomarkers for AFP-negative HCC

Owing to the fact that AFP is HCC biomarker with lower sensitivity and specificity and high percentage of false negative results, several studies investigated the diagnostic potential of miRNAs in detecting AFP-negative HCC patients. MiR-125b possibility to distinguish AFP-negative HBV-HCC patients (AFP levels < 200 ng/mL) from chronically infected HCC-free HBV patients (with AFP levels < 200 ng/mL as well) was addressed. The results showed that the calculated area under the curve (AUC) for plasma miR-125b levels was 0.943, and the effectiveness of miR-125b in discriminating the patients under the study was of 100% sensitivity and 75.5% specificity [132]. Furthermore, another study included 279 HCC patients with 38.7% of the HCC individuals showing negative AFP levels, miR-4651 proved high accuracy in distinguishing HCC patients with normal AFP levels from healthy individuals with sensitivity and specificity of 70% and 90% respectively [318]. Similarly, serum miR-21 levels were positively correlated in 83% of HCC patients with AFP-positive results and in 77.5% of HCC patients with AFP-negative results, with sensitivity and specificity of 81.2% and 83.2% respectively [319].

The integration of several biomarkers might enhance the diagnostic significance. A panel of four miRNAs was examined to distinguish HCC patients from CHB patients or healthy individuals. All candidates with AFP levels less than 20 ng/mL were included as AFP-negative cases. The combined panel of miR-26a, miR-27a, miR-125b and miR-223 was highly effective in differentiating HCC patients from non-HCC individuals [320]. Similar results were obtained after examining the miRNAs expression profiles in HCC biopsies and the adjacent non-tumor tissues. MiR-15b and miR-130b were highly expressed in tumor tissues, and produced 96.7% sensitivity in detecting HCC patients with lower AFP levels (< 20 ng/mL), in addition to accurate detection of early-stages HCC patients with normal AFP levels [321].

1.8.5. MicroRNA is HCC metastasis

Cancer metastasis is a serious complication of cancer, and it accounts for high mortality rates in cancer patients. Numerous studies proved direct correlation between regulation of miRNAs expression and HCC progression. A decrease in MiR-124, miR-139, miR-151 and miR-200 family expression in HCC tissues is observed, and these miRNAs are involved in the modulation of RHO/RHO-associated protein kinase (ROCK) pathway. A cytoskeletal reorganization pathway participated in the inhibition of motility and invasion in cancer cell lines [322–325]. Furthermore, miR-17 and miR-29b were known by their tumor suppressive potential in HCC, and they negatively regulate matrix metalloproteinase protein. The presence of this enzyme is essential in cancer metastasis as it digests extracellular proteins [326, 327]. Another mechanism is through tumor growth factor β (TGFβ)-enhanced epithelial to mesenchymal transition (EMT) in HCC is influenced by miR-181a, miR-216 and miR-200 family [328–331]. The effect of miR-200 family on the EMT was extensively studied and researchers concluded that miR-200 indirectly suppresses E-cadherin gene expression and the whole EMT processes is inhibited [332, 333].

Moreover, miRNAs participate in regulation of immune cells located in the tumor's microenvironment which support colonization of scattered HCC cells. TGFβ is also involved in downregulation of miR-34a in HCC cell lines, which promotes CC-chemokine ligand 22 production and recruits regulatory T-cells in the tumor's microenvironment [334]. Similarly, in vivo studies showed that downregulation of miR-28-59 in HCC mouse cells enhanced interleukin-34 production that promotes the infiltration of tumor-associated macrophages and in a forward

feedback mechanism, tumor associated macrophage infiltration inhibits miR-28-5p expression via release of TGFβ, thus regulated HCC metastasis [335].

1.8.6. MicroRNAs as therapeutic agents

Since miRNAs are modulating gene expression, targeting certain miRNAs could provide potential therapy against cancer development. The therapeutic approach is achieved by using oligonucleotides or RNAs duplex sharing complementary sequence to the target miRNA to mimic or suppress its action. Oligonucleotide's therapy provides direct and cost-effective therapeutic process, with high stability and efficacy [336]. Upregulated oncogenic miRNAs are selected in the HCC treatment. For instance, antisense 2′-O-methyl oligoribonucleotide can be used to targets miR-221, thus inhibiting tumor growth in mouse models [337, 338]. The first miRNA-targeting drug is miravirsen; 15-nucleotides locked nucleic acid, designed for treatment of chronic HCV to regulate HCV replication. Miravirsen studies on animals and second phase of clinical trials on chronic HCV patients revealed the efficiency of suppressing HCV levels over prolonged periods in a dose-dependent manner excluding any risks of toxicity, although further investigations on the long-term safety and efficacy of miravirsen are still required [339, 340]. Moreover, circulating miRNA can be used as therapeutic target or adjunct therapy in personalized medicine, such as miR-221 that showed potential therapeutic effect when used in conjunction with sorafenib (a kinase inhibitor used to block tumor growth) in the treatment of HCC patients [341]. Another therapeutic approach is the use of HCC downregulated miRNAs with tumor suppressor activity. Studies on MiR-26a therapeutic potential in HCC mouse model showed that marked reduction in tumor size and in focal lesions number with limited toxicity was obtained upon miR-26a administration [342]. However, lentivirus vector technique was used to systemically deliver miR-101in a liver tumor mouse model resulting in massive reduction in tumor size and metastasis [343]. Also, downregulation of miR-122 was observed in diethyl nitrosamine-induced HCC mouse model, introduction of agomiR-122 leads to restoration of miR-122 level, thus inhibits chemically-induced HCC [344]. Therefore, differentially expressed miRNAs (DE-miRNAs) in HCC could be introduced as potential therapeutic agents.

1.9. Rationale

The current serum biomarker (AFP) lacks sensitivity and specificity in HCC detection; therefore, the rationale of the current study is to identify a prognostic miRNAs panel capable of distinguishing HCC patients in a more accurate, sensitive and specific approach.

1.10. Hypothesis

The computationally assigned miRNAs possess a prognostic potential in predicting HCC in HCV-infected subjects using minimally invasive serum samples.

1.11. Objectives and aims

The objective of this research is to identify a panel of miRNAs with a differential expression pattern between HCV and HCV-associated HCC patients that could serve as a signature for early detection of HCC. While the aims of the current study are:

i) Identifying a DE-miRNAs miRNAs panel in the liver tissues of HCV and HCV-HCC patients through computational bioinformatic analysis of microarray dataset and RNA sequencing dataset deposited on NCBI's gene expression omnibus (GEO) and The Cancer Genome Atlas (TCGA); respectively.

ii) Collection of serum samples from HCV and HCC patients, in addition to healthy individuals with subsequent isolation of total RNAs from these samples.

iii) Quantitative measurement of the liver function's biomarkers to monitor the disease severity.

iv) Measuring the expression patterns of the identified miRNAs panel using quantitative real time PCR (qPCR).

1.12. Novelty of this research

The novelty of this research is deciphered in highlighting the potential ability of serum miR-142 in distinguishing HCC patients from non-HCC individuals, in addition to miR-424 in

discriminating HCV from HCC patients. A novel miRNAs panel composed of miR-142, miR-183, miR-199a, miR224 and miR-424 was examined as prognostic biomarker for HCC.

2. CHAPTER 2: MATERIALS AND METHODS

2.1. Materials

2.1.1. Chemicals and reagents

Ethanol (80% and 100%) (Absolute ethanol HPLC grade – Fisher Scientific, Leicestershire, UK - Cat. no E/0665DF/17), chloroform (molecular grade - Fisher Scientific, Leicestershire, United Kingdom – Cat no. C/492017), nuclease-free water (Lonza, Basel, Switzerland – Cat no. 51200), 0.9% Sodium Chloride (for direct bilirubin determination) and bleach (5% sodium hypochlorite, diluted 1:5).

2.1.2. Equipment and tools

Centrifuge(s) (with rotors for 2 mL tubes and for 10 mL tubes) for centrifugation at 4°C and at room temperature (15–25°C) (Centurion Scientific benchtop centrifuge - K2015R, West Sussex, UK and Hettich EBA 20 centrifuge - Merck, Darmstadt, Germany), vortex mixer, microplate reader spectrophotometer (SPECTRO star Nano BMG LABTECH, Germany), thermocycler (Applied Biosystems Veriti 96 well thermal cycler – ThermoFisher Scientific, Carlsbad, CA), photometer (5010 V5+ semi-automated clinical chemistry analyzer – RIELE, Germany), applied biosystems Realtime polymerase chain reaction (PCR) machine (ABI 7500 - ThermoFisher Scientific, Carlsbad, CA).

Micropipettes (p1000, p200, p100 and p10), sterile, RNase-DNase-free pipette tips (QSP 10 microL and Axygen scientific 100 microL), DNase-RNase free filter pipette tips. 1.5 mL or 2 mL microcentrifuge tubes, sterile RNase-DNase-free PCR tubes (0.2 mL), RNase-DNase-free sterile PCR tube strips (8 tubes per strip, 0.1 mL) (Geneaid qPCR Tube Strips and caps - Cat. No. QP8120), gel and clot activator 5mL collection tubes, butterfly scalp vein set, disposable gloves

2.2. Methods

Bioinformatic study was performed on microarray and RNA sequencing datasets in order to identify the target miRNAs panel.

2.2.1. Bioinformatic analysis

2.2.1.1. Analysis of microarray dataset

Analysis was performed on non-coding RNA microarray dataset GSE40744, deposited on the National Center for Biotechnology Information - Gene Expression Omnibus (NCBI-GEO) repository [345]. In such study, Diaz et.al, analyzed miRNA expression among three groups; HCC patients, cirrhotic patients and healthy individuals. A total of 76 liver specimens were isolated from 43 patients classified as the following: first, 26 liver specimens were obtained from HCV-related HCC patients; 9 specimens from the tumor focal lesions and 17 specimens from the neighboring non-tumor cirrhotic tissues. Second, 18 cirrhotic liver specimens were isolated from 10 HCV-associated cirrhotic patients, and 13 specimens from 4 HBV-related acute liver failure patients. Third, 12 specimens were obtained from 7 healthy normal liver donors and 7 subjects performed hepatic resection for liver angioma [346]. In our study, miRNA bioinformatic expression analysis was performed between 18 HCV cirrhotic samples and 9 HCV-HCC samples on R software (R x64 v.3.6.2) (R code is included in appendix 1).

2.2.1.2. Analysis of TCGA RNA sequencing dataset

Analysis of the RNA sequencing data deposited on The Cancer Genome Atlas (TCGA) was performed [347] to identify the target dataset. Data downloaded from TGCA portal comprised RNA expression in HCC patients from different etiologies. HCC expression data with HCV etiology only was filtered using R software (R x64 v.3.6.2) to obtain smaller dataset composed of 31 samples and was further processed for downstream analysis. Filtering criteria was applied to retain only the miRNAs with expression more than 10 reads or FPKM (Fragments Per Kilobase Million) in $\geq$ 85% of the dataset. After that differential expression analysis between HCV cirrhotic and HCC samples was performed using TCGABiolinks R package.

2.2.1.3. Gene ontology enrichment analysis

The molecular functions associated with the common miRNAs between the microarray and the RNA sequencing datasets were identified by gene ontology enrichment analysis using R software (R x64 v.3.6.2). First, target identification for the four common miRNAs was done using SpidermiR package. Second, targets were mapped to molecular functions gene ontologies and

check for enriched terms. Enrichment analysis for molecular function terms was done using hypergeometric test.

2.2.2. Patients and samples

This study included 245 individuals; 44 healthy volunteers and 201 HCV infected and HCV-associated HCC patients who attended the radiofrequency clinic at the National Hepatology and Tropical Medicine Research Institute (NHTMRI) during the period from July to December 2019. Patients' health history records were collected, with full clinical and ultrasonographic examinations.

2.2.2.1. Ethical approval

All patients have participated in the current study after giving a written consent (appendix 2,3) approved by the Institutional Review Board (IRB) of the American University in Cairo (case number 2018-2019-060) (appendix 4) and the IRB of NHTMRI (serial number 25-2019) (appendix 5). The study was performed in agreement with the Helsinki Declaration, by applying good clinical practice principles. NIH (national institute of health) web-based training course "Protecting Human Research Participants" was also completed (certification number 2875591) before sampling.

2.2.2.2. Inclusion criteria

Healthy individuals with normal liver functions, no history of viral hepatitis or any liver disease, general good health condition with no major disorders in kidney, heart, lungs or other vital organs were included in the study. HCV patients (assumed to be genotype 4; the most predominant genotype among the Egyptian population) with positive circulating anti-HCV antibodies were classified into two sub-groups based on the presence or the absence of cirrhosis. Diagnosis of HCV based upon ultrasonography and blood examination (complete blood count, liver function tests as AST (aspartate aminotransferase), ALT (alanine aminotransferase), albumin, total and direct bilirubin). Degree of fibrosis in CHC patients was diagnosed according to non-invasive AST to platelet ratio (APRI), Fibrosis-4 (FIB-4) and AST to ALT ratio (AAR) indices. APRI score is calculated based on levels of AST and platelets count, by applying the formula [AST (IU/L) / (AST upper limit for normal) / platelet count (10^9/L)] x 100, where upper normal limit used was 40 [348].

While calculation of FIB-4 score utilizes AST, ALT, platelets count in addition to patient's age, using the formula [age (in years) x AST (IU/L)) / platelet count (10^9/L) x $ALT^{1/2}$ (IU/L)] [349]. Combining both indices resulted in higher diagnostic accuracy [350, 351]. Whereas, degree of cirrhosis and severity of the liver condition were determined using CTP score. APRI, FIB-4, and CTP scores were assessed using MDCalc medical calculator [352]. METAVIR scoring system classifies chronic viral hepatitis patients into F0 = no fibrosis, F1 = portal fibrosis without septa, F2 = fibrosis with rare septa, F3 = numerous septa without cirrhosis, F4 = cirrhosis [353]. Comparison of the fibrosis indices is presented in table 1. However, for HCV-HCC patients, diagnosis primarily relied on abdominal ultrasonography and triphasic CT scan or MRI for examination of the FL, in addition to AFP blood levels. BCLC staging system was used for classification of HCC patients based on tumor stage, cancer-related symptoms, and serological liver function tests [354]. HCC patients enrolled in the study were classified in to BCLC stages 0, A and B.

Table 2.1. Classification of non-invasive fibrosis indices

Fibrosis index	Serum markers	Grading	Cut-off	Significance	References
APRI	AST and platelets count	F0-F1	≤ 0.5	Excluding significant fibrosis with a predictive estimate of 39%,	[355]
		F2-F4	> 1.5	Predicting significant fibrosis in 56% of patients	
		F0-F3	< 1	Excluding cirrhosis with a predictive value of 32%	
		F4	> 2	Predicting cirrhosis	
FIB-4	AST, ALT, platelets count and patient's age	F0-F1	≤ 1.45	Excluding significant fibrosis with a predictive value of 47%	[353, 356]
		F2-F4	> 3.27	Predicting significant fibrosis in 83% of patients	
AAR	AST and ALT		< 1	Exclude cirrhosis	[357]
			≥ 1	Predicting cirrhosis	
CTP	Bilirubin, albumin, international normalized ratio, ascites and encephalopathy	A	5-6 points	Prediction of post-operative mortality rate as10%	[358, 359]
		B	7-9 points	Prediction of post-operative mortality rate as 30%	
		C	10-15 points	Prediction of post-operative mortality rate as 70-80%	

2.2.2.3. Exclusion criteria

HCV patients who had other viral (e.g., HBV) or non-viral liver disease (e.g., alcoholic liver disease or non-alcoholic fatty liver) in conjunction with HCV were excluded. HCC patients with other liver disorders as hemangioma or cholangiocarcinoma were disqualified. In addition to excluding HCC patients with extrahepatic metastatic cancer, another type of cancer, or other comorbid condition such as kidney or heart disorders.

2.2.2.4. Sampling and serum preparation

Five mL of blood was withdrawn from each patient into labeled disposable serum collection tube (global roll gel and clot activator yellow tube). For complete clotting, blood samples were kept for one hour at 15–25°C, then samples were processed for serum separation following miRNeasy serum/plasma handbook – Qiagen – 2012. Briefly, blood samples were centrifuged at 1538 x *g* "equivalent to 4000 rotation per minute (rpm)" using benchtop centrifuge (Hettich EBA 20 centrifuge - Merck, Germany) for 10 min at 20°C, then tubes were placed at 15–25°C for 5 min, after that the centrifugation was repeated under the same conditions. The serum was separated as supernatant, and it was carefully transferred into a sterile DNase-RNase-free 1.5 mL microcentrifuge tube, then it was stored at -80°C for further analysis.

2.2.3. Liver function's biomarkers testing and HCV antibodies testing

Liver function biomarkers (ALT, AST, albumin, bilirubin total and direct) were assessed for all samples. AFP serum levels were assessed for diseased samples only. Absence of antibodies to HCV were determined in healthy individuals' samples.

2.2.3.1. Quantitative determination of ALT

Determination of ALT was done using SPINREACT kit, Barcelona, Spain (NADH. Kinetic UV. IFCC rec. Liquid, Cat. No. 41283) following the manufacturer's protocol [360]. Briefly, frozen serum samples were thawed at 15–25°C, working reagent was prepared by mixing 4 volumes of the buffer (100 mmol/L TRIS, Tris hydroxymethyl aminomethane; pH 7.8), 1200 U/L lactate

dehydrogenase, and 500 mmol/L L-Alanine) to 1 volume of the substrate (0.18 mmol/L NADH, nicotinamide adenine dinucleotide hydride, and 15 mmol/L α-ketoglutarate). The instrument was calibrated to zero using distilled water. 20 µL of the serum was added to 200 µL of the working reagent, mixed and kept for 1 min at 15–25°C. Absorbance (Abs.) of the sample was measured at 340 nm at 15–25°C using spectrophotometer (Photometer 5010 V5+ semi-automated clinical chemistry analyzer - RIELE, Germany) at time zero (initial Absorbance at 340 nm) and at 1 min interval for 3 min. The average between absorbances and the average absorbance difference per minute (ΔA/min) were calculated. Serum level of ALT was calculated using the formula [ΔA/min x 1750 = U/L of ALT].

2.2.3.2. Quantitative determination of AST

Determination of AST was done using SPINREACT kit, Barcelona, Spain (NADH. Kinetic UV. IFCC rec. Liquid, Cat. No. 41273) following the manufacturer's protocol [361]. Briefly, frozen serum samples were thawed are 15–25°C, working reagent was prepared by mixing 4 volumes of the buffer (provided by the kit, composed of 80 mmol/L TRIS pH 7.8, 800 U/L lactate dehydrogenase, 600 U/L malate dehydrogenase, and 200 mmol/L L-Aspartate) to 1 volume of the substate (provided by the kit, composed of 0.18 mmol/L NADH (nicotinamide adenine dinucleotide hydride), and 12 mmol/L α-ketoglutarate). The instrument was calibrated to zero using distilled water. 20 µL of the serum was added to 200 µL of the working reagent, mixed and kept for 1 min at 15–25°C. Absorbance (Abs.) of the sample was measured at 340 nm at room temperature using Photometer 5010 V5+ semi-automated clinical chemistry analyzer at time zero (initial Absorbance at 340 nm) and at 1 min interval for 3 min. The average between absorbances and the average absorbance difference per minute (ΔA/min) were calculated. Serum level of AST was calculated using the formula [ΔA/min x 1750 = U/L of AST or ALT].

2.2.3.3. Quantitative determination of albumin

Determination of albumin was done using SPINREACT kit, Barcelona, Spain (bromocresol green, colorimetric, Cat. No. 1001022) following the manufacturer's protocol [362]. Briefly, three tubes labeled blank, standard and sample were prepared by mixing 1 mL blank reagent (provided by the kit, composed of 0.12 mmol/L bromocresol green pH 4.2) with 5 µL standard reagent (provided by the kit, composed of 5 g/dL albumin aqueous primary standard calibrator) or 5 µL of

the sample. The instrument was calibrated to zero using distilled water. After mixing, tubes were incubated for 10 min at 15–25°C, then absorbance of the samples and standard were measured against the blank at 630 nm at room temperature using Photometer 5010 V5+ semi-automated clinical chemistry analyzer. Serum albumin concentration was calculated using the formula [((“A” sample – “A” blank) / (“A” standard – “A” blank)) x 5 “standard concentration” = g/dL albumin].

2.2.3.4. Quantitative determination of bilirubin

Determination of serum total bilirubin (T. Bil) and direct bilirubin (D. Bil) were done using RANDOX kit, UK (Cat. No. BR 412) following the manufacturer’s protocol [363]. Briefly, the instrument was calibrated to zero using distilled water. Four tubes labeled blank (total), T. Bil sample, blank (direct), and D. Bil sample were prepared by mixing kit’s reagents. For total and direct bilirubin determination, 40 µL of sample was mixed with 40 µL reagent 1 (R1; 29 mmol/L sulfanilic acid and 0.17 N HCl), and reagent 2 (R2; 38.5 mmol/L sodium nitrite). For T. Bil. reagent 200 µL reagent 3 (R3; 0.26 mol/L caffeine and 0.52 mol/L sodium benzoate) was used, while 400 µL sodium chloride (NaCl) 0.9% (not provided by the kit) was used for D. Bil. determination. After mixing, tubes were placed at 15–25°C for 10 min, then 200 µL reagent 4 (R4; 0.93 mol/L tartrate and 1.9 N NaOH) was added for T. Bil. assay only. The absorbance of the T. Bil and D. Bil tubes were measured against the blank at 578 nm and 546 nm respectively at room temperature, using Photometer 5010 V5+ semi-automated clinical chemistry analyzer. Total bilirubin serum concentration was calculated using the formula [Abs. x 10.8 = T. Bil concentration mg/dL], while direct bilirubin concentration was calculated using the formula [Abs. x 14.4 = D. Bil concentration mg/dL].

2.2.3.5. Quantitative determination of AFP

The quantitative determination of AFP was done on fully automated Cobas analyzer using Elecsys AFP (Roche, Mississauga, Canada - Cat. No. 04481798-190) by applying Sandwich principle [364]. Briefly, 10 µL of sample was incubated with a biotinylated monoclonal AFP-specific antibody. Then streptavidin-coated microparticles were added to the reaction forming biotin-streptavidin complex. The reaction mixture was after that aspirated and the microparticles were magnetically captured on an electrode surface, and chemiluminescent signal is captured and the AFP concentration was determined using 2-point calibration and a master curve.

2.2.3.6. Testing of antibodies against HCV

All samples were subjected to qualitative detection of antibodies to HCV in the serum using HCV rapid test cassette (ACON, San Diego, CA - Cat. No. L031-10341). Briefly, - 80°C frozen serum samples were thawed at room temperature. Test cassette was removed from the sealed foil pouch and the test was performed immediately. 10 µL of the serum was added followed by 2 drops (equivalent to 80 µL) of the buffer (included in the kit). The test cassette was kept at flat surface without movement and results were recorded within 2 min.

2.2.4. RNA isolation

Total RNA was extracted using miRNeasy minikit (Qiagen, Germantown, MD - Cat. No. 217004) guided by the manufacturer's protocol miRNeasy serum/plasma handbook (February 2012) with minor modification. Previously -80°C frozen serum samples were thawed at 15–25°C, and once thawed; samples were centrifuged at 16000 x *g* using benchtop centrifuge (Centurion Scientific - K2015R, UK) for 10 min at 4°C for removal of additional cellular nucleic acids attached to cellular debris. Supernatants were moved in to new 1.5 mL microcentrifuge tubes without disrupting the pellet which appeared as a smear on the outer sides of the microcentrifuge tubes. 200 µL of the serum samples were transferred in to 2 mL microcentrifuge tubes, followed by the addition of 1 mL QIAzol lysis reagent (provided within the kit) (contains phenol and guanidine thiocyanate) for cell lysis and the release of cellular components without affecting RNA integrity. Complete mixing was insured by pipetting up and down several times, then the homogenates were kept for 5 min at 15–25°C. For phase separation, 200 µL of chloroform (molecular grade - fisher UK – Cat no. C/492017) was added to the homogenate, tubes were securely capped and were vigorously shaked for 15 sec, followed by 2 – 3 min incubation at 15–25°C, then samples were centrifuged for 15 min at 12000 x *g* at 4°C. After centrifugation, phase separation occurred and samples were separated in to three phases; upper colorless RNA-containing aqueous phase, white protein-containing interphase, and red-colored organic lower phase. The upper aqueous phases of the samples were transferred in to new collection tubes without touching the middle interphase to prevent contamination of the aqueous phase with proteins. The aqueous phase total volume (600 – 700 µL) varied based on the RNA content of each sample. To ensure appropriate binding of RNA molecules, 900 – 1050 µL of absolute ethanol (HPLC grade –

fisher - UK - Cat. no E/0665DF/17) was added to the aqueous phase, and mixed rigorously by pipetting up and down several times. Immediately after ethanol addition, 700 µL of each sample was transferred into RNeasy MinElute spin column hold on 2 mL collection tube (provided within the kit), where total RNA got attached to the membrane, while other contaminants were discarded. The column lids were closed and centrifuged at 8000 x *g* for 30 sec at 20°C, flow-throughs were disposed and collection tubes were re-used. The last step was repeated by addition of the remaining of the sample into the spin column followed by centrifugation. 700 µL RWT stringent washing buffer (contains guanidine thiocyanate, provided within the kit and previously reconstituted with 100% ethanol) was added to the RNeasy MinElute spin column to wash protein contaminants, followed centrifugal force equivalent to 8000 x *g* for 30 sec at 20°C, the flow-throughs were disposed, and the collection tubes were re-used. Then 500 µL RPE mild washing buffer (provided within the kit and previously reconstituted with 100% ethanol) was placed on the RNeasy MinElute spin column to remove traces of salts, followed by applying centrifugal force of 8000 x *g* for 30 sec at 20°C, the flow-throughs were disposed, and the collection tubes were re-used. Afterwards, 500 µL of 80% ethanol (prepared using 100% ethanol and RNase-free water) were placed on the RNeasy spin column. The lids were closed and centrifuged for 2 min at 8000 x *g* at 20°C to ensure complete washing of the membrane, then the collection tubes having the flow-throughs were discarded. After centrifugation, RNeasy MinElute columns were moved to clean collection tubes, and were left with the lids opened for 5 min on the bench top to air dry. Finally, RNeasy MinElute spin columns were transferred to clean 1.5 mL collection tubes, and 14 µL RNase-free water (provided within the kit) was added precisely to the middle of the column membranes. The lids were gently closed, and columns centrifuged for 1 min at 14000 x *g* at 20°C to elute the RNA. Isolated RNA was frozen at -80ºC for subsequent use in reverse transcription.

2.2.5. Reverse transcription and cDNA synthesis

Frozen RNA samples were thawed on ice, upon complete thawing; both the quality and quantity of the extracted RNA were obtained using microplate reader spectrophotometer (SPECTRO star Nano BMG LABTECH, Germany) through measuring RNA concentration in ng/µL and measuring the absorbance at different wavelengths (230, 260, and 280 nm) for the calculation of A260/A280 and A260/A230 ratios. Reverse transcription (RT) was conducted using miScript II

RT kit (Qiagen, Germantown, MD - Cat. No. 218161), guided by the manufacturer's protocol of miScript PCR system handbook. Components of the miScript II RT kit (10x miScript nucleic mix, RNase-free water, and 5x miScript hiflex buffer) were thawed at 15–25°C. Solutions were shaked, briefly centrifuged and then tubes were stored on ice. The RT master mix was prepared on ice by mixing 4 µL HiFlex buffer, 2 µL 10x miScript nucleic mix and 2 µL reverse transcriptase mix and was gently mixed and then stored on ice. 8 µL of RT master mix were dispensed in RNase-DNase-free sterile PCR tubes (0.2 mL). Variable volume of template RNA (equivalent to 50 ng of RNA) and RNase-free water (up to final volume of 12 µL) were added to the RT master mix, then tubes were shaked, quickly centrifuged, and then placed on ice. Using conventional thermocycler (Applied Biosystems Veriti 96 well thermal cycler – ThermoFisher Scientific, Carlsbad, CA), the samples were incubated for 60 min at 37ºC, followed by 5 min incubation at 95ºC to deactivate reverse transcriptase mix. Then cDNA (commentary deoxyribonucleic acid) samples were stored at -20ºC freezer for subsequent use in real time PCR.

2.2.6. Real time PCR amplification of miRNAs

Quantitative real time PCR (qPCR) of the target miRNAs was conducted utilizing miScript SYBR Green PCR kit (Qiagen, Germantown, MD - Cat. no. 218073) and miScript primer assays (SNORD 68 as a housekeeping gene and specific primers for the target miRNAs (Qiagen, Germantown, MD - Cat. no. 218300), guided by manufacturer's protocol of miScript PCR system handbook. Components of miScript SYBR Green PCR kit (2x QuantiTect SYBR green PCR master mix, 10x miScript universal primer, and RNase-free water), in addition to 10x miScript primer assays, and template cDNA were thawed at 15–25ºC. Solutions were mixed using vortex except for the SYBR green master mix tube was mixed by flicking the tube, then solutions were briefly centrifuged to collect residual liquid from the sides of the tubes. qPCR master mix was prepared by adding 5 µL 2x QuantiTect SYBR Green PCR master mix, 1 µL 10x miScript universal primer and 2 µL RNase-free water. 8 µL of the master mix was dispensed in RNase-DNase-free sterile 0.1 mL PCR tube strips, followed by the addition of 1 µL 10x miScript primer assay specific for the target miRNAs (primers' nucleotide sequences are presented in table 2.2), and 1 µL cDNA (concentration: 2.5 ng/µL) (following the manufacturer's recommendation for mature miRNA quantification to ensure 50 pg - 3 ng cDNA per PCR). PCR strips were tightly sealed with their caps, the reaction mixtures were mixed using vortex and briefly centrifuged for

1 min at 1000 x *g* at 15–25°C to remove bubbles. qPCR amplification was performed on applied biosystems 7500 real time PCR machine (ABI 7500; Themo Fisher Scientific, Foster city, CA) according to qPCR cycling program presented in table 2.3.

Table 2.2. Primer sequences of the target mature miRNAs

miRBase ID	miRBase Accession	Primer sequence	Catalog No.
hsa-miR-142-3p	MIMAT0000434	5' UGUAGUGUUUCCUACUUUAUGGA 3'	MS00031451
hsa-miR-150-5p	MIMAT0000451	5' UCUCCCAACCCUUGUACCAGUG 3'	MS00003577
hsa-miR-183-5p	MIMAT0000261	5' UAUGGCACUGGUAGAAUUCACU 3'	MS00031507
hsa-miR-199a-3p (and)	MIMAT0000232	3' ACAGUAGUCUGCACAUUGGUUA 5'	MS00007602
hsa-miR-199b-3p	MIMAT0004563		
hsa-miR-215-5p	MIMAT0000272	5' AUGACCUAUGAAUUGACAGAC 3'	MS00003829
hsa-miR-217-5p	MIMAT0000274	5' UACUGCAUCAGGAACUGAUUGGA 3'	MS00003843
hsa-miR-224-5p	MIMAT0000281	5' UCAAGUCACUAGUGGUUCCGUUUAG 3'	MS00003878
hsa-miR-424-5p	MIMAT0001341	5' CAGCAGCAAUUCAUGUUUUGAA 3'	MS00004186
hsa-miR-3607-5p	MIMAT0017984	5' GCAUGUGAUGAAGCAAAUCAGU 3'	MS00011960
Housekeeping gene	**Entrez Gene ID**	**Sequence**	**Catalog No.**
68 (small nucleolar RNA, C/D box 68)	606500	5'CGCGTGATGACATTCTCCGGAATCGCTG TACGGCCTTGATGAAAGCACATTTGAACC CTTTTCCATCTGATT 3'	MS00033712

N.B. The sequences of miR-199a-3p and 199b-3p on miRbase were similar, thus miR-199a-3p primer was chosen for qPCR amplification.

Table 2.3. Cycling conditions for real time PCR

Step	Time	Temperature	Comments
PCR initial activation step	15 min	95ºC	Heating initiation step for Taq DNA Polymerase
3-step cycling (45 cycles):			
Denaturation	15 sec	94ºC	
Annealing	30 sec	55ºC	
Extension	34 sec	70ºC	

2.2.7. Data analysis

Real-time PCR results are conveyed as cycle threshold (Ct), which is the number of cycles required for the fluorescent signal to intercross the determined threshold. Data calculation was conducted first as ΔCt, which was computed by deducting the Ct value of SNORD68 from the Ct of each targeted miRNA for the exact sample. Then ΔΔCt was computed by deducting the arithmetic average ΔCt of the reference group (healthy controls) from ΔCt of each sample for each miRNA. ΔΔCt of certain mi-RNA = [(Ct target miRNA- Ct SNORD68) for each sample – mean (Ct target miRNA- Ct SNORD68) of the control group]. Finally fold change of expression was calculated by transforming ΔΔCt to log2 fold change using the formula $2^{-\Delta\Delta Ct}$ [365]. Handling of non-detects (undetermined values) in qPCR results was done through excluding all samples that failed to have true amplification curve. However, if true amplification curve was recorded, non-detects were replaced by the maximum possible Ct value (Ct = 40). Similarly, Ct values ≥ 40 were replaced by Ct = 40 [366–368].

2.2.8. Statistical analysis

Statistical analysis was performed by applying statistical package for the social sciences (IBM-SPSS) - version 25 (SPSS Inc., Chicago, IL, USA). Normality testing was performed using Anderson-Darling test, D'Agostino and Person test, Shapiro-Wilk test and Kolmogorov-Smirnov tests using GraphPad Prism (version 8.4.3). Additionally, MDCalc Software (version 15.0 for Microsoft Windows, Ostend, Belgium) was used for the calculation of degree of fibrosis and cirrhosis scoring indices. Quantitative data were demonstrated as mean ± SEM, range (minimum – maximum) or number (percentages) as appropriate. For non-normally distributed data, values were analyzed using Mann-Whitney U (for comparison between two groups), and Kruskal-Wallis H (for comparison among three or more groups), however normally distributed quantitative data was analyzed using one way ANOVA (analysis of variance) to compare three or more groups. Analysis of qualitative data was performed using Chi-square test. Spearman's rank correlation was used to study the inter-relation between target miRNAs. Receiver operator characteristic (ROC) curve was constructed to determine the diagnostic effectiveness and to highlight the best cutoff value which maximizes the summation of sensitivity and specificity of each biomarker. Moreover, ROC curve was used to calculate area under the curve (AUC). Figures were designed using SPSS

and GraphPad prism. For microarray dataset analysis, *P*-value was corrected by performing Bonferroni method. All statistical tests were two-tailed, and *P*-value ≤ 0.05 was considered statistically significant.

3. CHAPTER 3: RESULTS

3.1. Microarray bioinformatic analysis

Filtering criterion was set to log fold change cutoff of 1.5 and adjusted *P*-value of 0.01 (Fig. 3.1). Twenty-two DE-miRNAs between cirrhotic HCV and HCC groups were generated, 4 miRNAs were upregulated and 18 were downregulated in HCC group (Table 3.1).

Table 3.1. Differentially expression miRNAs from microarray dataset

miRNA ID	log fold change	Average expression	t	*P*-value	adjusted *P*-value	B statistics
Upregulated						
hsa-mir-1269	3.980556	3.006296	7.573041	3.48E-08	2.58E-05	8.862391
hsa-mir-224	2.268889	5.132963	4.317145	0.000186	0.00811	0.691497
hsa-mir-452	2.004444	5.007037	4.287352	0.000201	0.008498	0.615536
hsa-mir-130b	1.673889	8.126296	7.236449	8.09E-08	3.60E-05	8.064353
Downregulated						
hsa-mir-503	-1.56833	6.736667	-4.54318	0.000101	0.005233	1.270147
hsa-mir-424	-1.70222	6.841481	-5.2379	1.55E-05	0.00172	3.060813
hsa-mir-23a	-1.77944	4.24963	-4.71964	6.27E-05	0.004113	1.724066
hsa-miR-29b	-1.82667	5.335556	-4.69036	6.79E-05	0.004268	1.648638
hsa-mir-150	-1.82722	9.885926	-4.28367	0.000203	0.008498	0.60616
hsa-mir-139	-1.84667	5.137778	-4.99007	3.02E-05	0.002688	2.421497
hsa-mir-10a	-1.88222	7.034815	-4.77929	5.34E-05	0.003715	1.877774
hsa-mir-4269	-1.89722	4.128148	-7.62543	3.05E-08	2.58E-05	8.985176
hsa-mir-130a	-1.91	8.736667	-9.22381	6.86E-10	1.53E-06	12.5379
hsa-mir-27a	-1.98	3.592222	-4.42072	0.000141	0.00666	0.956184
hsa-mir-203	-2.28278	4.461852	-4.64132	7.75E-05	0.004542	1.522428
hsa-mir-886	-2.35333	7.171111	-5.02797	2.72E-05	0.002585	2.519308
hsa-mir-200c	-2.355	5.542222	-5.80061	3.41E-06	0.000632	4.504642
hsa-mir-214	-2.67	11.09444	-4.55014	9.92E-05	0.005233	1.288025
hsa-mir-214	-2.67667	5.091111	-7.08254	1.19E-07	4.43E-05	7.694318
hsa-mir-199b	-3.05111	10.51185	-5.73493	4.06E-06	0.000695	4.337026
hsa-miR-199a-3p	-3.22889	10.41593	-5.2558	1.47E-05	0.00172	3.106947
hsa-miR-199a-5p	-3.31389	10.00259	-5.88751	2.70E-06	0.000547	4.725912

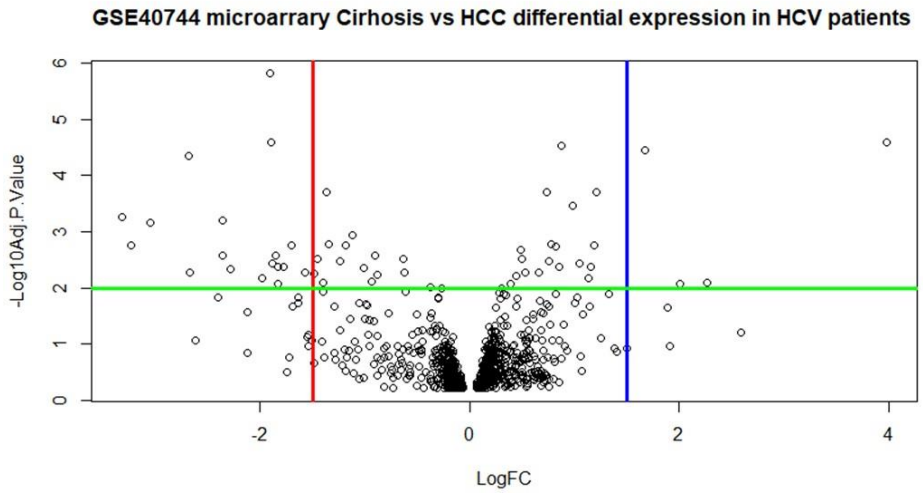

Figure 3.1. Volcano plot of microarray DE-miRNAs. Filtering criterion was adjusted using fold change cutoff of 1.5, and adjusted *P*-value cutoff of 0.01.

3.2. RNA sequencing bioinformatic analysis

MiRNAs differential expression analysis was conducted using false discovery rate (FDR) cutoff of 0.05, and fold change cutoff of 1 (Fig. 3.2). Nine significant DE-miRNAs were obtained, 3 were upregulated and 6 were downregulated (Table 3.2).

Table 3.2. Differentially expression miRNAs from TCGA dataset

miRNA ID	Log fold change	False discovery rate	Tumor	Normal	Delta
Upregulated					
hsa-mir-217	4.237359	0.00095	2742.886	145.6502	11622.59
hsa-mir-224	3.02565	0.027267	349.2049	42.85636	1056.572
hsa-mir-183	2.730561	0.048386	4087.799	617.5533	11161.99
Downregulated					
hsa-mir-142	-1.95755	0.011533	1599.147	6242.973	3130.404
hsa-mir-199b	-1.72226	0.046202	946.2798	3129.33	1629.743
hsa-mir-150	-2.17145	0.002423	471.3316	2131.151	1023.473
hsa-mir-424	-2.72822	1.42E-05	140.6106	936.6654	383.6167
hsa-mir-215	-3.54143	4.24E-10	93.39001	1090.393	330.7346
hsa-mir-3607	-2.83414	7.02E-06	50.00577	358.5205	141.7232

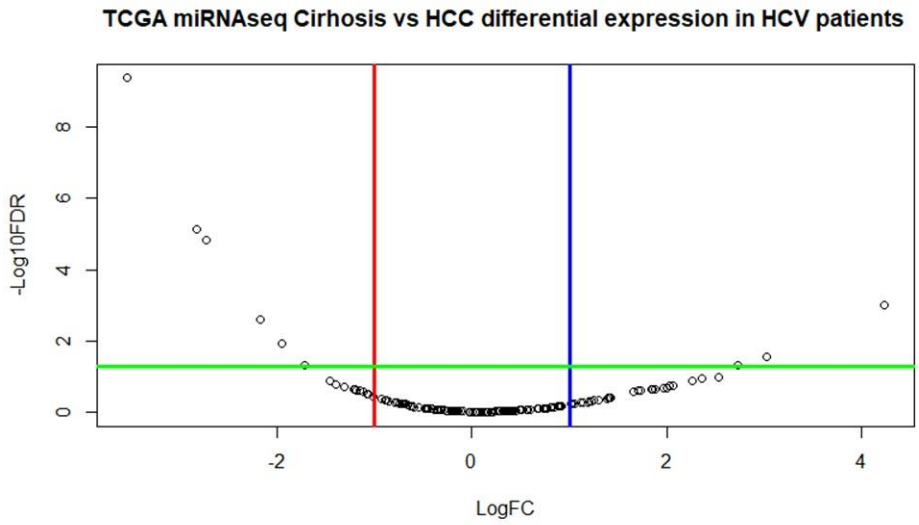

Figure 3.2. Volcano plot of TCGA DE-miRNAs. Filtering criterion was adjusted using fold change cutoff of 1, and false discovery rate cutoff of 0.05.

3.3. Gene Ontology (GO) enrichment analysis

The top ten enriched terms with lowest *P*-value were plotted. Terms related to protein binding, transcription regulation and kinase activity were frequently and significantly enriched (Fig.3.3).

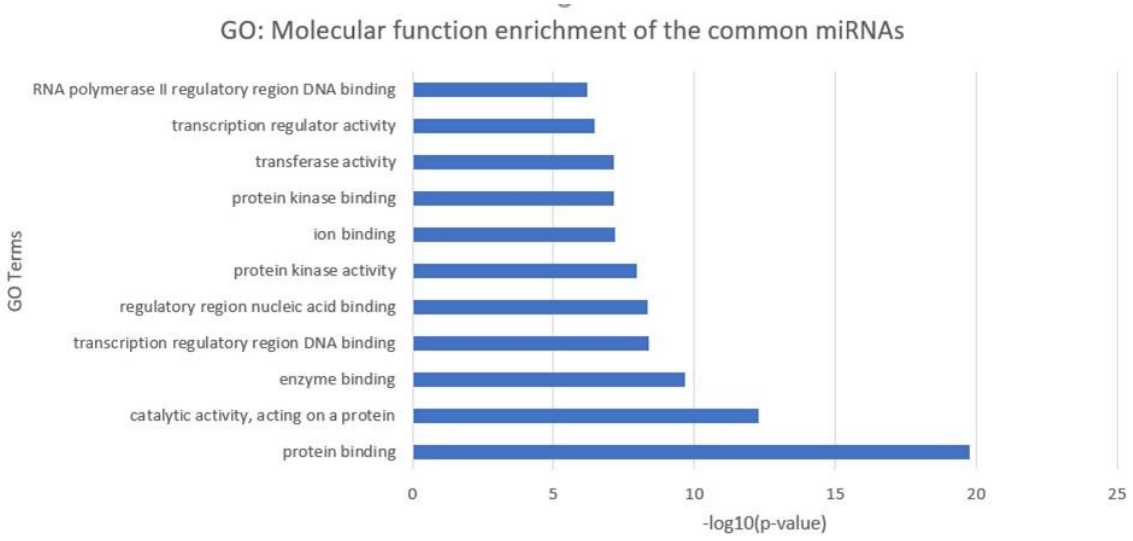

Figure 3.3. Molecular function enrichment of the common miRNAs

3.4. Antibodies to HCV rapid testing

All healthy controls serum samples included in the study were tested negative against HCV antibodies, while HCV and HCC samples showed positive anti-HCV antibodies (Fig. 3.4).

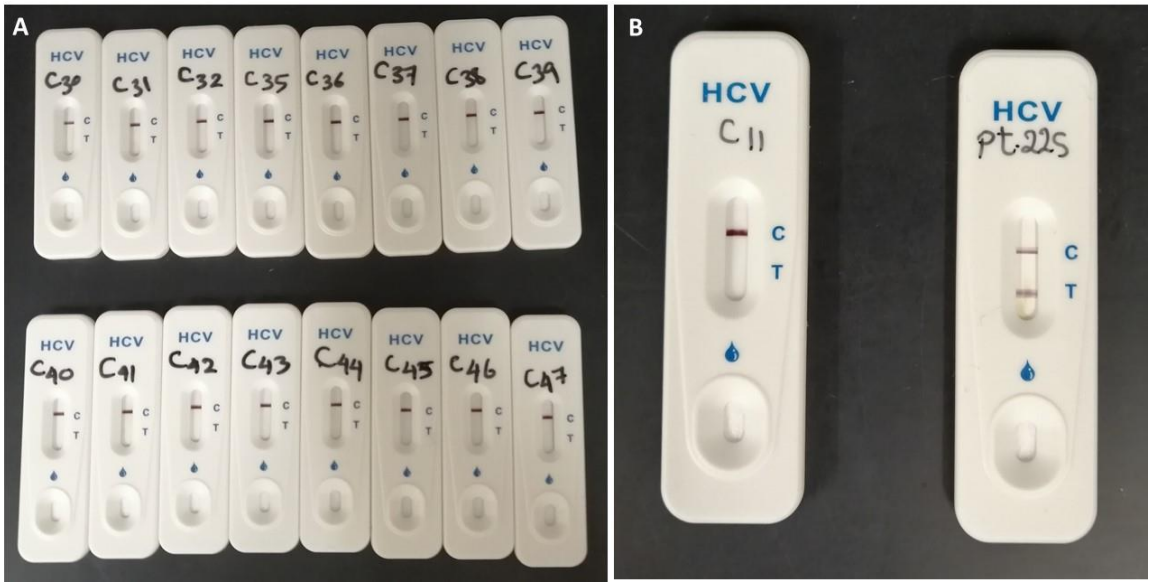

Figure 3.4. Qualitative detection of antibodies to HCV in the healthy individuals' serum samples. (A) HCV rapid test negative results. (B) Negative result in one control sample compared to positive result of a diseased sample.

3.5. Study subjects and laboratory testing

3.5.1. Subjects were classified into the following groups

I) Group 1 (Healthy controls)

Serum of 44 normal healthy samples were donated by global research lab, age range from 25-75 years old, median age was 58 years old, mean age ± SD was 54.6 ± 12.8.

II) Group 2 (HCV non-cirrhotic group)

Blood samples from 62 patients with non-cirrhotic liver condition were collected, either from HCV treatment naïve (chronically infected with HCV, without receiving any treatment for HCV) or HCV treated patients, who have achieved sustained virological response (HCV-SVR), which is guaranteed by the absence of HCV particles in the patient's blood 12 weeks after the last dose of

HCV therapy. Patients' age range from 28-68 years old, median age was 54 years old, mean age ± SD was 52.6 ± 8.8.

III) Group 3 (HCV cirrhotic group)

Blood samples from 67 patients with cirrhotic liver condition, HCV treatment naïve or HCV-SVR were collected. Patients' age range from 27-76 years old, median age was 62 years old, mean age ± SD was 59.2 ± 10.8. Treatment naïve patients are those awaiting a line to receive their HCV treatment, or have some contraindications to HCV treatment including decompensated liver cirrhosis.

IV) Group 4 (HCV-associated HCC)

Blood samples from 72 patients with HCC hepatic focal lesions post HCV infection (either HCV treatment naïve-HCC or HCV-SVR-HCC) were collected. Patients' age range from 36-81 years old, median age was 61 years old, mean age ± SD was 61.4 ± 8.1.

3.5.2. Clinicopathological and demographic features of the study groups

Demographic and clinical information are compiled in (Tables 3.3 and 3.4) and (Fig. 3.5). No significant difference was noted in gender distribution between healthy control and HCC group ($P = 0.5294$), and between non-cirrhotic and cirrhotic groups ($P = 0.1508$). Moreover, no statistical difference was observed in age distribution among the healthy individuals, cirrhotic and HCC groups ($P = 0.0662$). Elevated levels of ALT showed highly significant difference among the three diseased groups (non-cirrhotic, cirrhotic, and HCC) upon comparison with the healthy individuals ($P < 0.0001$). Similarly, AST elevated levels were highly significant in cirrhotic and HCC groups relative to healthy individuals ($P < 0.0001$), and non-cirrhotic group ($P = 0.0005$). Total bilirubin elevated levels in cirrhotic and HCC groups didn't provide statistical significance ($P > 0.99$) although lower T. Bil concentrations in non-cirrhotic groups was reported with high statistical significance ($P < 0.0001$). Statistical significance was detected in the elevated direct bilirubin concentrations among the three diseased groups upon comparison with healthy individuals [D. Bil ($P < 0.0001$, 0.003 respectively), ALB ($P < 0.0001$)], however statistical significance was recorded in decreased albumin levels in cirrhotic and HCC groups only ($P < 0.0001$), and P-value = 0.453 was calculated for the non-cirrhotic patients. Analysis of the 5 liver markers' concentrations

between cirrhotic HCV and HCC groups didn't show any statistically significant difference [ALT ($P > 0.9999$), AST ($P = 0.2786$), T. Bil ($P > 0.9999$), D. Bil ($P > 0.9999$), and ALB ($P = 0.9807$)]. AFP serum concentrations were assessed in the three diseased groups, showing high statistical significance in non-cirrhotic ($P = 0.0002$) and cirrhotic groups ($P = 0.0016$) upon comparison with the HCC group ($P < 0.0001$), while no statistical significance was seen between both HCV groups ($P > 0.9999$).

Serum levels of blood cells were examined among the study groups. Difference in hemoglobin concentrations were noticed in the cirrhotic group in relation to the healthy control subjects ($P < 0.0001$), while there was no significant statistical difference in the non-cirrhotic and the HCC groups compared to controls ($P = 0.453$, 0.237; respectively). However elevated red blood cells (RBCs) and decreased total leukocytes counts (TLCs) and platelets counts were significant among the disease groups in comparison with the healthy individuals ($P < 0.0001$). Nevertheless, no absence of statistically significant divergence was recorded in RBC count between non-cirrhotic and HCC groups ($P = 0.99$), and TLCs counts among cirrhotic and HCC groups relative to non-cirrhotic groups ($P = 0.275$, 0.97; respectively). While platelet count was not significant in cirrhotic and HCC groups ($P = 0.847$).

Table 3.3. Laboratory and clinical data of the study population

Parameter	Control	HCV non-cirrhotic	HCV cirrhotic	HCV HCC	Statistics / *P*-value	
Age	54.6 ± 1.927	52.6 ± 1.253	59.2 ± 1.45	61.4 ± 0.963	26.53^a	< 0.0001
ALT (IU/L)	11.84 ± 0.67	27.48 ± 2.207	33.94 ± 2.42	45.14 ± 4.914	90.3^a	< 0.0001
AST (IU/L)	16.99 ± 1.32	30.26 ± 2.947	39.95 ± 3.61	50.94 ± 4.04	70.1^a	< 0.0001
Alb (g/dL)	4.42 ± 0.1	4.26 ± 0.046	3.658 ± 0.09	3.698 ± 0.07	23.82^b	< 0.0001
T.Bil (mg/dL)	0.98 ± 0.03	0.8 ± 0.057	1.157 ± 0.17	0.984 ± 0.0825	33.12^a	< 0.0001
D.Bil (mg/dL)	0.15 ± 0.009	0.41 ± 0.0473	0.84 ± 0.13	0.603 ± 0.066	71.23^a	< 0.0001
AFP (ng/mL)	NA	18.561 ± 7.42	41.75 ± 11.78	834.47 ± 156.41	19.01^a	< 0.0001
Hb (g/dL)	13.44 ± 0.268	12.89 ± 0.226	11.49 ± 0.22	12.7877 ± 0.234	12.37^b	< 0.0001
RBCs ($\times 10^3/mm^3$)	4.77 ± 0.274	12.9 ± 0.226	11.491 ± 0.22	12.788 ± 0.234	106.9^a	< 0.0001
TLC ($\times 10^9/L$)	7.626 ± 0.417	4.748 ± 0.191	4.194 ± 0.09	4.614 ± 0.09	61.1^a	< 0.0001
Platelets ($\times 10^9/L$)	300.5 ± 12.37	219.85 ± 13.7	130.1 ± 7.75	141.202 ± 9.122	84.6^a	< 0.0001

Data are expressed as mean ± standard error of mean, statistical significance is considered as *P*-value ≤ 0.05
Statistical analysis was performed using (^{a}) Kruskal-Wallis and (^{b}) ANOVA test.

Table 3.4. Clinicopathological and demographic features of the study population

Clinicopathological features	No. of participants [n = 245]	Groups				Statistics	
		Control [n = 44 (% within group)]	HCV non-cirrhotic [n = 62 (% within group)]	HCV cirrhotic [n = 67 (% within group)]	HCV HCC [n = 72 (% within group)]	$\chi^{2(a)}$	*P*-value
Age							
Mean age (≤ 57)	136	25 (56.8%)	48 (77.4%)	36 (53.7%)	27 (37.5)	21.624	< 0.0001
Mean age (> 57)	109	19 (43.2%)	14 (22.6%)	31 (46.3%)	45 (62.5%)		
Gender							
Male	122	30 (68.2%)	15 (24.2%)	24 (35.8%)	53 (73.6%)	43.775	< 0.0001
Female	123	14 (31.8%)	47 (75.8%)	43 (64.2%)	19 (26.4%)		
HCV infection							
Negative	44	44 (100%)	0	0	0	245	NA
Positive (SVR)	126	0	48 (77.4%)	42 (62.7%)	36 (50%)		
Positive (Treatment naïve)	75	0	14 (22.6%)	25 (37.3%)	36 (50%)		
Cirrhosis							
Negative	106	44 (100%)	62 (100%)	0	0	245	NA
Positive	139	0	0	67 (100%)	72 (100%)		
ALT							
≤ 40 IU/L	187	42 (100%)	51 (83.6%)	50 (77%)	44 (63%)	22.745	NA
> 40 IU/L	51	0	10 (16.4%)	15 (23%)	26 (37%)		
Missing	7	2	1	2	2		
AST							
≤ 40 IU/L	167	41 (97.6%)	51 (83.6%)	39 (60%)	36 (51.4%)	35.336	< 0.0001
> 40 IU/L	71	1 (2.4%)	10 (16.4%)	26 (40%)	34 (48.6%)		
Missing	7	2	1	2	2		
ALB							
> 4 g/dL	122	28 (66.7%)	51 (83.6%)	22 (33.8%)	21 (30.4%)	49.41	< 0.0001
≤ 4 g/dL	115	14 (33.3%)	10 (16.4%)	43 (66.2%)	48 (69.6%)		
Missing	8	2	1	2	3		
T. Bil							
≤ 1.25 mg/dL	191	41 (97.6%)	57 (93.4%)	44 (67.7%)	49 (71%)	25.186	< 0.0001
> 1.25 mg/dL	46	1 (2.4%)	4 (6.6%)	21 (32.3%)	20 (29%)		
Missing	8	2	1	2	3		
D. Bil							
≤ 0.35 mg/dL	134	42 (100%)	33 (54.1%)	27 (41.5%)	32 (46.4)	41.285	NA

> 0.35 mg/dL	103	0	28 (45.9%)	38 (58.5%)	37 (53.6%)		
Missing	8	2	1	2	3		
AFP							
< 20 ng/ml	153	NA	56 (91.8%)	55 (83.33%)	42 (60.9%)	19.706	< 0.0001
20-400 ng/ml	16	NA	5 (8.2%)	10 (15.15%)	1 (1.4%)	8.448	0.015
> 400 ng/ml	27	NA	0	1 (1.52%)	26 (37.7%)	51.296	NA
Missing	5	NA	1	1	3		

Statistical significance is considered as *P*-value ≤ 0.05.
Statistical analysis was performed using ([a]) Chi-square test
NA: not applicable, as the number of participants in one or more groups (n=0)

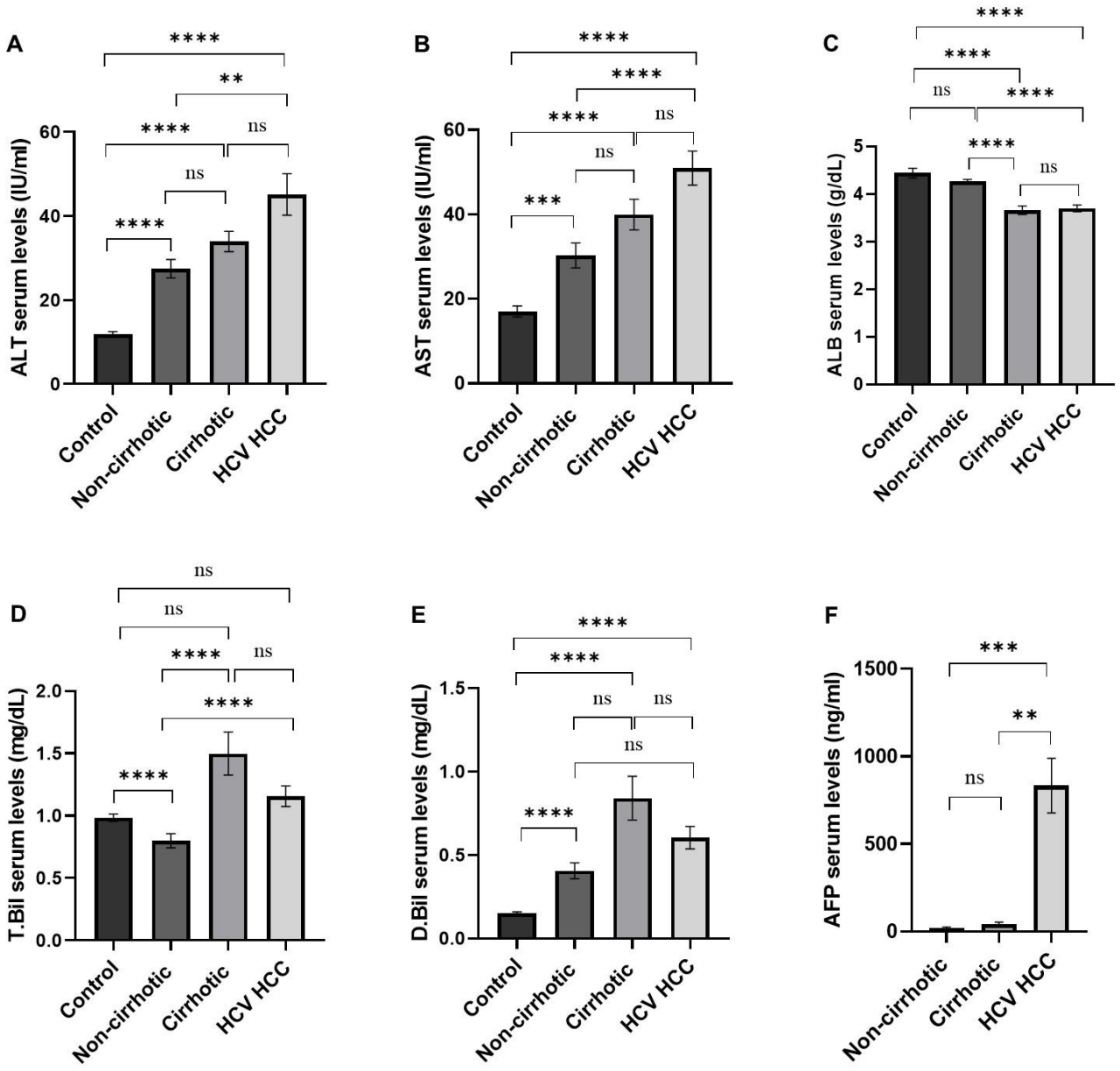

Figure 3.5. Mean of serum concentration of liver biomarkers in the study groups. (A) Comparison of mean values of (A) ALT, (B) AST, (C) albumin, (D) total bilirubin, (E) direct bilirubin and (F) AFP. values are expressed as mean ± SEM. Statistical significance (**** indicates $P \leq 0.0001$, *** indicates $P \leq 0.001$, ** indicates $P \leq 0.01$, ns indicates non-significance). [AFP: alpha-fetoprotein, ALB: albumin, ALT: alanine aminotransferase, AST: aspartate aminotransferase, D. Bil: direct bilirubin, T. Bil: total bilirubin].

Different indices as APRI, FIB-4 and AAR were used to assess the degree of fibrosis and cirrhosis in the study groups (Table 3.5, and Fig. 3.6). Two cutoffs were chosen for APRI, using cutoff score less than 0.5, excluded the possibility of fibrosis in 76.6% of non-cirrhotic group, 33.9% of the cirrhotic patients and 24.6% of HCC group. While APRI score > 1.5 indicated significant fibrosis in 2.1%, 16.9% and 23.1% of non-cirrhotic, cirrhotic and HCC patients respectively. However, the selected FIB-4 cutoffs were 1.45 and 3.27. Having FIB-4 score < 1.45 exclude advanced fibrosis in 62.2% of the non-cirrhotic group, 6% of the cirrhotic, and 11.1% of the HCC patients. Whereas, FIB-4 score > 3.25 indicated higher percentages of advanced fibrosis in 10.8%, 36%, and 49.2% in non-cirrhotic, cirrhotic and HCC patients respectively. Moreover, AAR < 1 suggested normal liver condition, and it was reported in 24.6%, 26.2% and 15.7% of non-cirrhotic, cirrhotic and HCC groups respectively. On the other hand, AAR > 1 suggested the presence of cirrhosis in 75.4%, 73.8% and 84.3% of the three diseased groups respectively. Results obtained from the non-invasive indices indicated the importance of combining different indices in addition to imaging techniques as US for accurate determination of the degree of fibrosis and cirrhosis.

Table 3.5. Non-invasive indices for determination of fibrosis and cirrhosis degrees

Parameter	No. of Participants	Groups			Statistics	
		HCV non-cirrhotic	HCV cirrhotic	HCV HCC	$\chi^{2(a)}$	*P-value*
APRI score	213	0.424 ± 0.051	0.992 ± 0.13	01.365 ± 0.202	102.65	< 0.0001
< 0.5	113	36 (76.6%)	20 (33.9%)	16 (24.6%)	73.747	< 0.0001
0.5 - 1.5	74	10 (21.3%)	29 (49.2%)	34 (52.3%)	37.409	< 0.0001
> 1.5	26	1 (2.1%)	10 (16.9%)	15 (23.1%)	20.165	< 0.0001
Missing	32	15	8	7		
FIB-4 score	192	1.684 ± 0.204	3.767 ± 0.399	4.534 ± 0.476	86.193	< 0.0001
< 1.45	67	23 (62.2%)	3 (6%)	7 (11.1%)	85.387	< 0.0001
1.45 - 3.27	71	10 (27%)	29 (58%)	25 (39.7%)	18.686	< 0.0001
> 3.27	54	4 (10.8%)	18 (36%)	31 (49.2%)	34.641	< 0.0001
Missing	53	25	17	9		
AST/ALT	238	1.14 ± 0.041	1.17 ± 0.043	1.25 ± 0.047	9.73	0.001
≤ 1	54	15 (24.6%)	17 (26.2%)	11 (15.7%)	2.805	0.423
> 1	184	46 (75.4%)	48 (73.8%)	59 (84.3%)		
Missing	7	1	2	2		

[a]: Statistical analysis was performed using Chi-square test.

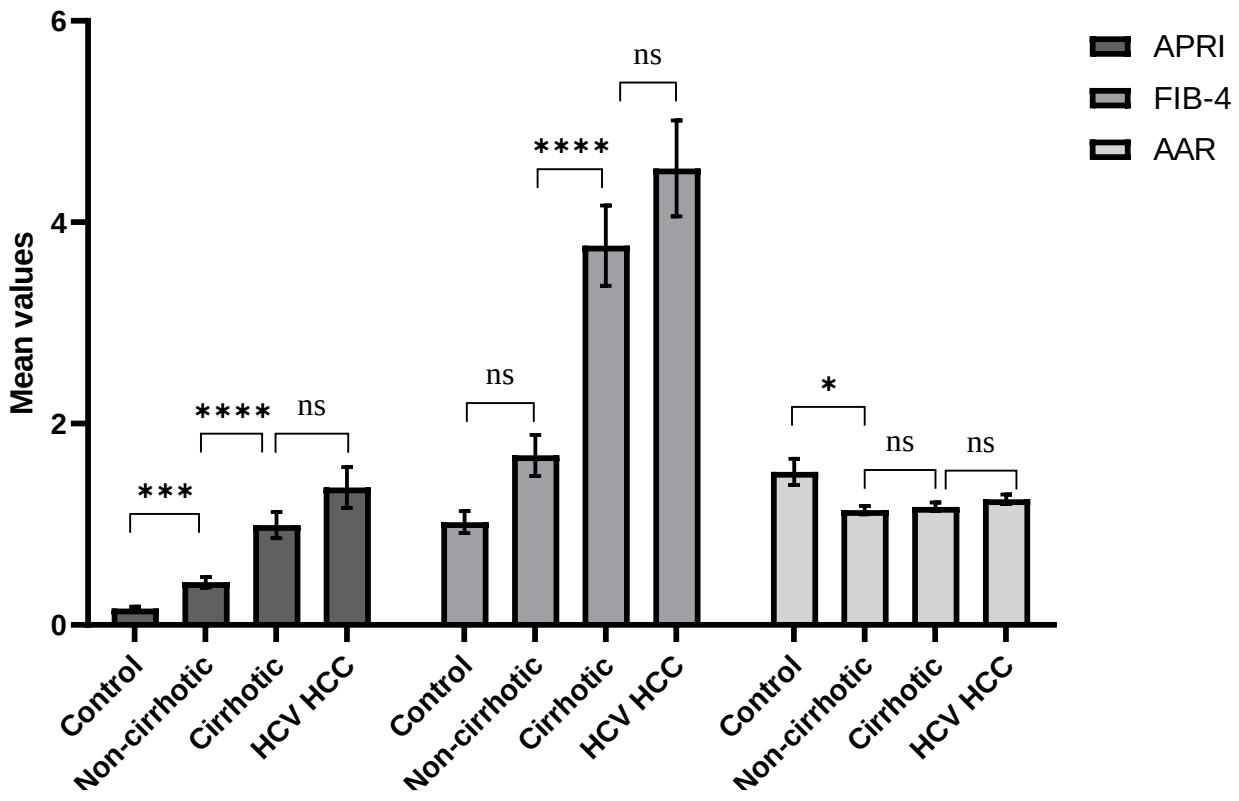

Figure 3.6. Mean values of the non-invasive indices APRI, FIB-4, and AAR in the study groups. Comparison of the statistical significance of the three non-invasive indices in differentiation between different disease stages. Values are expressed as mean ± SEM. Statistical significance (**** indicates $P \leq 0.0001$, *** indicates $P \leq 0.001$, * indicates $P \leq 0.05$, ns indicates non-significance). [AAR: AST to ALT ratio, APRI: Aspartate aminotransferase to platelet ratio index, FIB-4: fibrosis-4 index].

Tumor features and classification of patients in to different disease stages were assessed (Table 3.6). CTP score for measuring the possibilities of liver transplantation in chronic liver diseases as cirrhosis, was determined in the cirrhotic and HCC groups. Patients were categorized into Child A, B, and C in 69.7%, 24.2% and 6.1% of the cirrhotic patients, in addition to 78.3%, 20.3% and 1.4% of the HCC patients respectively. Furthermore, ascetic condition was assessed in the two groups, 22.4% of the cirrhotic patients and 22.2% of the HCC patients showed slight to moderate ascites. Single FL was reported in 63.9% of the HCC patients, while 36.1% had multiple FLs. Additionally, 40.7% of the HCC patients had FL ≤ 3cm in diameter. Overall patients' well-being

and health conditions were examined aiming to classify the patients for the accessibility to chemotherapy in to performance status (PS) = 0 in 48.7%, PS = 1-2 in 43%, and PS > 2 in 8.3% of the HCC patients. BCLC staging system determine the liver condition and the possibility of liver transplantation based on the number and the size of the FL. Patients were classified into three groups: very early (stage 0; 17.9%), early (stage A; 64.2%), and intermediate stage (stage B; 17.9%).

Table 3.6. Characteristics and staging of HCC patients

Parameter		No. of participants	HCV cirrhotic	HCV HCC
CTP score	A	100	46 (69.7%)	54 (78.3%)
	B	30	16 (24.2%)	14 (20.3%)
	C	5	4 (6.1%)	1 (1.4%)
	Missing	4	1	3
Ascites	Absent	117	20 (29.8%)	35 (48.6%)
	Present	31	15 (22.4%)	16 (22.2%)
	Unknown	53	32 (47.8%)	21 (29.2%)
Focal lesions number	Single		----	46 (63.9%)
	Multiple		----	26 (36.1%)
Focal lesions size (By CT)	Tumor ≤ 3cm		----	22 (40.7%)
	Tumor > 3cm		----	32 (59.2%)
	Missing		----	18
Performance status	PS = 0		----	35 (48.7%)
	PS = 1 - 2		----	31 (43%)
	PS > 2		----	6 (8.3%)
BCLC staging system	0		----	10 (17.9%)
	A		----	36 (64.2%)
	B		----	10 (17.9%)
	Missing		----	16

3.6. Real time qPCR

3.6.1. qPCR amplification and data analysis of the candidate miRNAs

The study design relied on determination of the differential expression signature of the circulating miRNAs that have been obtained from the bioinformatic analysis and were previously reported to participate in either the oncogenicity or the progression of HCC disease. The expression levels of the target miRNAs were assessed using SYBR Green based qPCR in the aforementioned diseased groups compared to healthy individuals as a control group. The expression of the target miRNA in each sample was normalized to SNORD 68 as an endogenous reference gene for the same sample to calculate ΔCt values (Table 3.7). The relative expressions of the candidate miRNAs were assessed using $2^{-\Delta\Delta Ct}$ method. Failure to have true amplification plot for the SNORD 68 gene or if no true amplification was recorded in three or more miRNAs, the results of this sample became disqualified and were disqualified from the analysis. Each experiment was implemented using two technical replicates.

Fold changes of the DE-miRNAs among the study groups were represented in Fig. 3.7. The results of this study revealed that serum levels of the nine candidate miRNAs were differentially expressed in HCV and HCC patients in comparison to healthy individuals with high statistical significance (*P*-value < 0.0001) using Mann-Whitney U statistical test (Table 3.9). However, only miR-424 serum level showed statistical significance upon comparing HCV patients with those having HCC. The expression levels of miR-424, miR-199a, miR-142, and miR-224 were significantly altered in HCC patients relative to the non-cirrhotic subjects ($P < 0.0001$, $P = 0.0001$, $P = 0.023$, and $P = 0.027$ respectively). Whereas, miR-199a and miR-183 showed difference in differential expression between HCV cirrhotic and non-cirrhotic patients ($P = 0.012$ and $P = 0.036$ respectively).

Comparison of the mean rank (which represents the arithmetic average of the positions in the list, preferred to be used in non-parametric test) of the fold change among the study groups (Table 3.8) showed that the increase in the fold change of miR-142, miR-199a, miR-215, miR-224 and miR-424 was compatible with the disease progression. Whereas, for miR-183 and miR-217, the mean rank increased in non-cirrhotic and cirrhotic patients followed by reduction in the mean expression in the HCC patients. However, the mean rank of miR-150 expression was elevated in

the non-cirrhotic and the cirrhotic patients compared to health controls, without any marked difference in the fold change values between the two HCV groups, followed by an increase in expression of the HCC group. As for miR-3607, the increase in mean rank expression in the non-cirrhotic patients, was followed by reduction in expression in patients with cirrhosis, then non-significant increase in expression HCC group.

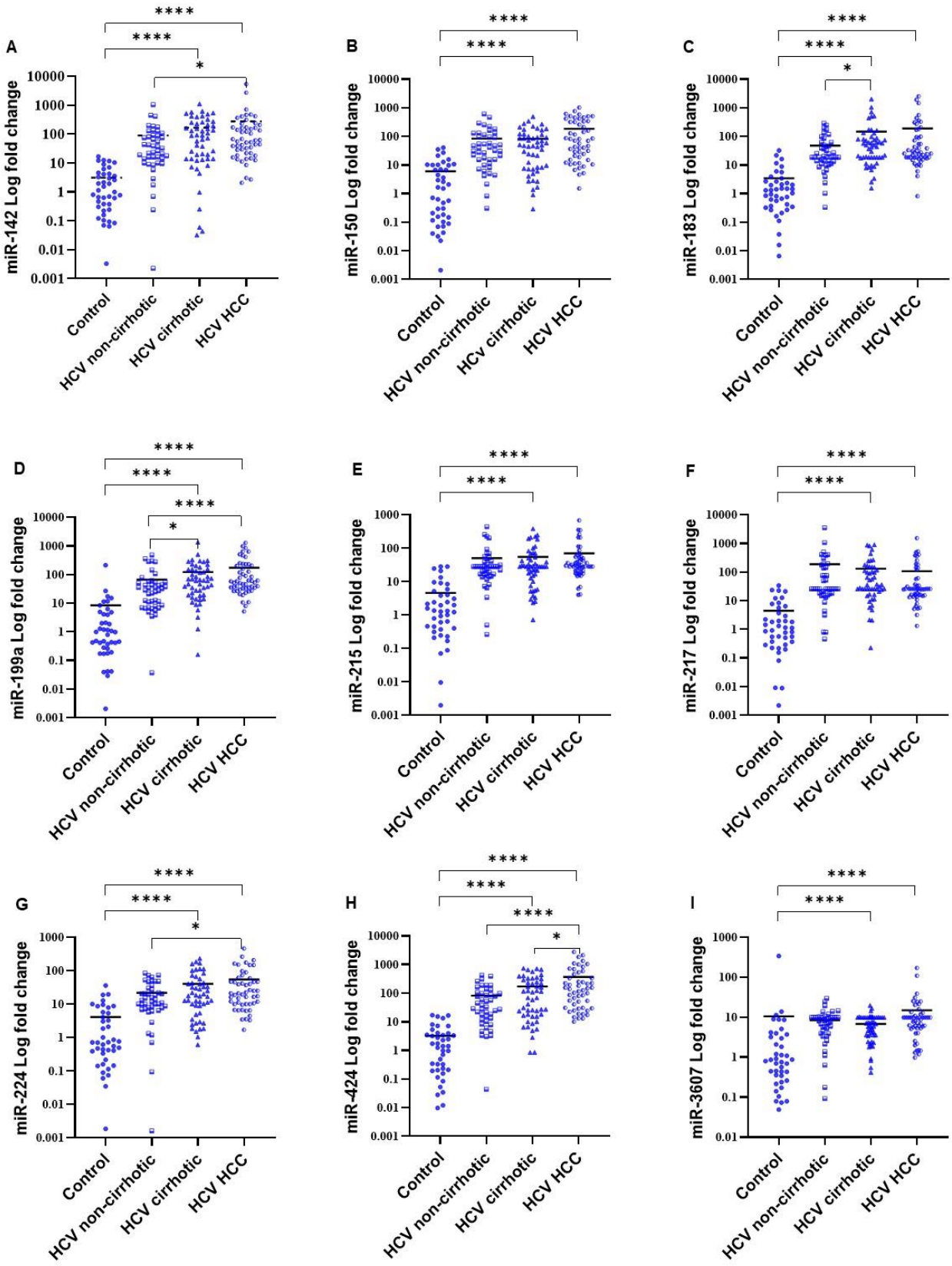
A
miR-142 Log fold change
B
miR-150 Log fold change
C
miR-183 Log fold change
D
miR-199a Log fold change
E
miR-215 Log fold change
F
miR-217 Log fold change
G
miR-224 Log fold change
H
miR-424 Log fold change
I
miR-3607 Log fold change
Control
HCV non-cirrhotic
HCV cirrhotic
HCV HCC
****
*

Figure 3.7. Fold change of the DE-miRNAs in the study groups. Scatter dot plots demonstrating the fold change of serum expression of the target miRNAs (miR-142, miR-150, miR-183, miR-199a, miR-215, miR-217, miR-224, miR-424, and miR-3607) among the study groups. Y-axis represents log of the fold change of each miRNA; X-axis shows the study groups. Each experiment was performed in duplicates.

Table 3.7. Mean of ΔCt of target miRNAs among the studied groups.

Target	Groups				Statistics		
	Control mean ΔCt (n = 41)	HCV non-cirrhotic mean ΔCt (n = 44)	HCV cirrhotic mean ΔCt (n = 51)	HCV HCC mean ΔCt (n = 52)	Statistical test[a]	*P*-value (cont. vs HCV and HCC)[b]	*P*-value (HCV vs HCC)[b]
miR-142	3.847 ± 0.42	-0.816 ± 0.47	-1.58 ± 0.5	-2.25 ± 0.32	74.022	< 0.0001	0.853(N.S.)
miR-150	-2.402 ± 0.55	-7.42 ± 0.35	-7.37 ± 0.35	-8.49 ± 0.33	64.834	< 0.0001	0.051(N.S.)
miR-183	4.21 ± 0.401	-0.254 ± 0.29	-1.24 ± 0.303	-1.22 ± 0.32	80.109	< 0.0001	0.689(N.S.)
miR-199a	2.13 ± 0.49	-2.62 ± 0.35	-3.63 ± 0.32	-4.213 ± 0.26	81.468	< 0.0001	0.413(N.S.)
miR-215	4.81 ± 0.45	0.217 ± 0.29	0.148 ± 0.27	-0.374 ± 0.21	76.745	< 0.0001	0.248(N.S.)
mir-217	4.684 ± 0.48	-0.54 ± 0.395	-0.759 ± 0.33	-0.358 ± 0.29	72.422	< 0.0001	0.112(N.S.)
miR-224	3.469 ± 0.46	-0.012 ± 0.41	-0.737 ± 0.3	-1.294 ± 0.25	60.309	< 0.0001	0.314(N.S.)
miR-424	2.401 ± 0.45	-2.79 ± 0.37	-3.663 ± 0.36	-4.796 ± 0.303	90.225	< 0.0001	0.05
miR-3607	3.358 ± 0.4	0.77 ± 0.25	0.93 ± 0.17	0.317 ± 0.21	46.934	< 0.0001	0.07(N.S.)

Data are expressed as mean ± standard error of mean, statistical significance is considered as *P*-value ≤ 0.05. (N.S.) Not significant, indicates absence of statistical significance.
Statistical analysis was performed using ([a]) Kruskal-Wallis or ([b]) Mann-Whitney test

Table 3.8. Fold change mean rank of target miRNAs among the studied groups.

Target	Groups				Statistics	
	Control fold change mean rank (n = 41)	HCV non-cirrhotic fold change mean rank (n = 44)	HCV cirrhotic fold change mean rank (n = 51)	HCV HCC fold change mean rank (n = 52)	Statistical test[(a)]	*P*-value
miR-142	31.634	98.659	115.098	120.346	74.0224	< 0.0001
miR-150	35.976	104.636	104.235	122.519	64.3728	< 0.0001
miR-183	28.879	99.705	119.971	116.856	80.1087	< 0.0001
miR-199a	30.39	92.886	116.431	124.904	81.4677	< 0.0001
miR-215	31.488	104.989	109.069	121.019	72.812	< 0.0001
mir-217	31.39	111.875	119.039	105.49	72.4221	< 0.0001
miR-224	38.146	98.091	110.235	120.462	60.2673	< 0.0001
miR-424	27.049	95.568	111.549	130.058	90.2253	< 0.0001
miR-3607	44.634	108.92	99.4314	116.779	46.9342	< 0.0001

Statistical significance is considered as *P*-value ≤ 0.05
Statistical analysis was performed using ([a]) Kruskal-Wallis.

3.6.2. Receiver operating characteristic (ROC) analysis

Assessment of the diagnostic performance for the nine candidate miRNAs was performed using receiver operating characteristic (ROC) analyses. ROC curves were created using SPSS software version 25, and the capability of each potential biomarker to identify the diseased persons was demonstrated as the area under the ROC curve (AUC). ROC analysis was assessed based on RNAs' relative quantification (RQ) values to highlight the threshold value for the best sensitivity and specificity. The cutoffs were set by calculating the true positive samples (sensitivity percent) and false positive samples (1 - specificity) of each RNA's RQ values at several cutoff points. Accordingly, the best cutoff values were selected for each of the RNAs. Samples were considered positive if the RQ was greater than or equal to this cutoff value. The distribution of the positive cases of each miRNA among the four groups was examined using Chi-Square test. Evaluation of

the diagnostic potential of the DE-miRNAs through calculation of sensitivity, specificity, positive predictive value (PPV), negative predictive value (NPV), and accuracy among different comparative study groups. For better diagnostic accuracy, ROC analysis was implemented for combined panels of the statistically significant miRNAs. Additionally, the diagnostic performance of the combined panel was compared to AFP in HCV and HCC patients.

3.6.2.1. Diagnostic potential of the DE-miRNAs in HCC patient compared to healthy individuals

ROC analysis calculations were assessed for the candidate miRNAs to discriminate HCC patients from healthy controls (Fig. 3.8 and Table 3.9). The AUC values were 0.993, 0.972, 0.968, 0.958, 0.957, 0.933, 0.928, 0.921, 0.868 corresponding to miR-424, miR-142, miR-199a, miR-215, miR-183, miR-217, miR-150, miR-224, and miR-3607 respectively with high statistical significance (*P*-value < 0.0001). All of the targets showed high sensitivity (ranging from 100% to 80.77%) and accuracy (ranging from 95.7% to 81.72%) for diagnosis of HCC patients. Having combined panel of 5 miRNAs; in which if 5 miRNAs tested positive, the whole panel is considered positive; increased the sensitivity, specificity and accuracy of detection to 100%, 95.12%, and 97.85% respectively with high statistical significance (*P*-value < 0.0001).

3.6.2.2. Diagnostic potential of the DE-miRNAs in HCV patient compared to healthy individuals

To identify HCV patients from healthy individuals, ROC curves were drawn for the candidate miRNAs (Fig. 3.9 and Table 3.10). The AUC values were 0.941, 0.94, 0.927, 0.919, 0.913, 0.903, 0.882, 0.863, and 0.824 corresponding to miR-183, miR-424, miR-217, miR-199a, miR-215, miR-142, miR-150, miR-224, and miR-3607 respectively with high statistical significance (*P*-value < 0.0001). All of the targets showed high sensitivity (ranging from 91.58% to 80%) and accuracy (ranging from 90.44% to 79.41%) for discrimination of HCV patients. Combined panel of 5 miRNAs improved overall sensitivity, specificity and accuracy of detection to 90.53%, 85.37%, and 88.97% respectively with high statistical significance (*P*-value < 0.0001).

3.6.2.3. Diagnostic potential of the DE-miRNAs in HCC patient compared to non-HCC individuals

In a comparison between HCC patients with others without malignancy (healthy individuals, HCV non-cirrhotic and HCV cirrhotic patients), AUC were calculated and eight potential miRNAs

had statistically significant values (Fig. 3.10 and Table 3.11). For miR-424, miR-199a, miR-150, miR-215, miR-224, miR-142, miR-183, and miR-3607 had AUC equal to 0.761, 0.724, 0.706, 0.695, 0.691, 0.69, 0.664, and 0.664 respectively with high statistical significance (*P*-value < 0.0001). Acceptable sensitivities (80.77% to 61.54%) and accuracies (65.96% to 57.98%) were recorded for the different targets. Using a combined panel of 5 miRNAs resulted in 80.77% sensitivity and 61.03% specificity for HCC detection with a statistically significant *P* -value < 0.0001.

3.6.2.4. Diagnostic potential of the DE-miRNAs in HCC (SVR / treatment naïve) patient compared to non-HCC (SVR / treatment naïve) patients

Classifying the study groups in to those who have received HCV treatment and reached sustained virological response (SVR) (Fig. 3.11 and Table 3.12) and those who haven't received any treatment (treatment naïve; Fig. 3.12 and Table 3.13) remarkably increased AUC and the overall ROC analysis measurements. The highest AUC for both HCC (SVR) group HCC (treatment naïve) group was recorded for miR-424 (0.8, and 0.835 respectively) (*P*-value < 0.0001). Similar to the previously reported results, combined panel of 5 miRNAs increased the overall sensitivity, specificity and accuracy for HCC (SVR) patients' diagnosis to (83.33%, 63.73% and 67.46% respectively). While combining 6 miRNAs in one panel, improved the calculated measurements in HCC (treatment naïve patients) (sensitivity 89.29%, specificity 72.6% and accuracy 77.23%).

3.6.2.5. Diagnostic potential of the DE-miRNAs in HCC patients compared to patients with HCV

In order to develop potential biomarker to differentiate between HCC patients from HCV subjects, ROC analysis was performed and resulted in three statistically significant targets; miR-424, miR-199a, and miR-150, with *P*-values 0.001, 0.018, and 0.028 respectively (Fig. 3.13 and Table 3.14). The highest calculations were obtained for miR-424. Comparison between miRNA-424 and AFP (the current HCC serum biomarker) resulted in comparable sensitivities, 63.46% for the former and 62.32% for the later. Although AFP specificity and accuracy (64.57% and 63.78%) were better than those for miR-424 (57.9% and 59.86%). However, the choice of a combined panel of 2 miRNAs with or without AFP didn't provide significant improvements in the ROC analysis measurements.

3.6.2.6. Diagnostic potential of the DE-miRNAs in HCC (SVR) patients compared to patients with HCV (SVR)

Similarly, ROC curves were constructed to determine the best AUC for patients with HCC (SVR) compared to HCV (SVR) (Fig. 3.14, and Table 3.15). Three miRNAs had statistically significant results (miR-424, miR142, and miR-3607) with *P*-values 0.01, 0.018, and 0.014; respectively. The ROC measurements obtained (sensitivity: 66.67%, 66.67%, and 70.83%, accuracy: 62.1%, 68.97%, 58.62%) were remarkably higher than sensitivity and accuracy recorded for AFP (51.43% and 58.1% respectively). Using combined panel of 2 miRNAs enhanced the sensitivity, specificity and accuracy of detection (70.83%, 61.9%, and 64.37% respectively). Addition of AFP biomarker to the combined panel improved only the sensitivity with a reduction in the specificity and accuracy. However, ROC analysis to discriminate patients with HCC (treatment naïve) for HCV (treatment naïve) patients didn't show any statically significant AUC for any of the targets.

3.6.3. Correlation between the studied miRNAs

Spearman's correlation test was performed to investigate the correlation between the fold change of expression of each individual miRNA and the other miRNAs. Positive correlation was recorded between the expression of all miRNAs among the study groups, with high statistical significance ($P < 0.0001$) (Table 3.16). Moreover, the correlation between the miRNAs under study and some clinicopathological characteristics was performed (Table 3.17). MiR-183, miR-199a and miR-215 were positively correlated with the age of the patients ($P = 0.007$, 0.037 and 0.026 respectively), while only miR-142 and miR-217 were positively correlated with gender ($P = 0.036$ and 0.001 respectively). Whereas, the whole panel of the nine miRNAs was positively correlated with the cirrhotic liver conditions ($P < 0.0001$), ALT and AST levels ($P < 0.001$). High statistically significant positive correlation was also found between the nine targets and D. Bil ($P < 0.0001$). On the other hand, negative correlation was recorded between T. Bil levels, with statistical significance shown only in miR-150 ($P = 0.003$). Similarly, miRNAs concentrations were negatively correlated with albumin levels ($P < 0.001$ in most of the targets). Moreover, the association between the tumor characteristics and the miRNAs expression was investigated. Only miR-199a showed significant positive correlation with the AFP levels ($P = 0.04$). While for child-Pugh score, miR-150 was negatively correlated ($P = 0.009$), while miR-217 and miR-3607 were

positively correlated (P = 0.02, P = 0.032 respectively). Interestingly, no significant correlation was reported with BCLC staging.

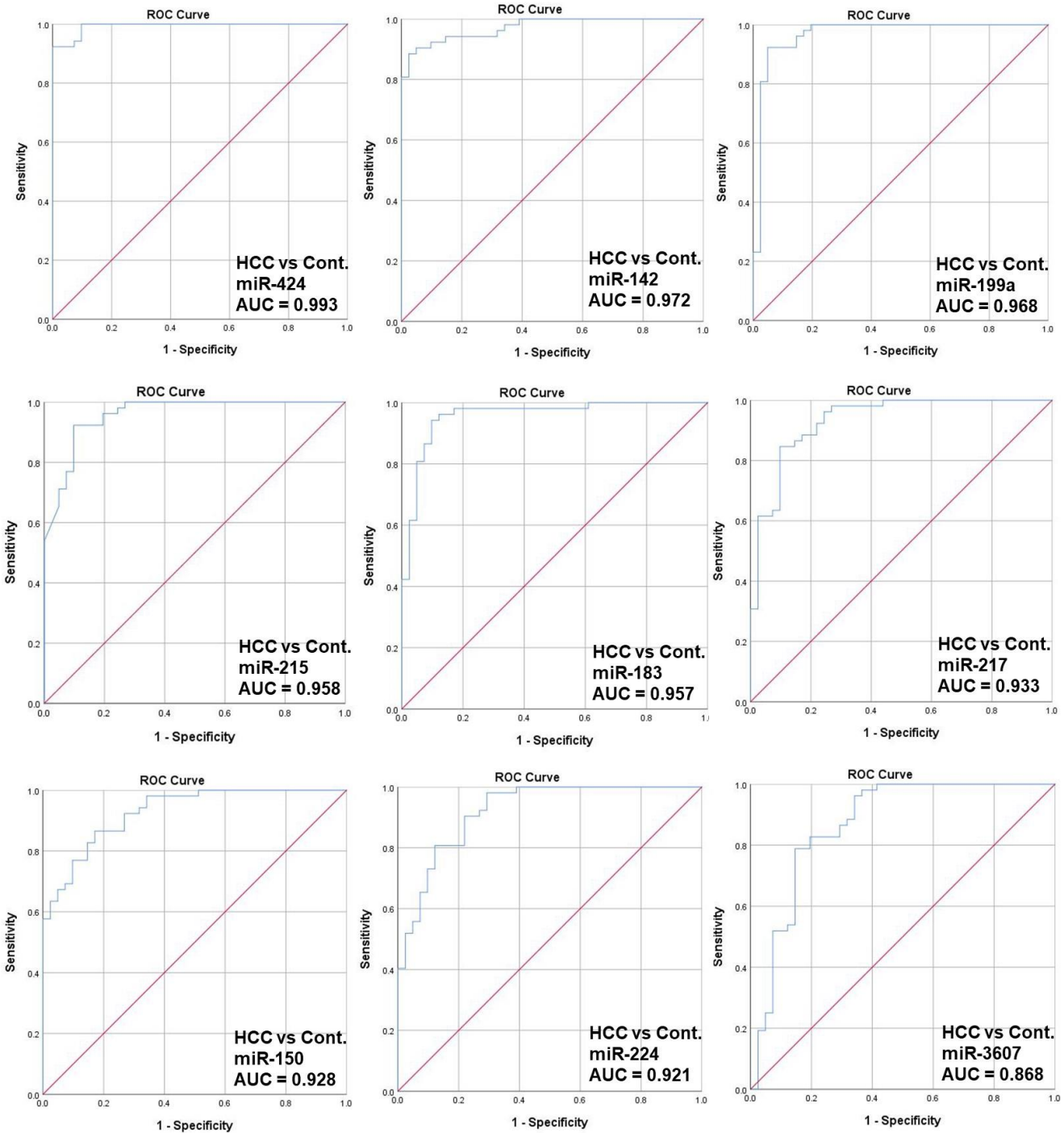

Figure 3.8. ROC curves and AUC for the DE-miRNAs in the differentiation between HCC patients and healthy individuals. The diagnostic potential and AUC of nine DE-miRNAs (miR-424, miR-142, miR-199a, miR-215, miR-183, miR217, miR150, miR-224 and miR-3607 were calculated.

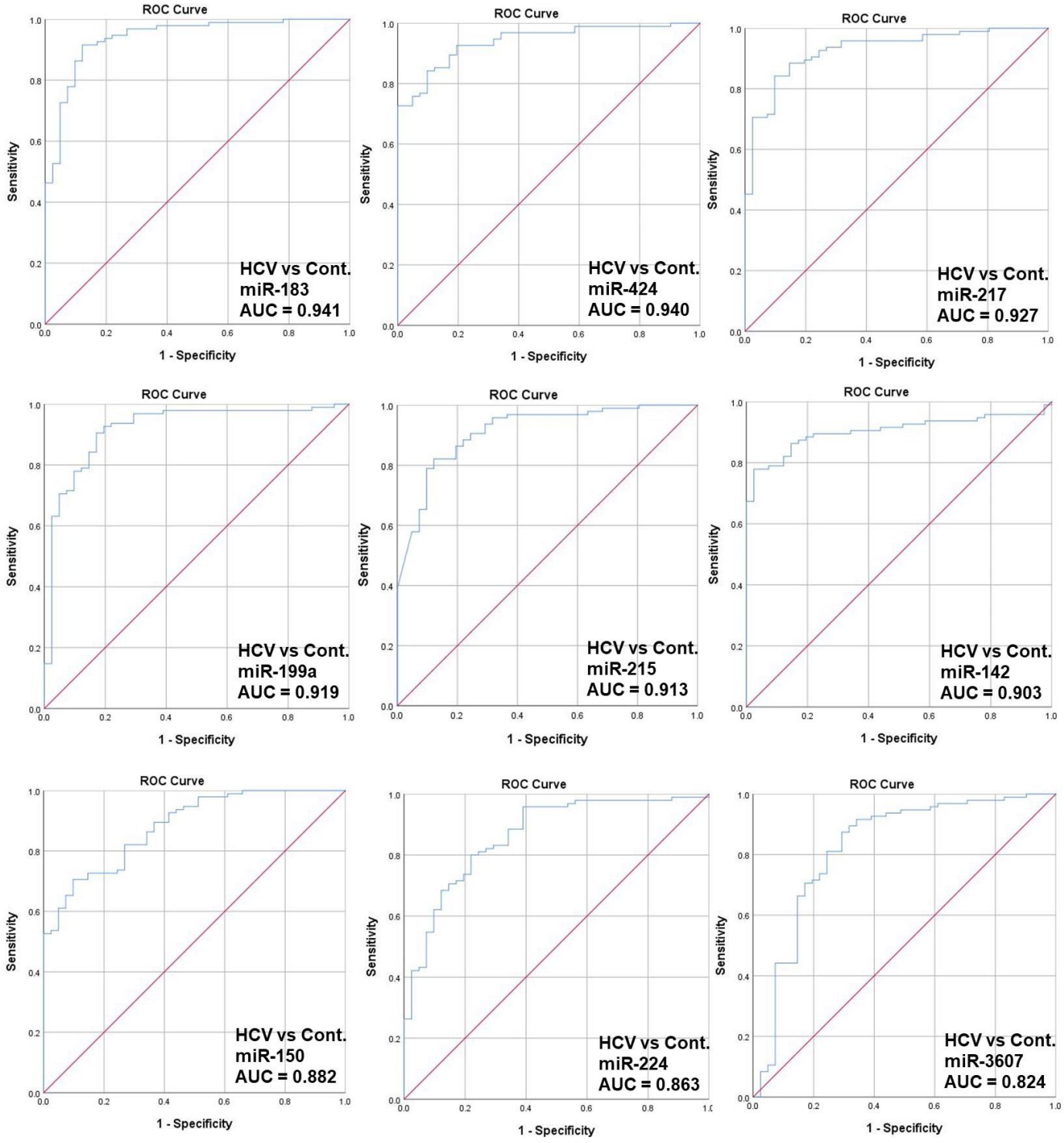

Figure 3.9. ROC curves and AUC for the DE-miRNAs in the differentiation between HCV patients and healthy individuals. The diagnostic potential and AUC of nine DE-miRNAs (miR-183, miR-424, miR-217, miR-199a, miR-215, miR-142, miR-150, miR-224, and miR-3607) were calculated.

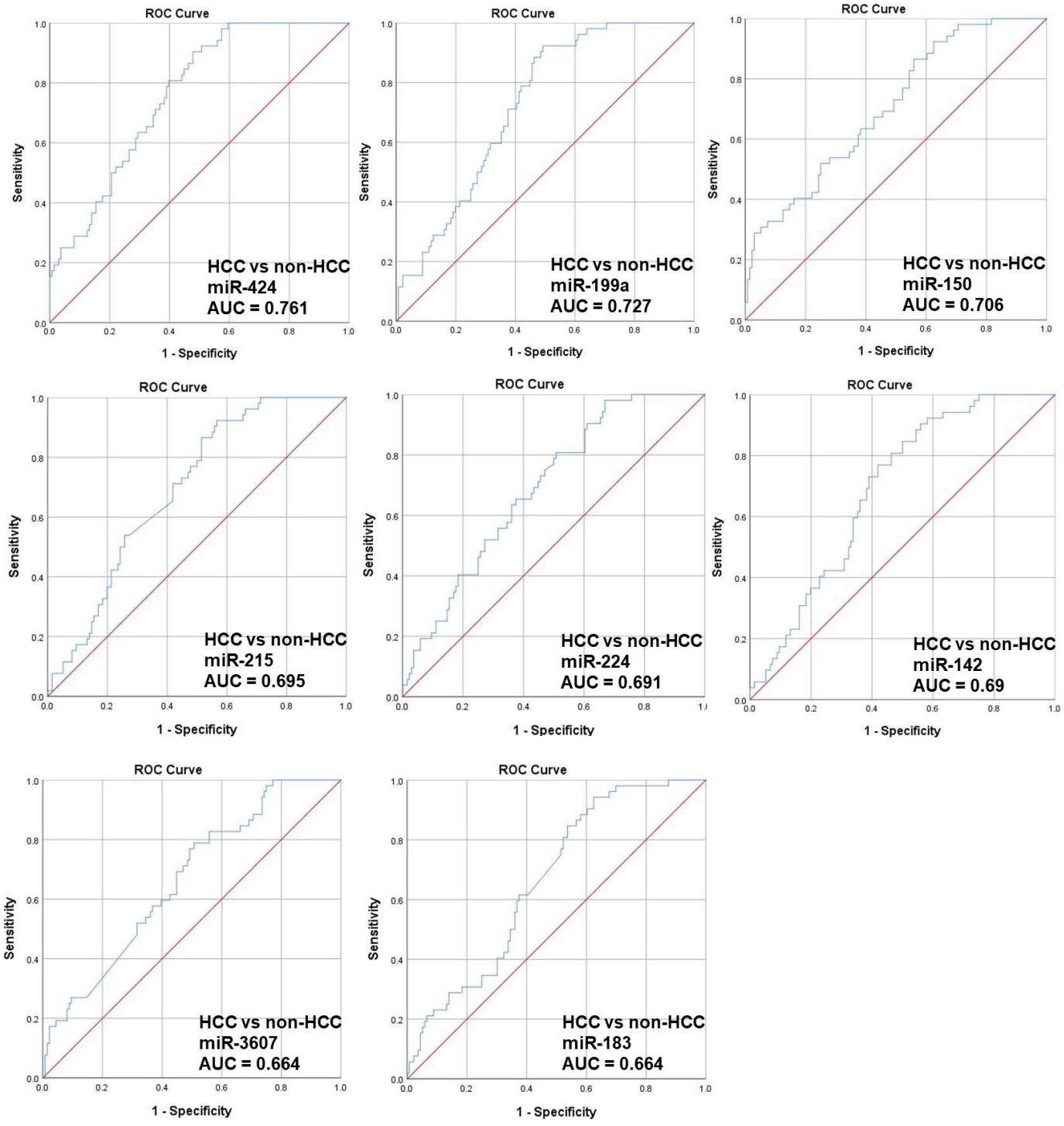

Figure 3.10. ROC curves and AUC for DE-miRNAs in the differentiation between HCC patients and non-HCC (healthy controls, non-cirrhotic and cirrhotic HCV patients). The diagnostic potential and AUC of the eight DE-miRNAs (miR-424, miR-199a, miR-150, miR-215, miR-224, miR-142, miR-183, and miR-3607) were calculated.

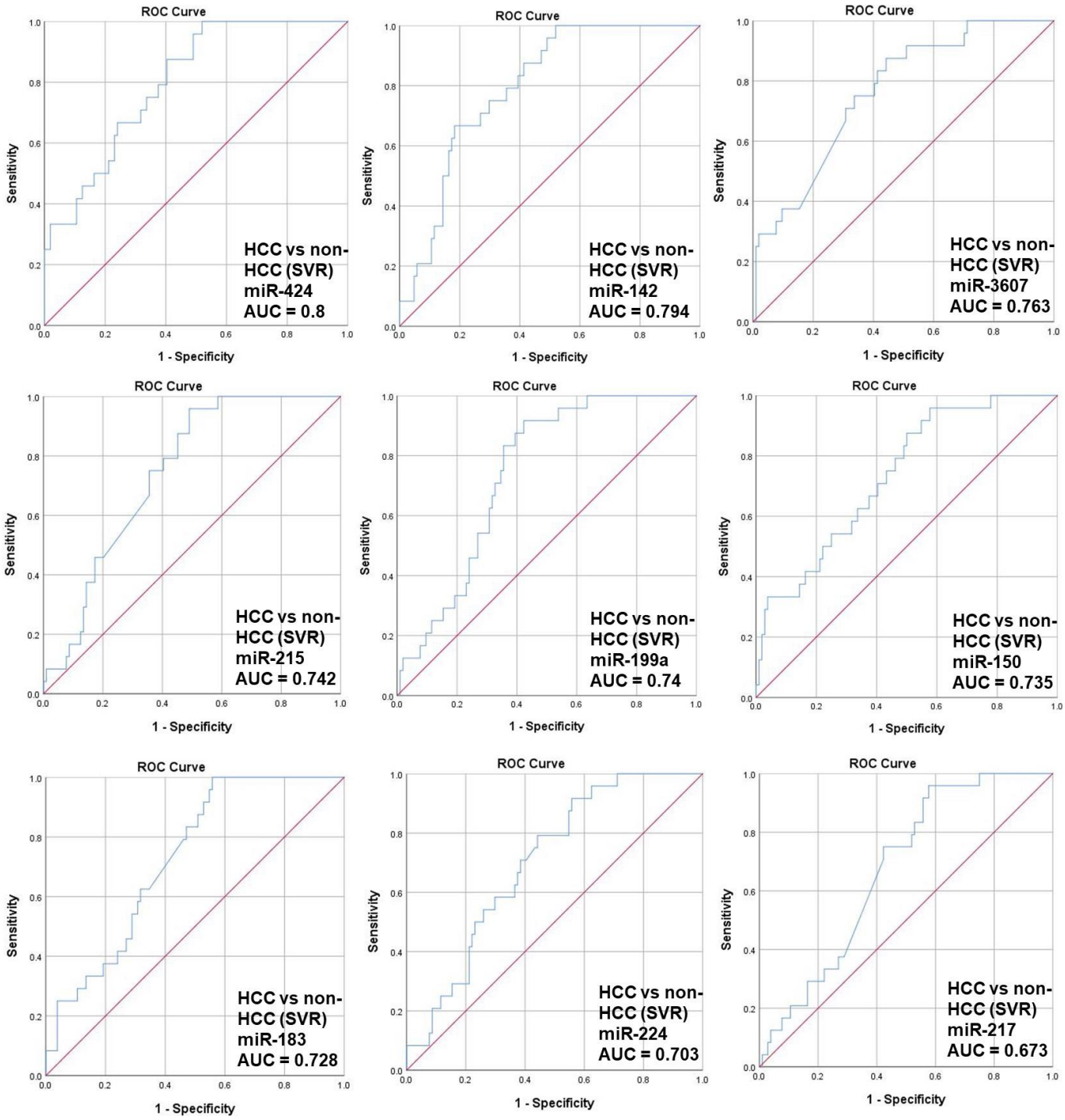

Figure 3.11. ROC curves and AUC for the DE-miRNAs in the differentiation between HCC (SVR) patients and non-HCC (healthy controls, non-cirrhotic (SVR) and cirrhotic (SVR) HCV patients). The diagnostic potential and AUC of nine DE-miRNAs (miR-424, miR-142, miR-3607, miR-215, miR-199a, miR-150, miR-183, miR-224, and miR-217) were calculated.

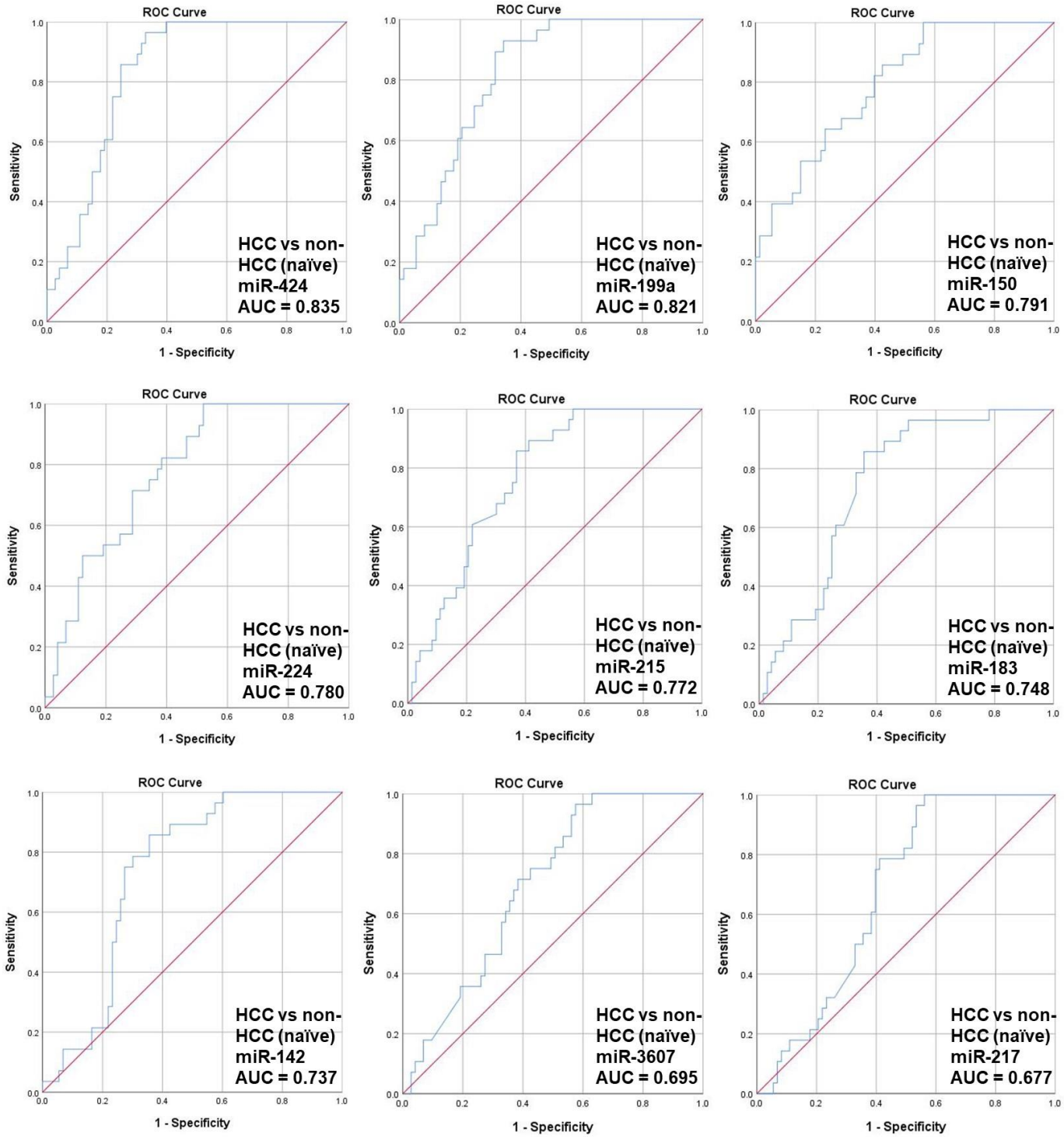

Figure 3.12. ROC curves and AUC for the DE-miRNAs in the differentiation between HCC (treatment naive) patients and non-HCC (healthy controls, non-cirrhotic (treatment naive) and cirrhotic (treatment naive) HCV patients). The diagnostic potential and AUC of nine DE-miRNAs (miR-424, miR-199a, miR-150, miR-224, miR-215, miR-183, miR-142, miR-3607, and miR-217) were calculated.

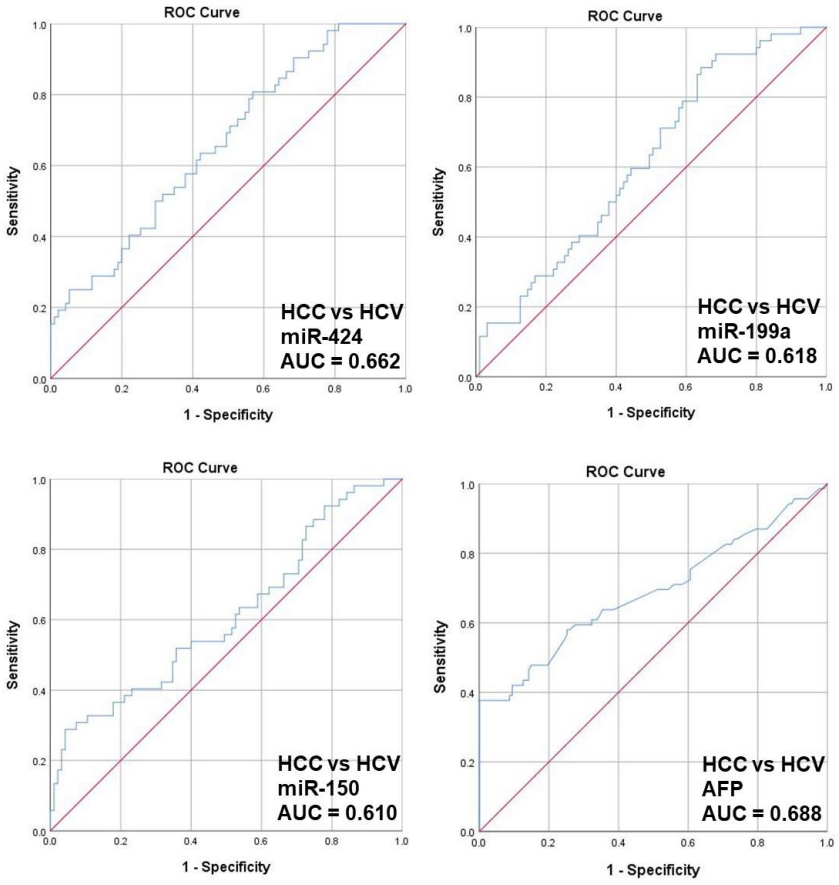

Figure 3.13. ROC curves and AUC for DE-miRNAs in comparison to AFP in the differentiation between HCC and HCV patients. The diagnostic potential and AUC of three DE-miRNAs (miR-424, miR-199a, and miR-150) in addition to AFP were calculated.

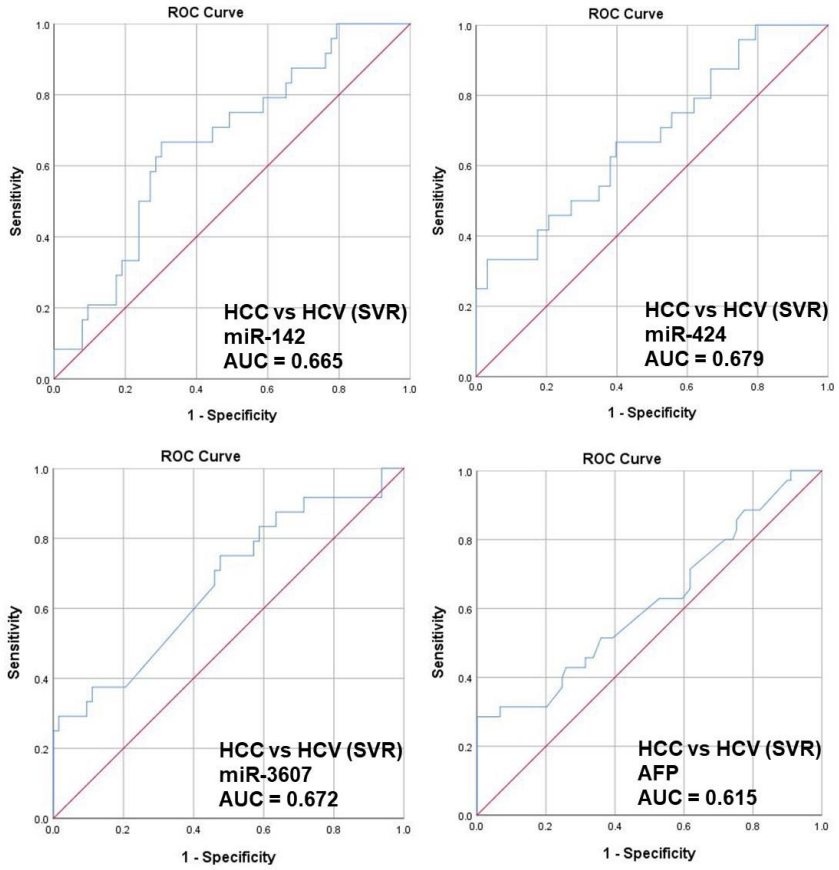

Figure 3.14. ROC curves and AUC for DE-miRNAs in comparison to AFP in the differentiation between HCC (SVR) and HCV (SVR) patients. The diagnostic potential and AUC of three DE-miRNAs (miR-142, miR-424, and miR-3607) in addition to AFP were calculated.

Table 3.9. ROC curve analysis of the investigated biomarkers in discriminating HCC patients from healthy individuals

Target	AUC	SE	*P*-value	95% CI	Cut-off	Sensitivity	Specificity	PPV	NPP	Accuracy	Chi-sq	*P*-value (2 sided)
HCC vs Control												
miR-424	0.993	0.005	< 0.0001	0.98-1	9.05	100	90.24	92.86	100	95.70	77.93	< 0.0001
miR-199a	0.968	0.02	< 0.0001	0.93-1	18.22	92.31	95.12	96.00	90.70	93.55	70.49	< 0.0001
miR-142	0.972	0.014	< 0.0001	0.95-0.99	10.80	92.31	90.24	92.31	90.24	91.40	63.38	< 0.0001
miR-215	0.958	0.019	< 0.0001	0.92-0.994	13.89	92.31	90.24	92.31	90.24	91.40	63.38	< 0.0001
miR-224	0.921	0.027	< 0.0001	0.87-0.97	9.60	80.77	87.80	89.36	78.26	83.87	43.13	< 0.0001
miR-150	0.928	0.024	< 0.0001	0.88-0.98	10.36	88.46	82.93	86.79	85.00	86.02	47.66	< 0.0001
miR-3607	0.868	0.041	< 0.0001	0.79-0.95	3.96	82.69	80.49	84.31	78.57	81.72	36.95	< 0.0001
miR-183	0.957	0.021	< 0.0001	0.92-0.998	9.14	94.23	90.24	92.45	92.50	92.47	66.74	< 0.0001
miR-217	0.933	0.026	< 0.0001	0.88-0.98	9.54	86.54	85.37	88.24	83.33	86.02	47.86	< 0.0001
Combined panel (3 out of 9 miRNAs)						100	80.49	86.67	100	91.40	64.87	< 0.0001
Combined panel (4 out of 9 miRNAs)						100	85.37	89.66	100	93.55	71.18	< 0.0001
Combined panel (5 out of 9 miRNAs)						**100**	**95.12**	**96.30**	**100**	**97.85**	**85.19**	**< 0.0001**
Combined panel (6 out of 9 miRNAs)						96.15	97.56	98.04	95.24	96.77	81.3	< 0.0001

Statistical significance is considered as *P*-value ≤ 0.05. ROC analysis was done on nine statistically significantly candidate miRNAs.

Table 3.10. ROC curve analysis of the investigated biomarkers in discriminating HCV patients from healthy individuals

Target	AUC	SE	*P*-value	95% CI	Cut-off	Sensitivity	Specificity	PPV	NPV	Accuracy	Chi-sq	*P*-value (2 sided)
HCV vs Control												
miR-424	0.94	0.019	< 0.0001	0.9-0.98	7.17	85.26	85.37	93.1	71.43	85.29	61.99	< 0.0001
miR-199a	0.919	0.028	< 0.0001	0.86-0.97	8.40	84.21	85.37	93.02	70	84.56	59.64	< 0.0001
miR-142	0.903	0.026	< 0.0001	0.85-0.96	7.17	86.32	85.37	93.18	72.92	86.03	64.44	< 0.0001
miR-215	0.913	0.06	< 0.0001	0.86-0.96	6.2	86.32	80.49	91.11	71.74	84.55	57.1	< 0.0001
miR-224	0.863	0.034	< 0.0001	0.8-0.93	5.73	80	78.05	89.41	62.75	79.41	41.18	< 0.0001
miR-150	0.882	0.029	< 0.0001	0.83-0.94	6.97	82.11	73.17	87.64	63.83	79.41	38.69	< 0.0001
miR-3607	0.824	0.044	< 0.0001	0.74-0.91	3.27	81.05	75.61	88.51	63.27	79.41	39.9	< 0.0001
miR-183	0.941	0.022	< 0.0001	0.9-0.98	6.27	91.58	87.8	94.57	81.82	90.44	82.47	< 0.0001
miR-217	0.927	0.023	< 0.0001	0.88-0.97	8.5	88.42	85.37	93.33	76.09	87.5	69.66	< 0.0001
Combined panel (3 out of 9 miRNAs)						98.95	78.05	91.26	96.97	92.64	92.39	< 0.0001
Combined panel (4 out of 9 miRNAs)						96.84	80.49	92	91.67	91.91	87.99	< 0.0001
Combined panel (5 out of 9 miRNAs)						**90.53**	**85.37**	**93.48**	**79.55**	**88.97**	**75.37**	**< 0.0001**
Combined panel (6 out of 9 miRNAs)						86.32	87.8	94.25	73.47	86.76	68.27	< 0.0001

Statistical significance is considered as *P*-value ≤ 0.05. ROC analysis was done on nine statistically significantly candidate miRNAs.

Table 3.11. ROC curve analysis of the investigated biomarkers in discriminating HCC patients from non-HCC individuals [healthy controls, non-cirrhotic and cirrhotic HCV patients]

Target	AUC	SE	*P*-value	95% CI	Cut-off	Sensitivity	Specificity	PPV	NPV	Accuracy	Chi-sq	*P*-value (2 sided)
HCC vs non-HCC												
miR-424	0.761	0.035	< 0.0001	0.7-0.83	27.94	80.77	60.29	43.75	89.13	65.96	25.38	< 0.0001
miR-199a	0.724	0.037	< 0.0001	0.65-0.8	28.77	78.85	58.09	41.84	87.78	63.83	20.56	< 0.0001
miR-142	0.69	0.039	< 0.0001	0.61-0.77	21.81	76.92	58.09	41.24	86.81	63.3	18.46	0.001
miR-215	0.695	0.039	< 0.0001	0.62-0.77	22.14	73.1	55.15	38.38	84.27	60.1	12.02	0.001
miR-224	0.691	0.04	< 0.0001	0.61-0.77	10.32	73.1	54.41	38	84.09	59.57	11.42	0.001
miR-150	0.706	0.041	< 0.0001	0.06-0.08	23.53	71.15	54.41	37.37	83.15	59.04	9.863	0.002
miR-3607	0.664	0.042	0.001	0.58-0.75	5.8	71.15	52.94	36.63	82.76	57.98	8.784	0.003
miR-183	0.664	0.041	< 0.0001	0.59-0.74	18.87	61.54	59.56	36.78	80.2	60.11	6.735	0.009
miR-217	0.581	0.042	0.087 (N.S.)	0.5-0.66								
Combined panel (3 out of 8 miRNAs)						94.23	41.91	38.28	95	56.38	22.61	< 0.0001
Combined panel (4 out of 8 miRNAs)						90.39	53.68	42.73	93.59	63.83	30.08	< 0.0001
Combined panel (5 out of 8 miRNAs)						**80.77**	**61.03**	**44.21**	**89.25**	**66.49**	**26.29**	**< 0.0001**
Combined panel (6 out of 8 miRNAs)						65.39	70.59	45.95	84.21	69.15	20.4	< 0.0001

Statistical significance is considered as *P*-value ≤ 0.05. ROC analysis was done on eight statistically significantly candidate miRNAs
(N.S.) Not significant, indicates absence of statistical significance

Table 3.12. ROC curve analysis of the investigated biomarkers in discriminating HCC (SVR) patients from non-HCC individuals [healthy controls, non-cirrhotic (SVR) and cirrhotic (SVR) HCV patients]

Target	AUC	SE	*P*-value	95% CI	Cut-off	Sensitivity	Specificity	PPV	NPV	Accuracy	Chi-sq	*P*-value (2 sided)
HCC vs non-HCC (SVR groups)												
miR-424	0.8	0.044	< 0.0001	0.72-0.89	24.17	79.17	62.5	32.76	92.86	65.63	13.66	< 0.0001
miR-199a	0.74	0.045	< 0.0001	0.65-0.83	28.8	83.33	64.42	35.09	94.37	67.97	18.01	< 0.0001
miR-142	0.794	0.042	< 0.0001	0.71-0.88	38.56	75	70.19	36.73	92.41	71.1	16.86	< 0.0001
miR-215	0.742	0.045	< 0.0001	0.65-0.83	24.66	75	64.42	32.73	91.78	66.41	12.37	< 0.0001
miR-224	0.703	0.051	0.002	0.6-0.8	11.04	70.83	61.54	29.82	90.14	63.28	8.273	0.004
miR-150	0.735	0.053	< 0.0001	0.63-0.84	23.53	75	59.62	30	91.18	62.5	9.383	0.002
miR-3607	0.763	0.05	< 0.0001	0.67-0.86	8.7	75	66.35	33.96	92	67.97	13.74	< 0.0001
miR-183	0.728	0.048	0.001	0.63-0.82	18.87	62.5	65.38	29.41	88.31	64.84	6.326	0.012
miR-217	0.673	0.052	0.008	0.57-0.78	24.75	75	57.69	29.03	90.91	60.93	8.345	0.004
Combined panel (4 out of 9 miRNAs)						91.67	55.88	32.84	96.61	62.69	17.64	< 0.0001
Combined panel (5 out of 9 miRNAs)						**83.33**	**63.73**	**35.09**	**94.2**	**67.46**	**17.37**	**< 0.0001**
Combined panel (6 out of 9 miRNAs)						66.67	69.9	34.04	90	69.29	11.17	0.001

Statistical significance is considered as *P*-value ≤ 0.05. ROC analysis was done on nine statistically significantly candidate miRNAs.

Table 3.13. ROC curve analysis of the investigated biomarkers in discriminating HCC (treatment naive) patients from non-HCC individuals [healthy controls, non-cirrhotic (treatment naive) and cirrhotic (treatment naive) HCV patients]

Target	AUC	SE	*P*-value	95% CI	Cut-off	Sensitivity	Specificity	PPV	NPV	Accuracy	Chi-sq	*P*-value (2 sided)
HCC vs non-HCC (Naïve group)												
miR-424	0.835	0.039	< 0.0001	0.76-0.91	29.1	85.71	75.34	57.14	93.22	78.22	31.06	< 0.0001
miR-199a	0.821	0.041	< 0.0001	0.74-0.9	22.67	89.29	68.49	52.08	94.34	74.26	27.09	< 0.0001
miR-142	0.737	0.049	< 0.0001	0.64-0.83	12.93	85.71	64.38	48	92.16	70.29	20.32	< 0.0001
miR-215	0.772	0.046	< 0.0001	0.68-0.86	17.09	85.71	63.01	47.06	92	69.31	19.22	< 0.0001
miR-224	0.78	0.046	< 0.0001	0.7-0.87	9.76	82.14	61.64	45.1	90	67.33	15.52	< 0.0001
miR-150	0.791	0.046	< 0.0001	0.7-0.88	11.15	82.14	60.27	44.23	89.8	66.34	14.76	< 0.0001
miR-3607	0.695	0.052	0.002	0.59-0.8	5.09	71.43	61.64	41.67	84.91	64.46	8.876	0.003
miR-183	0.748	0.049	< 0.0001	0.65-0.84	14.5	85.71	64.38	48	92.16	70.3	20.32	< 0.0001
miR-217	0.677	0.052	0.006	0.58-0.78	13.52	75	60.27	42	86.27	64.36	10.07	0.002
Combined panel (4 out of 9 miRNAs)						100	61.64	50	100	72.28	31.13	< 0.0001
Combined panel (5 out of 9 miRNAs)						92.86	66.67	52	96	74	28.57	< 0.0001
Combined panel (6 out of 9 miRNAs)						**89.29**	**72.6**	**55.56**	**94.64**	**77.23**	**31.38**	**< 0.0001**

Statistical significance is considered as *P*-value ≤ 0.05. ROC analysis was done on nine statistically significantly candidate miRNAs

Table 3.14. ROC curve analysis of the investigated biomarkers in discriminating HCC patients from HCV patients

Target	AUC	SE	*P*-value	95% CI	Cut-off	Sensitivity	Specificity	PPV	NPV	Accuracy	Chi-sq	*P*-value (2 sided)
HCC vs HCV (cirrhotic & non-cirrhotic)												
miR-424	0.662	0.046	0.001	0.57-0.75	79.387	63.46	57.89	45.21	74.32	59.86	6.131	0.013
miR-199a	0.618	0.047	0.018	0.53-0.71	38.725	63.46	50.53	41.25	71.64	55.1	2.651	0.103 (N.S)
miR-150	0.61	0.05	0.028	0.51-0.71	45.166	55.77	50.53	38.16	67.61	52.38	0.533	0.465 (N.S)
miR-142	0.568	0.048	0.172 (N.S)	0.47-0.66								
miR-215	0.582	0.048	0.103 (N.S)	0.49-0.68								
miR-224	0.592	0.048	0.066 (N.S)	0.5-0.69								
miR-3607	0.576	0.05	0.129 (N.S)	0.47-0.67								
miR-183	0.538	0.05	0.445 (N.S)	0.44-0.64								
miR-217	0.429	0.049	0.154 (N.S)	0.332-0.525								
AFP	0.688	0.043	< 0.0001	0.60-0.77	6.25	62.32	64.57	48.86	75.93	63.78	13.06	< 0.0001
Combined panel (1 out of 3 miRNAs)						84.62	32.63	40.74	79.49	51	5.128	0.024
Combined panel (2 out of 3 miRNAs)						**61.54**	**56.84**	**43.84**	**72.97**	**58.5**	**4.542**	**0.033**
Combined panel (3 out of 3 miRNAs)						36.54	69.47	39.58	66.67	57.82	0.552	0.457 (N.S)
Combined panel + AFP (2 out of 4 +ve)						76.47	45.74	43.33	78.18	56.55	6.93	0.008
Combined panel + AFP (3 out of 4 +ve)						54.9	67.02	47.46	73.26	62.75	6.585	0.01

Statistical significance is considered as *P*-value ≤ 0.05. ROC analysis was done on only three statistically significant candidate miRNAs.
(N.S) Not significant, indicates absence of statistical significance

Table 3.15. ROC curve analysis of the investigated biomarkers in discriminating HCC (SVR) patients from HCV (SVR) patients

Target	AUC	SE	*P*-value	95% CI	Cut-off	Sensitivity	Specificity	PPV	NPV	Accuracy	Chi-sq	*P*-value (2 sided)
HCC vs HCV (cirrhotic & non-cirrhotic) (SVR)												
miR-424	0.679	0.065	0.01	0.55-0.81	79.387	66.67	60.32	39.02	82.61	62.07	5.08	0.024
miR-142	0.665	0.063	0.018	0.54-0.79	112.42	66.67	69.84	45.71	84.62	68.97	9.63	0.002
miR-3607	0.672	0.067	0.014	0.54-0.8	9.3248	70.83	53.97	36.96	82.93	58.62	4.29	0.038
miR-199a	0.594	0.064	0.177 (N.S)	0.47-0.72								
miR-215	0.599	0.066	0.157 (N.S)	0.47-0.72								
miR-224	0.566	0.07	0.34 (N.S)	0.44-0.7								
miR-150	0.608	0.069	0.119 (N.S)	0.47-0.75								
miR-183	0.57	0.069	0.314 (N.S)	0.44-0.71								
miR-217	0.494	0.069	0.932 (N.S)	0.36-0.63								
AFP	0.615	0.059	0.047	0.5-0.73	6.05	51.43	60.67	33.96	76.06	58.06	1.50	0.22 (N.S)
Combined panel (1 out of 3 miRNAs)						91.67	33.33	34.38	91.3	49.43	5.59	0.018
Combined panel (2 out of 3 miRNAs)						**70.83**	**61.9**	**41.46**	**84.78**	**64.37**	**7.48**	**0.006**
Combined panel (3 out of 3 miRNAs)						41.667	88.89	58.82	80	75.86	10.32	0.001
Combined panel + AFP (2 out of 4 +ve)						79.167	47.62	36.54	85.71	56.32	5.19	0.023
Combined panel + AFP (3 out of 4 +ve)						54.167	80.95	52	82.26	73.56	10.47	0.001

Statistical significance is considered as *P*-value ≤ 0.05. ROC analysis was done on only three statistically significant candidate miRNAs
(N.S) Not significant, indicates absence of statistical significance miRNAs.

Table 3.16. Correlation between the target miRNAs in the study groups

miRNAs		miR-142-fold change	miR-150-fold change	miR-183-fold change	miR-199a-fold change	miR-215-fold change	miR-217-fold change	miR-224-fold change	miR-424-fold change	miR-3607-fold change
miR-142-fold change	rho	1.000	0.619	0.403	0.624	0.371	0.350	0.579	0.651	0.359
	P-value		< 0.0001	< 0.0001	< 0.0001	< 0.0001	< 0.0001	< 0.0001	< 0.0001	< 0.0001
miR-150-fold change	rho	0.619	1.000	0.378	0.656	0.409	0.315	0.767	0.774	0.420
	P-value	< 0.0001		< 0.0001	< 0.0001	< 0.0001	< 0.0001	< 0.0001	< 0.0001	< 0.0001
miR-183-fold change	rho	0.403	0.378	1.000	0.617	0.707	0.725	0.439	0.495	0.497
	P-value	< 0.0001	< 0.0001		< 0.0001	< 0.0001	< 0.0001	< 0.0001	< 0.0001	< 0.0001
miR-199a-fold change	rho	0.624	0.656	0.617	1.000	0.659	0.541	0.727	0.828	0.581
	P-value	< 0.0001	< 0.0001	< 0.0001		< 0.0001	< 0.0001	< 0.0001	< 0.0001	< 0.0001
miR-215-fold change	rho	0.371	0.409	0.707	0.659	1.000	0.681	0.527	0.582	0.621
	P-value	< 0.0001	< 0.0001	< 0.0001	< 0.0001		< 0.0001	< 0.0001	< 0.0001	< 0.0001
miR-217-fold change	rho	0.350	0.315	0.725	0.541	0.681	1.000	0.339	0.441	0.503
	P-value	< 0.0001	< 0.0001	< 0.0001	< 0.0001	< 0.0001		< 0.0001	< 0.0001	< 0.0001
miR-224-fold change	rho	0.579	0.767	0.439	0.727	0.527	0.339	1.000	0.769	0.569
	P-value	< 0.0001	< 0.0001	< 0.0001	< 0.0001	< 0.0001	< 0.0001		< 0.0001	< 0.0001
miR-424-fold change	rho	0.651	0.774	0.495	0.828	0.582	0.441	0.769	1.000	0.545
	P-value	< 0.0001	< 0.0001	< 0.0001	< 0.0001	< 0.0001	< 0.0001	< 0.0001		< 0.0001
miR-3607-fold change	rho	0.359	0.420	0.497	0.581	0.621	0.503	0.569	0.545	1.000
	P-value	< 0.0001	< 0.0001	< 0.0001	< 0.0001	< 0.0001	< 0.0001	< 0.0001	< 0.0001	

Association between miRNAs expression was determined using Spearman's correlation. Rho: Spearman's rho coefficient. Correlation is significant as *P*-value ≤ 0.01 (two-tailed).

Table 3.17. Correlation between clinicopathological factors and the target miRNAs

Factor		miR-142-fold change	miR-150-fold change	miR-183-fold change	miR-199a-fold change	miR-215-fold change	miR-217-fold change	miR-224-fold change	miR-424-fold change	miR-3607-fold change
Age	rho	0.021	0.049	.206**	.160*	.170*	0.081	0.082	0.127	-0.047
	P-value	0.781	0.527	0.007	0.037	0.026	0.291	0.285	0.098	0.538
Gender	rho	.153*	0.103	.168*	0.074	0.084	.251**	0.046	0.056	0.055
	P-value	0.036	0.159	0.021	0.315	0.252	0.001	0.530	0.442	0.450
Cirrhosis	rho	.472**	.385**	.485**	.532**	.418**	.360**	.424**	.535**	.278**
	P-value	<0.0001	<0.0001	<0.0001	<0.0001	<0.0001	<0.0001	<0.0001	<0.000	<0.0001
ALT	rho	.452**	.402**	.404**	.481**	.422**	.322**	.483**	.511**	.268**
	P-value	<0.0001	<0.0001	<0.0001	<0.0001	<0.0001	<0.0001	<0.0001	<0.0001	<0.0001
AST	rho	.379**	.299**	.323**	.402**	.356**	.244**	.387**	.416**	.202**
	P-value	<0.0001	<0.0001	<0.0001	<0.0001	<0.0001	<0.0001	<0.0001	<0.0001	<0.0001
AFP	rho	0.131	-0.067	0.081	.170*	0.082	-0.046	0.082	0.127	0.090
	P-value	0.117	0.420	0.332	0.040	0.324	0.583	0.328	0.128	0.281
T. Bil	rho	-0.064	-.219**	-0.008	-0.006	-0.005	-0.139	-0.057	-0.059	-0.139
	P-value	0.392	0.003	0.915	0.930	0.945	0.060	0.443	0.427	0.059
D. Bil	rho	.293**	.179*	.423**	.364**	.423**	.389**	.312**	.353**	.284**
	P-value	<0.0001	0.015	<0.0001	<0.0001	<0.0001	<0.0001	<0.0001	<0.0001	<0.0001
Albumin	rho	-.211**	-0.071	-.229**	-.258**	-.266**	-.159*	-.195**	-.265**	-0.132
	P-value	0.004	0.339	0.002	<0.0001	<0.0001	0.031	0.008	<0.0001	0.074
CTP score	rho	-0.037	-.259**	0.154	0.055	0.123	.231*	-0.057	0.045	.214*
	P-value	0.715	0.009	0.124	0.587	0.219	0.020	0.570	0.658	0.032
BCLC	rho	-0.295	-0.110	-0.035	0.136	0.168	-0.042	-0.210	-0.115	-0.056
	P-value	0.065	0.500	0.829	0.404	0.301	0.798	0.194	0.481	0.730

Association between miRNAs expression and the clinicopathological factors was determined using Spearman's correlation. Rho: Spearman's rho coefficient. * Correlation is significant as *P*-value ≤ 0.05 (two-tailed), ** correlation is significant as *P*-value ≤ 0.01 (two-tailed).

4. CHAPTER 4: DISCUSSION

HCC is rated as one of the widely spread and highly aggressive malignancies worldwide, that represents more than 80% of primary liver cancers [369]. HCV virus plays major role in the in hepatic carcinogenicity [370] that computes around 25% of the global HCC cases [371]. Generally, the poor prognosis nature of HCC greatly affects the overall patients' survival rates and drives the global attention for the determination of new biomarkers that aid in the disease's early detection [372]. Thus, the aim of this research study was to specify miRNA panel to serve as a non-invasive biomarker for prediction of HCC in chronic HCV patients.

In the current study, patients' inclusion criteria relied on current or previous HCV infection, because the hazardous probability of HCC development remains elevated even after achievement of SVR, especially in the presence of other co-morbid conditions as diabetes mellitus [373, 374]. HCC incidence could be manifested up to 5 to 10 years after viral clearance [375, 376]. The choice of the healthy control group was sex matched with the HCC group ($P = 0.5294$), as HCC is a male predominant disease [377], and both HCV groups were sex matched ($P = 0.1508$). Also, inclusion of study subjects in the control groups was aged matched to the cirrhotic and HCC groups ($P = 0.0662$); excluding the non-cirrhotic group, since the risk of cirrhosis and HCC shows exponential increments with age [378].

The results obtained from our bioinformatics analysis highlighted four overlapping miRNAs sharing the same expression patterns between the GEO microarray and TCGA datasets. MiR-224 was upregulated, while miR-150, miR-199b and miR-424 were downregulated in liver tissues. In addition to these 4 non-coding RNAs, analysis of TGCA datasets resulted in 5 DE-miRNAs; 2 upregulated miRNAs (miR-183 and miR-217) and 3 downregulated miRNAs (miR-142, miR-215, and miR-3607) in HCC liver tissues. The 9 candidate miRNAs obtained from TCGA dataset analysis were chosen for further validation of their serum expression using qPCR. Similar results were obtained by a previously published study, through analyzing a GEO microarray dataset. They identified 13 DE-miRNAs in liver tissues, in which 2 folds increased in miR-224 expression, and 2 folds decrease in miR-150 and miR-199a-3p expression in HCC tissues were reported [379]. However, analysis of TGCA datasets was also a beneficial approach in several studies to compare significant miRNAs expression in HCC from different etiologies. Analysis of tissue biopsies

isolated from 48 HCC patients including tumor tissues and surrounding non-tumor tissues, in addition to 302 HCC patients' tumorous tissues was performed in a previous study. The analysis resulted in 33 DE-miRNAs in HCC, 5 were upregulated including miR-183, and 28 miRNAs were downregulated, including miR-199b, miR-424, miR-150 and miR-142, which was also consistent with our TCGA results. Down regulation of miR-424 and miR-3607 were validated via qPCR, and the importance of miR-424 was highlighted due to the significant downregulation of this miRNA in all HCC types among the different etiologies [380].

Previous tissue expression research studies reported downregulation of miR-142 [380–382], miR-150 [383, 384], miR-199a [385], miR-215 [386], miR-424 [387] and miR-3607 [388] in the liver tumor cells relative to non-tumor adjacent tissues, which were comparable to our bioinformatic analysis results. Such downregulation is associated with poor disease's clinicopathological features and bad prognosis. The major mechanism through which these miRNAs control liver carcinogenesis is the regulation of invasion and migration of HCC cells, resulting in stimulation of EMT and consequently metastasis occurs. A previously published study suggested tumor suppressor ability of miR-142-3p, via direct gene expression regulation, to high mobility group box protein 1 (HMGB1); an oncogene that stimulates metastasis in HCC cells [389]. Upregulation of miR-142 prohibits cell proliferation, migration, invasion, and EMT [390, 391]. MiR-150 is also downregulated in metastatic cancer relative to primary liver cancer, which was confirmed by stimulation of cellular proliferation, migration and invasion upon miR-150 inhibition, suggesting an important role of miR-150 in HCC metastasis [392, 393]. Moreover, analysis to the downregulation mechanisms revealed targeting of miR-199a to the tumor promotor protein activated kinase 4 (PAK4), which regulates cell adhesion, migration, survival and proliferation. Thus, inhibition of HCC progression is achieved via inhibition of PAK4/Raf/MEK/ERK pathway [394]. Moreover, EMT features of HCC are regulated by Notch1 activation which influences E-cadherin expression [395]. A negative correlation was explained between miRNA-199a expression and Notch1 or E-cadherin levels in HCC patients. MiR-199a-5p and 3p were proved to regulate E-cadherin expression by targeting Notch1. However, on post-transcriptional level, miR-199-a/b-5p inhibits Rho-associated coiled-coil kinase 1 (ROCK1), resulting in repression of ROCK1/MLC and PI3K/Akt signaling pathways, which are essential for HCC proliferation and metastasis. Consequently, miR-199a/b can strongly influence HCC

aggressiveness by playing an important role as a tumor suppressor in HCC, which might provide potential therapeutic option in HCC treatment [396]. Upregulation of miR-424 in HCC cells results in suppression of invasion and proliferation in-vitro and restraining tumor growth in-vivo, suggesting a tumor suppressor role for miR-424 [380, 397, 398]. This role was explained via suppression of c-Myb proto-oncogene [387] or through modulation of Tripartite motif-containing 29; which is linked to HCC cell invasion and proliferation [399]. As for miR-3607, this novel non-coding RNA that hasn't been hugely investigate in HCC. Few studies concluded downregulation of miR-3607 in HCC tissues relative to normal cells. MiR-3607 decreased expression was linked to poor outcomes in HCC patients and was linked to patient's tumor size and HCC TNM stage [400]. A recently published study addressed the inhibitory effect of miR-3607 on the growth, colony formation, invasion and migration of HCC cells. Multiple miR-3607 target genes were proposed to demonstrate the inhibition to the EMT process, either by targeting mini-chromosome maintenance (MCM5) gene [388], or through suppressing X-linked inhibitor of apoptosis [401]. The tumor suppressor effects in the previously mentioned pathways suggested potential prognostic role of miR-142, miR-150, miR-199a, miR-424 and miR-3607 in HCC.

Furthermore, another mechanism by which these downregulated miRNAs antagonize HCC progression is through blockage of certain pathways involved in the cell cycle process. It was reported that overexpression of miR-150 promotes cell cycle arrest and apoptosis, and that this non-coding RNA might be required in the self-renewal mechanism of the liver cancer stem cells via regulation of c-Myb transcription factor [402]. Whereas, miR-199a was found to inhibit cell cycle arrest in G2/M stage [394, 396]. However, in a recently published study, the importance of cell division cycle 6 as one of the potential genes involved in cancer process was highlighted [403]. They revealed the mechanism by which cell division cycle 6 enhances the cell proliferation via controlling G1 phase checkpoint. This mechanism is negatively regulated by miR-215, thus inhibits HCC proliferation. Additionally, the inhibitory effect of miR-424-5p on HCC cell proliferation was explained in another study via targeting E2F7 transcription factor; which is involved in angiogenesis, thus inhibition of G0/G1 phase of the cell cycle occurs [404]. Another approach for miR-424 downregulation is through inhibition of retinoblastoma tumor suppressor protein (pRb) and E2F transcription factor via pRb-E2F pathway, and that miR-424 inhibits proliferation of HCC cells via modulating Akt3 and E2F3 [405]. Besides, the expression

of miR-424 in HCC patients after liver transplantation, was measured and it was found that patients with lower miR-424 levels displayed earlier HCC recurrence, suggesting that miR-424 might provide a prediction tool for tumor recurrence [406]

Moreover, several research studies identified alternative mechanisms for the regulation of HCC development. MiR-215 downregulation in HCC tissues was found to target Wnt/ β-catenin cascade proteins (β-catenin, APC and c-myc), and that the expression of this miRNA was correlated with the liver disease stage [386]. Similarly, another study highlighted the miR-215 downregulation in HCC via targeting cyclin-dependent kinases 13 in an inversely proportional correlation [407]. While miR-142-3p overexpression was demonstrated to inhibit aerobic glycolysis by targeting lactate dehydrogenase, which subsequently affects HCC cells proliferation [408]

On the contrary, upregulation of miR-183 [409], miR-217 [410, 411] and miR-224 [281, 379] was predominant in HCC tumor tissues compared to healthy controls, chronic hepatitis (HBV or HCV), liver cirrhosis and adjacent non-tumor tissues, proposing that such increased expressions might be attributed to the onset of cancer. Previous studies suggested an oncogenic role for miR-183 in HCC either through suppression of apoptosis by inhibition of programmed cell death protein 4 (PCDC4) or via reduction in the expression of AKAP12 in the hepatic carcinogenic cells, which is known by its tumor suppressor activity [409, 412–414]. Generally, upregulation of miR-183 might be related to HCC onset and progression, although it won't affect overall patients' survival. While knockdown of miR-183-5p results in significant inhibition in survival, proliferation, migration and invasion in HCC cell lines via deactivation of Wnt/β-catenin signaling pathway [415, 416]. Similarly, activation of Wnt signaling pathway was a suggested mechanism for miR-217 upregulation in the tissues [417]. Moreover, a previously published study identified miRNAs panel associated with HCC recurrence, they claimed increased expression of miR-216a/217 cluster in HCC tissue specimens. This was correlated with early tumor recurrence, decreased overall survival, in addition to activation of EMT. MiR-216a/217 cluster increased expression in HCC cell lines resulted in increased cell migration and metastasis [418].

Besides, miR-224 tissue upregulation was heavily studied in HCC. MiR-224 expression is strongly linked to the activation of the protein coding gene phosphorylated serine/threonine protein kinase (pAKT). Increased levels of both miR-224 and pAKT in the HCC cells are

significantly correlated with serum AFP levels, tumor stage and tumor grade [419]. It was also observed that upregulated miR-224 and pAKT protein can induce HCC progression and worsen patient's overall survival rates. Thus miR-224 might act as predicator of HCC poor prognosis [420, 421]. Furthermore, a recently published study highlighted the role of cytoplasmic polyadenylation element-binding protein 3 (CPEB3) as a new target for miR-224 in HCC progression. They reported that CPEB3 is negatively regulated by miR-224, and they highlighted the negative correlation between their expressions in HCC cells. Their data also showed inhibition of proliferation and motility of SMMC-7721 cancer cell; with increased expression miR-224, upon the increase of CPEB3 expression. In addition to enhancement of motility and proliferation of HuH-7 cells; with downregulated miR-224, upon knocking-down CPEB3. These results suggested that the mechanism through which miR-224 enhances HCC proliferation and motility is by targeting CPEB3 protein [422].

Real time PCR results in our study showed highly significant increase in serum concentration of the nine-candidate miRNA in HCC patients relative to healthy individuals ($P < 0.0001$). Similarly, the expressions of all targets were significantly increased in HCV patients' serum ($P < 0.0001$) compared to healthy subjects. However, the expression levels of miR-424, miR-199a, miR-142, and miR-224 were significantly altered in HCC patients upon comparison with the non-cirrhotic subjects ($P < 0.0001$, $P = 0.0001$, $P = 0.023$, and $P = 0.027$ respectively). While miR-199a and miR-183 showed differential expression in HCV cirrhotic patients relative to non-cirrhotic ones ($P = 0.012$ and $P = 0.036$ respectively). The only target that showed significant alteration between HCV patients with LC and HCC patients was miR-424 ($P = 0.05$). To the best of our knowledge, this research is the first to report circulatory differential expression of miR-142, miR-217 and miR-3607 in serum of HCV and HCC patients. In a previous study, miR-142-5p Serum levels were reported to be inversely correlated with the albumin concentrations in serum of HCV HCC patients, although the differential expression wasn't reported [423]. It is worth mentioning that 20% of our qPCR signals in serum miR-217 amplification were undetectable. Thus, these samples were normalized by replacing their Ct values by the maximum allowed number of cycles = 40 [366], in order to avoid losing a significant number of samples that showed true amplification with other targets in the data analysis and to have a consistent samples number for all miRNAs. Therefore, based on the scarce data on circulatory miR-217 expression in

literature, and on our findings, we suggest that miR-217 serum differential expression might not affect the regulation of HCC progression.

Serum expression of miR-183, miR-215 and miR-224 were previously studied in HCC and the results were consistent with our findings. Several research studies reported a significant increase in miR-183 concentration in the serum of cirrhotic and HCC patients relative to healthy individuals. They also concluded that the sensitivity and specificity of using miR-183 as a biomarker for HCC detection were 57.9% and 76.2% in serum respectively, proposing a diagnostic potential of miR-183 in differentiating HCC patients from those with liver cirrhosis without malignancy with high sensitivity and specificity [424, 425]. Additionally, serum miR-183 level in HCC patients after surgery was significantly lower compared to the expression before surgery [321], confirming that the increase in miR-183 serum levels is positively correlated with the presence of HCC FLs. Furthermore, elevated serum expression levels of miR-224 were explained in several studies [426–428]. Serum miR-224 level was reported to be corelated with AFP levels and with other serum parameters indicating liver damage, also it has been correlated with poor survival. MiR-224 increased serum expression was also correlated with the BCLC stage progression. Higher miR-224 expression was recorded in patients with BCLC stage C compared to stage B. Therefore, miR-224 concentration could be BCLC stage dependent, beside possessing prognostic biomarker ability in HCC patients' survival [429, 430]. In a previously published study conducted on the Egyptian population, overexpression of miR-224 and miR-215 in serum of HCV HCC Egyptian patients relative to healthy individuals was detected using qPCR [431, 432]. Although the increase in miR-215 serum levels failed to distinguish between HCV, HBV and HCC patients, as its expression was significantly increased in all groups relative to healthy controls [433]. However, multiple recent studies relied on the serum miR-215 expression levels to differentiation between patients with CHC infection or fibrosis and those with LC, and between HCC patients and other hepatic disease patients. It was also noticed that miR-215 level was positively correlated with HCV viral load [434, 435] suggesting that miR-215 might act as prognostic biomarker for liver disease. On the other hand, only one study reported downregulation of miR-215 in serum exosomes by 8.4 folds relative to liver cirrhosis [436].

Furthermore, contradicting results in literature were obtained after addressing the serum expression of miR-150, miR-199a and miR-424 in HCC. In a previously published study, the

increase in miR-150 serum levels in HCV HCC patients in African Americans and Caucasians relative to healthy controls were comparable to our findings. Also, a significant increase in the serum levels was recorded in HCV cirrhotic groups relative to healthy subjects in both ethnic groups [437]. However, analysis of miR-150 serum expression in HCV HCC Egyptian patients in a different study recorded a significant decrease in miR-150 expression levels in serum of HCC patients relative to healthy individuals and to non-cirrhotic HCV patients, and no significant difference was found between HCC and cirrhotic HCV patients. Moreover, the expression levels decreased in HCV cirrhotic patients relative to non-cirrhotic individuals. These results opposed our findings, as miR-150 serum expression was significantly higher in HCC group relative to controls, non-cirrhotic and cirrhotic subjects. Whereas, no significant difference was observed neither between non-cirrhotic and cirrhotic patients or between cirrhotic and HCC individuals [438]. Although few published studies addressed the regulation of miR-424 serum expression in HCC, their results were contradicting. Significant increase in serum miR-424-3p levels in HCC patients relative to healthy control was reported in a previous study [439]. Although, analysis of the miR-424 serum expression using qPCR showed that its expression was reduced in HCC patients relative to healthy individuals. The decreased expression was also correlated with serum AFP levels, with vein invasion and with the progression of the TNM [440]. Interestingly, qPCR results in a previously published research failed to have a significant difference in serum miR-424 levels in HCC patients relative to healthy controls [441].

As for miR-199a, multiple research studies performed on Egyptian patients concluded serum miR-199a overexpression in severe chronic hepatic inflammation and in HCV genotype 4 patients, especially in late-stage fibrosis compared to early fibrotic stages. This could be explained by the induced inflammation triggered by HCV to the hepatocytes, concluding that members of miR-199 family are linked to liver fibrosis progression in HCV patients [396, 432, 442]. On the other hand, other studies reported a reduction in miR-199a expression in the serum of HCC patients [416, 422, 424]. It was observed that the decrease in miR-199a serum expression was inversely proportional to apoptotic markers such as programmed cell death protein 4 and cytochrome C [443]. Additionally, the antiviral activity of miR-199a against HCV was proved, and the mechanism of inhibition is attributed to the interaction between miR-199a and the step loop II region at the 5’-UTR of HCV, resulting in inhibition of HCV replication. Thus, based on

their findings, increased expression of miR-199a was associated with cell cycle arrest, suppression of cellular invasion, improves sensitivity to chemotherapy, and hindering HCV genome replication [444–446]. Therefore, we suggest further analysis to the differential expression miR-150, miR-424 and miR-199a serum levels in HCV and HCC patients. A summary of the previously published research studies that have addressed the differential expression of the candidate miRNAs in the liver tissues and circulation is presented in table 4.1.

Besides the proposed role of the miRNAs panel in HCC, evidences on the engagement of these candidate targets in other liver disorders and different cancer types were also highlighted (table 4.2). Dysregulation in circulating miR-142 and miR-150 level were recorded in intrahepatic cholangiocarcinoma [447, 448]. Also, miR-142 serum expression and miR-150 serum exosome levels were significantly lower in colorectal cancer patients [423, 449–451]. Other studies highlighted the role of serum miR-217 in the pathogenesis of colorectal cancer [452, 453] Whereas, miR-3607 played important function in the regulation of DNA repair mechanisms and possessed inhibitory effect on colorectal cancer tumorigenesis [454] and pancreatic cancer development [455]. Deregulation in serum miR-217 levels were also involved in pancreatic cancer pathogenesis [456]. Multiple miRNAs were suggested to affect the incidence and development of gastric cancer, including miR-142 [457], miR-215 [458] and miR-217 [459]. Furthermore, breast cancer was considered to be highly influenced by alteration in circulatory miRNAs expression, such as miR-142 [460], miR-215 [461, 462] and mir-3607 [463, 464]. Generally, these targets might act as potential HCC specific biomarker, in addition to being common tumor markers for the other cancers. Therefore, further research is required to explore the exact role and suggested pathways through which these miRNAs regulate HCC progression.

The polygenic nature of HCC and the complexity of serum as a detection platform favored the use of multiple biomarkers approach over a single one [465]. In the current study, we proposed a novel miRNAs study panel that could play a pivotal role in HCC detection. A combined panel of 5 miRNAs dramatically increased the sensitivity and specificity of recognizing HCC patients from healthy individuals to 100% and 95.12% respectively, with 97.85% detection accuracy. A similar trend was obtained in identifying HCV patients to reach 90.5% sensitivity, 85.37% specificity and 89% accuracy upon relying on a 5-miRNAs-combined panel. The success chance of using multiple miRNAs in a single panel was manifested in distinguishing HCC patients from

non-HCC individuals in both the SVR and the treatment naïve groups. A combined 5 miRNAs panel enhanced the sensitivity and specificity of detection to 83.3% and 63.73% respectively in the SVR groups. Whereas 6 miRNAs-combined panel provided better results in the treatment naïve patients (89.3% sensitivity and 72.6% specificity). Moreover, the combined panel was used successfully used to assess the accuracy of distinguishing HCC from HCV patients. Only three (miRNAs 424, miR-199a and miR-150) showed statistically significant AUC after constructing the ROC curve. A combined panel of 2 miRNAs didn't provide an improvement in the detection sensitivity and specificity (61.54% and 56.84%) compared to AFP (62.3% and 64.57%). However, in the comparison of HCV and HCC patients belonging to the SVR groups, the AUC of miR-424, miR-142 and miR-3607 were statistically significant. Interestingly, 2-miRNAs combined panel ameliorated the sensitivity and specificity in the SVR group to 70.8% and 61.9% respectively, in comparison to AFP results (51.43% and 60.67% respectively). Nevertheless, the inclusion of AFP to the miRNAs combined panel improved the sensitivity of detection to 76.47% and 79.17% in HCC (SVR and treatment naïve) and HCC-SVR patients respectively, but it decreased the detection specificity in both groups to 45.74% and 47.62% respectively.

Finally, we believe that the choice of the candidate miRNAs within the panel provided a multifunctional tool for HCC early detection. The panel is composed of miR-199a, which could act as a marker for liver fibrosis progression, while miR-183 might be linked to HCC onset and progression. However, predication for HCC poor prognosis could be achieved via miR-224, whereas, miR-424 might provide a prediction tool for tumor recurrence, suggesting potential prognostic biomarker ability for both miRNAs. Moreover, the inclusion of miR-142 and miR-150 might provide information about the fibrosis and cirrhosis progression in HCV patients. Thus, the use of the miRNAs combined panel will facilitate and improve HCC diagnosis than conventional single biomarker approach.

Table 4.1. Dysregulated tissue and circulating miRNAs' expression in HCC

Target	Clinical sample	Expression	Population	Role as biomarker	Diagnosis	Reference
miR-142	Tissue	Decrease	NA	Diagnostic in HCC	HCC	[389]
	Tissue	Decrease	Chinese	Prognostic in HCC	HCC	[408]
	Tissue	Decrease	Chinese	Prognostic in HCC	HCC	[391]
	Tissue	Decrease	Chinese	NA	HCC	[381]
	Tissue	Decrease	NA	Diagnostic in HCC	HCC	[382]
	Plasma	Increase	Indian	Diagnostic in HCC	HBV-HCC	[466]
	Tissue	Decrease	American	Diagnostic in HCC	HCC	[380]
	Tissue	NA	Hong Kong	Prognostic in HCC	HCC	[390]
	Tissue	Increase	Egyptian	Diagnostic in HCC	HCV-HCC	[423]
	Cancer stem cells	Decrease	NA	NA	HCC	[467]
miR-150	Serum	Decrease	Egyptian	Diagnostic for HCC, prognostic for cirrhosis	HCV-HCC	[438]
	Tissue	Decrease	NA	Diagnostic for HCC, prognostic for cirrhosis	HBV-HCC	[468]
	Tissue	Decrease	Chinese	NA	HCC	[393]
	Tissue	Decrease	Chinese	NA	HCC	[392]
	Tissue	Decrease	Chinese	NA	HBV-HCC	[437]
	Tissue	Decrease	Chinese	Diagnostic and prognostic in HCC	HCC	[469]
	Serum	Decrease	Chinese	Diagnostic and prognostic in HCC	HBV-HCC	[470]
	Tissue	Decrease	NA	Prognostic in HCC	HCC	[384]
	Tissue / Cancer stem cells	Decrease	Chinese	NA	HBV-HCC	[402]
	Serum	Increase	African Americans and Caucasians	Diagnostic and prognostic in HCC	HCV-HCC	[437]
	Tissue	Decrease	Chinese	Prognostic in HCC	HCC	[471]
	Tissue	Decrease	NA	NA	HCC	[472]

miR-183	Tissue	Increase	Egyptian	Diagnostic in HCC	HCV-HCC	[423]
	Tissue / serum	Increase	Chinese	Diagnostic and prognostic in HCC	HCV and HBV-HCC	[409]
	Serum	Increase	New Delhi	Diagnostic and prognostic in HCC	HCC	[425]
	Tissue	Decrease	Chinese	Prognostic in HCC	HCV and HBV-HCC	[473]
	Tissue / serum	Increase	Chinese	NA	HBV-HCC	[321]
	Tissue	Increase	German	NA	HCV and HBV-HCC	[474]
	Tissue	Increase	NA	Diagnostic in HCC	HCC	[475]
	Tissue	Increase	Chinese	NA	HBV-HCC	[412]
	Tissue	Increase	NA	NA	HCC	[412]
	Tissue	Increase	Hong Kong	Prognostic in HCC	HBV-HCC	[415]
	Tissue	Increase	German	Diagnostic and prognostic in HCC	HCV and HBV-HCC	[415]
	Tissue	Increase	Chinese	Diagnostic and prognostic in HCC	HCC	[416]
	Tissue	Increase	Chinese	Prognostic in HCC	HBV-HCC / others	[413]
	Serum / plasma	Increase	Chinese	Diagnostic in HCC	HCC	[424]
miR-199a	Tissue	Increase	Egyptian	Diagnostic for HCC, prognostic for fibrosis	HCV-HCC	[423]
	Tissue	Decrease	Japanese	Prognostic for fibrosis	HCV	[476]
	Tissue	Decrease	NA	NA	HBV-HCC	[379]
	Tissue	Decrease	Chinese	Prognostic in HCC	HBV-HCC	[477]
	Serum	Decrease	American	NA	HCV-HCC	[478]
	Tissue	Decrease	Chinese	NA	HCC	[479]
	Serum	Decrease	Egyptian	Diagnostic in HCC	HCV and HBV-HCC	[443]
	Tissue	Decrease	Chinese	Diagnostic in HCC	HCC	[396]
	Tissue	Increase	Egyptian	Prognostic for fibrosis	HCC	[480]
	Tissue	Increase	Japanese	Prognostic for fibrosis	HCV	[481]
	Serum	Increase	Egyptian	Prognostic for fibrosis	HCV	[442]
	Serum	Decrease	NA	Diagnostic and prognostic in HCC	HCC	[482]
	Serum	Decrease	Chinese	Diagnostic in HCC	HCV / other etiologies	[483]
	Serum	Decrease	Egyptian	Diagnostic in HCC	HCV-HCC	[484]

	Tissue	Decrease	Japanese	Diagnostic in HCC	HCV and HBV-HCC	[281]
miR-215	Plasma	Decrease	Egyptian	Diagnostic and prognostic in HCC	HCC	[407]
	Serum	Increase	Egyptian	Diagnostic and prognostic in HCC	HCV-HCC	[431]
	Serum	Increase	Egyptian	Diagnostic and prognostic in HCC	HCV-HCC	[432]
	Plasma	Decrease	Egyptian	Diagnostic and prognostic in HCC	HCV-HCC	[485]
	Serum	Increase	Chinese	Diagnostic in HCC	HCV and HBV-HCC	[433]
	Tissue	Decrease	Egyptian	Prognostic in HCC	HCV / other etiologies	[386]
	Serum	Increase	Brazilian	Prognostic for fibrosis	HCV	[435]
	Serum	Increase	Chinese	NA	HCV-HCC	[426]
	Serum	Increase	Egyptian	Diagnostic and prognostic in CHC	HCV-HCC	[434]
miR-217	Tissue	Decrease	Chinese	Diagnostic in HCC	HCC	[486]
	Tissue	Decrease	Chinese	NA	HCC	[487]
	Tissue	Increase	Chinese	NA	HCC	[417]
	Tissue	Decrease	NA	Prognostic in HCC	HCC	[488]
	Tissue	Increase	Chinese	NA	HBV-HCC	[489]
	Tissue	Decrease	Chinese	NA	HCC	[490]
	Tissue	Increase	Chinese	NA	HBV-HCC	[410]
	Tissue	Increase	NA	Prognostic in HCC	HCC	[331]
miR-224	Tissue	Increase	NA	Diagnostic in HCC	HCV, HBV-HCC	[379]
	Tissue	Increase	French	NA	HBV-HCC / others	[411]
	Tissue	Increase	Japanese	Diagnostic in HCC	HCV, HBV-HCC	[281]
	Serum	Increase	Egyptian	Diagnostic and prognostic in HCC	HCV-HCC	[432]
	Serum	Increase	Chinese	Prognostic in HCC	HBV-HCC	[429]
	Plasma	Increase	Egyptian	Diagnostic in HCC	HCV-HCC	[491]
	Serum	Increase	Korean	NA	HCC	[428]
	Serum	Increase	Chinese	NA	HBV-HCC	[426]
	Serum	Increase	NA	Diagnostic in HCC	HCV-HCC	[427]
	Tissue	Increase	Chinese	Diagnostic and prognostic in HCC	HCC	[419]

	Serum	Decrease	Chinese	Diagnostic in HCC	HBV-HCC / others	[492]
mir-424	Tissue	Decrease	American	Diagnostic in HCC	HCC	[493]
	Serum	Decrease	Chinese	Diagnostic in HCC	HCC	[440]
	Serum	Decrease	Chinese	Prognostic in HCC	HCC	[494]
	Tissue	Decrease	Chinese	Prognostic in HCC	HCC	[398]
	Tissue	Decrease	Chinese	NA	HCC	[397]
	Tissue	Decrease	Chinese	Prognostic in HCC	HCC	[399]
	Tissue	Decrease	Chinese	Prognostic in HCC	HBV-HCC	[406]
	Tissue	Decrease	Chinese	Prognostic in HCC	HBV-HCC / others	[405]
	Tissue	Decrease	Chinese	Prognostic in HCC	HCC	[387]
	Serum	Increase	Chinese	Diagnostic in HCV	HCV	[439]
miR-3607	Tissue	Decrease	NA	Prognostic in HCC	HCC	[388]
	Tissue	Decrease	Chinese	Prognostic in HCC	HCC	[400]
	Tissue	Decrease	NA	NA	HCC	[401]

NA: Data not available

Table 4.2. Dysregulation of the target miRNAs in different cancers

Target	Disease / Cancer type	Clinical sample	Expression	Reference
miR-142	Colorectal cancer	Serum	Decrease	[449]
miR-142	Breast cancer	Serum	Decrease	[460]
miR-142	Colorectal cancer	Cell line	Decrease	[495]
miR-142	Breast cancer	Cell line	Decrease	[496]
miR-150	Colorectal cancer	Cell line	Decrease	[497, 498]
miR-150	Breast cancer	Serum	Decrease	[460]
miR-150	Intrahepatic cholangiocarcinoma	Serum	Decrease	[447]
miR-150	Intrahepatic cholangiocarcinoma	Serum	Increase	[448]
miR-150	Post-acute myocardial infarction heart failure	Serum	Decrease	[450]
miR-150	Colorectal cancer	Exosomes	Decrease	[451]
miR-183	Colorectal cancer	Exosomes	Increase	[499]
miR-183	Colorectal cancer	Cell line	Increase	[500]
miR-183	cerebral ischemia	Animal model	Decrease	[501]
miR-183	Skin cancer	Cell line	Decrease	[502]
miR-183	Ovarian cancer	Cell line	Increase	[503]
miR-199a	Lung cancer	Tissues	Decrease	[504, 505]
miR-199a	Glioblastoma	Cell line	Increase	[506]
miR-199a	Liver fibrosis	Cell line	Increase	[507]
miR-199a	laryngeal cancer	Tissues	Decrease	[508]
miR-215	Gastric cancer	Tissues	Increase	[458]
miR-215	Breast cancer	Tissues	Decrease	[461]
miR-215	Breast cancer	Serum	Decrease	[462]
miR-217	Gastric cancer	Tissues	Decrease	[459]
miR-217	Colorectal cancer	Serum	Increase	[452]
miR-217	Colorectal cancer	Exosomes	Decrease	[453]
miR-224	Gastric cancer	Tissues	Increase	[509]
miR-224	Bladder cancer	Tissues	Increase	[510]
miR-224	renal cell carcinoma	Tissues	Increase	[511]
miR-224	Prostate cancer	Cell line	Decrease	[512]
miR-224	uveal melanoma	Tissues	Decrease	[513]
miR-424	laryngeal cancer	Cell line	Increase	[514]
miR-424	Gastric cancer	Cell line	Increase	[515]
miR-424	Ovarian cancer	Cell line	Decrease	[516]
miR-424	Intrahepatic cholangiocarcinoma	Cell line	Decrease	[517]
miR-424	osteosarcoma	Cell line	Decrease	[518]
miR-424	Melanoma	tissues / serum	Increase	[519]
miR-3607	Colorectal cancer	Cell line	Decrease	[454]

miR-3607	Pancreatic cancer	Exosomes	Decrease	[455]
miR-3607	Breast cancer	Tissues	Decrease	[463]
miR-3607	Breast cancer	Cell line	Decrease	[464]

5. CHAPTER 5: CONCLUSION AND FUTURE PRESPECTIVES

5.1. Conclusion

Nearly 80% of HCC cases are untreatable owing to the presentation of the patients at their advanced stages. However, hepatic interventions and surgeries could improve the overall survival rates if the tumor is detected at early stages, especially if the tumor is only a single lesion with a size 2 of cm or smaller. Consequently, the identification of a specific non-invasive biomarker would enable early diagnosis of HCC, decrease the risks of surgical intervention, and permit the non-invasive monitoring and better therapeutic options. The choice of miRNAs as a reliable biomarker relied on the evidences that circulating miRNAs are sensitive predictors to physiological and pathological features of HCC. In this study, the serum differential expression of nine miRNAs (miR-142, miR-150, miR-183, miR-199a, miR-215, miR-217, miR-224, miR-424 and miR-3607) were significantly overexpressed in HCC and HCV patients relative to healthy individuals. However, the expression levels of miR-424, miR-199a, miR-142, and miR-224 were significantly altered in HCC patients relative to non-cirrhotic subjects. While miR-199a and miR-183 showed significant divergance in expression between the two HCV groups. MiR-424 showed potential power in differentiating HCC patients from HCV infected patients with sensitivity and specificity (63.46% and 57.9% respectively) compared to the current biomarker AFP (62.3% and 64.57%; respectively). Using combined panel of five miRNAs (miR-142, miR-183, miR-199a, miR-224 and miR-424) increased the overall sensitivity and specificity of HCC detection to 100% and 95.12%; respectively, and HCV diagnosis to 90.5% and 85.37%; respectively. Upon classifying the patients into SVR and treatment naïve groups, the overall sensitivity and specificity of detection of the combined miRNAs panel in the SVR patients (70.83% and 61.9%) were significantly higher than AFP (51.4% and 60.67%). In conclusion: A combined panel of 5 serum miRNAs could serve as an early prognostic marker for non-invasive early detection of HCC in chronic HCV patients (table 5.1).

Table 5.1. Summary of the potential role of the target miRNAs under this study

miRNA(s)	Potential role
miR-424, miR-199a, miR-142, and miR-224	Significantly dysregulated in HCC patients compared to non-cirrhotic HCV subjects
miR-199a and miR-183	Significantly dysregulated in cirrhotic HCV patients compared to non-cirrhotic HCV subjects
miR-424	Significantly dysregulated in HCC patients compared to cirrhotic HCV subjects
miR-142, miR-150, miR-183, miR-199a, miR-215, miR-217, miR-224, miR-424 and miR-3607	Significantly dysregulated in HCC patients compared to healthy individuals
miR-142, miR-150, miR-183, miR-199a, miR-215, miR-217, miR-224, miR-424 and miR-3607	Significantly dysregulated in HCV patients compared to healthy individuals
miR-142, miR-183, miR-199a, miR-224 and miR-424	Possess potential prognostic marker ability for detection of HCC in chronic HCV patients

5.2. Future perspectives

MicroRNAs are essential regulatory elements in gene expression and sophisticated signaling pathways. Further investigation will ameliorate the information on gene regulation and reveal the complex crosstalk in different cancer-associated characteristics including cancer stem cells formation and EMT. The possible diagnostic and therapeutic approaches of miRNAs in human HCC have been elucidated in previous research studies. However, further analysis to the differential expression of some miRNAs, such as miR-150, miR-424 and miR-199a in the serum of HCV and HCC patients is suggested, in order to highlight the exact mechanism of action and to investigate the potential therapeutic options in HCC treatment. It is also recommended to perform multicentric studies to validate the reliability of these miRNAs as biomarkers for HCC, beside applying longitudinal study to monitor the progression of HCC by those biomarkers.

Extensive investigation on novel non-invasive biomarker for HCC should be performed. Due to the limitations of AFP (including fair sensitivity and accuracy in HCC diagnosis and false negative results in early and advanced stages of HCC), discovering novel biomarkers capable of detecting HCC in AFP-negative patients is warranted. Moreover, conceptualizing a model for

health economics for the early assessment of HCC progression in viral hepatitis treated patients, would assist in reducing HCC death cases as a consequence of poor prognosis and late detection, in addition to overcoming misdiagnosis and improving patients' quality of life.

5.3. Study limitations

Study limitations include heterogenous cohort expressed in different HCV treatment options in HCV-SVR and HCC-SVR groups. The choice of the endogenous reference gene (SNORD 68) in qPCR amplification and data analysis was done following the previous research recommendations in literature, although data normalization using endogenous reference panel could have been done. Furthermore, the variation in Ct values among the technical replicates could be attributed to the low cDNA template concentration used in the qPCR amplification reaction, although the used concentration was approximately close to the upper recommended range by the kit's manufacturer. Lack of AFP measurements in the healthy control samples hindered the comparison of the efficacy of the miRNAs panel versus AFP in HCC and HCV detection.

REFERENCES

[1] Lavanchy D. The global burden of hepatitis C. In: *Liver International*. 2009, pp. 74–81.

[2] Bartosch B. Hepatitis B and C viruses and hepatocellular carcinoma. *Viruses* 2010; 2: 1504–1509.

[3] Petrick JL, McGlynn KA. The Changing Epidemiology of Primary Liver Cancer. *Curr Epidemiol Reports* 2019; 6: 104–111.

[4] Xu C, Zhou W, Wang Y, et al. Hepatitis B virus-induced hepatocellular carcinoma. *Cancer Letters* 2014; 345: 216–222.

[5] Schulze K, Nault JC, Villanueva A. Genetic profiling of hepatocellular carcinoma using next-generation sequencing. *Journal of Hepatology* 2016; 65: 1031–1042.

[6] Fiorino S, Bacchi-Reggiani L, Pontoriero L, et al. Tensegrity model hypothesis: May this paradigm be useful to explain hepatic and pancreatic carcinogenesis in patients with persistent hepatitis B or hepatitis C virus infection? In: *Journal of the Pancreas*. E.S. Burioni Ricerche Bibliografiche, pp. 151–164.

[7] Ji X, Zhang Q, Du Y, et al. Somatic Mutations, Viral Integration and Epigenetic Modification in the Evolution of Hepatitis B Virus-Induced Hepatocellular Carcinoma. *Curr Genomics* 2015; 15: 469–480.

[8] Forner A, Reig M, Bruix J. Hepatocellular carcinoma. *The Lancet* 2018; 391: 1301–1314.

[9] Gholamin S, Mirzaei H, Razavi SM, et al. GD2-targeted immunotherapy and potential value of circulating microRNAs in neuroblastoma. *Journal of Cellular Physiology* 2018; 233: 866–879.

[10] Bray F, Ferlay J, Soerjomataram I, et al. Global cancer statistics 2018: GLOBOCAN estimates of incidence and mortality worldwide for 36 cancers in 185 countries. *CA Cancer J Clin* 2018; 68: 394–424.

[11] World Health Organization International Agency for Research on Cancer. Latest global cancer data 2018, https://www.who.int/cancer/PRGlobocanFinal.pdf (2018, accessed 3 May 2021).

[12] Dasgupta P, Henshaw C, Youlden DR, et al. Global Trends in Incidence Rates of Primary Adult Liver Cancers: A Systematic Review and Meta-Analysis. *Front Oncol* 2020; 10: 171.

[13] Jiang Y, Han QJ, Zhang J. Hepatocellular carcinoma: Mechanisms of progression and immunotherapy. *World Journal of Gastroenterology* 2019; 25: 3151–3167.

[14] World Health Organization. GLOBOCAN 2020: Bladder cancer 10th most commonly diagnosed worldwide - World Bladder Cancer Patient Coalition, https://worldbladdercancer.org/news_events/globocan-2020-bladder-cancer-10th-most-commonly-diagnosed-worldwide/ (2020, accessed 3 May 2021).

[15] Bray F, Ferlay J, Soerjomataram I, et al. Global cancer statistics 2018: GLOBOCAN estimates of incidence and mortality worldwide for 36 cancers in 185 countries. *CA Cancer J Clin* 2018; 68: 394–424.

[16] El-Zayadi AR, Badran HM, Barakat EMF, et al. Hepatocellular carcinoma in Egypt: A single center study over a decade. *World J Gastroenterol* 2005; 11: 5193–5198.

[17] Fitzmaurice C, Akinyemiju T, Abera S, et al. The burden of primary liver cancer and underlying etiologies from 1990 to 2015 at the global, regional, and national level results from the global burden of disease study 2015. *JAMA Oncol* 2017; 3: 1683–1691.

[18] BioRender. BioRender Templates, https://app.biorender.com/biorender-templates (accessed 24 May 2021).

[19] Zhao C, Nguyen MH. Hepatocellular carcinoma screening and surveillance practice guidelines and real-life practice. *Journal of Clinical Gastroenterology* 2016; 50: 120–133.

[20] El-Serag HB, Rudolph KL. Hepatocellular Carcinoma: Epidemiology and Molecular Carcinogenesis. *Gastroenterology* 2007; 132: 2557–2576.

[21] Tang A, Hallouch O, Chernyak V, et al. Epidemiology of hepatocellular carcinoma: target population for surveillance and diagnosis. *Abdominal Radiology* 2018; 43: 13–25.

[22] Allison RD, Teleb N, Al Awaidy S, et al. Hepatitis B control among children in the Eastern Mediterranean Region of the World Health Organization. *Vaccine* 2016; 34: 2403–2409.

[23] Salama II, Sami SM, Said ZNA, et al. Effectiveness of hepatitis B virus vaccination program in Egypt: Multicenter national project. *World J Hepatol* 2015; 7: 2418–2426.

[24] Yang JD, Kim WR, Coelho R, et al. Cirrhosis Is Present in Most Patients With Hepatitis B and Hepatocellular Carcinoma. *Clin Gastroenterol Hepatol* 2011; 9: 64–70.

[25] El-Houseini ME, Ismail A, Abdelaal AA, et al. Role of TGF-β1 and C-Kit Mutations in the Development of Hepatocellular Carcinoma in Hepatitis C Virus-Infected Patients: in vitro Study. *Biochem* 2019; 84: 941–953.

[26] Neamatallah M, El-Bendary M, Elalfy H, et al. Impact of Toll-like Receptors 2(TLR2) and TLR 4 Gene Variations on HCV Susceptibility, Response to Treatment and Development of Hepatocellular Carcinoma in Cirrhotic HCV Patients. *Immunol Invest* 2020; 49: 462–476.

[27] Freeman A. Estimating progression to cirrhosis in chronic hepatitis C virus infection. *Hepatology* 2001; 34: 809–816.

[28] Ledda C, Loreto C, Zammit C, et al. Non-infective occupational risk factors for hepatocellular carcinoma: A review (Review). *Mol Med Rep* 2017; 15: 511–533.

[29] Rapisarda V, Loreto C, Malaguarnera M, et al. Hepatocellular carcinoma and the risk of occupational exposure. *World Journal of Hepatology* 2016; 8: 573–590.

[30] Choiniere J, Wang L. Exposure to inorganic arsenic can lead to gut microbe perturbations and hepatocellular carcinoma. *Acta Pharmaceutica Sinica B* 2016; 6: 426–429.

[31] Badawi A F MMS. Risk factors for hepatocellular carcinoma in Egypt: the role of hepatitis-B viral infection and schistosomiasis - PubMed, https://pubmed.ncbi.nlm.nih.gov/10650811/ (1999, accessed 3 May 2021).

[32] Griswold MG, Fullman N, Hawley C, et al. Alcohol use and burden for 195 countries and territories, 1990-2016: A systematic analysis for the Global Burden of Disease Study 2016. *Lancet* 2018; 392: 1015–1035.

[33] Fitzmaurice C, Akinyemiju T, Abera S, et al. The burden of primary liver cancer and underlying

etiologies from 1990 to 2015 at the global, regional, and national level results from the global burden of disease study 2015. *JAMA Oncol* 2017; 3: 1683–1691.

[34] Meroni M, Longo M, Dongiovanni P. Alcohol or Gut Microbiota: Who Is the Guilty? *International Journal of Molecular Sciences*; 20. Epub ahead of print 2 September 2019. DOI: 10.3390/ijms20184568.

[35] Stickel F. Alcoholic cirrhosis and hepatocellular carcinoma. *Adv Exp Med Biol* 2015; 815: 113–130.

[36] Fattovich G, Stroffolini T, Zagni I, et al. Hepatocellular carcinoma in cirrhosis: Incidence and risk factors. In: *Gastroenterology*. W.B. Saunders. Epub ahead of print 2004. DOI: 10.1053/j.gastro.2004.09.014.

[37] Ganne-Carrié N, Nahon P. Hepatocellular carcinoma in the setting of alcohol-related liver disease. *Journal of Hepatology* 2019; 70: 284–293.

[38] Ganne-Carrié N, Chaffaut C, Bourcier V, et al. Estimate of hepatocellular carcinoma incidence in patients with alcoholic cirrhosis. *J Hepatol* 2018; 69: 1274–1283.

[39] Baecker A, Liu X, La Vecchia C, et al. Worldwide incidence of hepatocellular carcinoma cases attributable to major risk factors. *Eur J Cancer Prev* 2018; 27: 205–212.

[40] Lee YCA, Cohet C, Yang YC, et al. Meta-analysis of epidemiologic studies on cigarette smoking and liver cancer. *Int J Epidemiol* 2009; 38: 1497–1511.

[41] Kur P, Kolasa-Wołosiuk A, Misiakiewicz-Has K, et al. Sex hormone-dependent physiology and diseases of liver. *International Journal of Environmental Research and Public Health*; 17. Epub ahead of print 2 April 2020. DOI: 10.3390/ijerph17082620.

[42] Kanda T, Takahashi K, Nakamura M, et al. Androgen receptor could be a potential therapeutic target in patients with advanced hepatocellular carcinoma. *Cancers (Basel)*; 9. Epub ahead of print 5 May 2017. DOI: 10.3390/cancers9050043.

[43] Ferlay J, Soerjomataram I, Dikshit R, et al. Cancer incidence and mortality worldwide: Sources, methods and major patterns in GLOBOCAN 2012. *Int J Cancer* 2015; 136: E359–E386.

[44] Omar A, Abou-Alfa GK, Khairy A, et al. Risk factors for developing hepatocellular carcinoma in Egypt. *Chinese Clinical Oncology* 2013; 2: 13–13.

[45] Maurizio S, Lydia G, Fabio D, et al. Interleukin-6 and its soluble receptor in patients with liver cirrhosis and hepatocellular carcinoma. *World J Gastroenterol* 2006; 12: 2563–2568.

[46] Naugler WE, Sakurai T, Kim S, et al. Gender disparity in liver cancer due to sex differences in MyD88-dependent IL-6 production. *Science (80-)* 2007; 317: 121–124.

[47] Wang YC, Xu GL, Jia WD, et al. Estrogen suppresses metastasis in rat hepatocellular carcinoma through decreasing interleukin-6 and hepatocyte growth factor expression. *Inflammation* 2012; 35: 143–149.

[48] Ma WL, Lai HC, Yeh S, et al. Androgen receptor roles in hepatocellular carcinoma, fatty liver, cirrhosis and hepatitis. *Endocrine-Related Cancer*; 21. Epub ahead of print 2014. DOI: 10.1530/ERC-13-0283.

[49] Kanda T, Jiang X, Yokosuka O. Androgen receptor signaling in hepatocellular carcinoma and pancreatic cancers. *World J Gastroenterol* 2014; 20: 9229–9236.

[50] Shi L, Lin H, Li G, et al. Targeting androgen receptor (AR)→IL12A signal enhances efficacy of sorafenib plus NK cells immunotherapy to better suppress HCC progression. *Mol Cancer Ther* 2016; 15: 731–742.

[51] Abd-Elsalam S, Elwan N, Soliman H, et al. Epidemiology of liver cancer in Nile delta over a decade: A single-center study. *South Asian J Cancer* 2018; 07: 24–26.

[52] Elghazaly H, Gaballah A, Eldin NB. Clinic-pathological pattern of hepatocellular carcinoma (HCC) in Egypt. *Ann Oncol* 2018; 29: v5–v6.

[53] Larsson SC, Wolk A. Overweight, obesity and risk of liver cancer: A meta-analysis of cohort studies. *Br J Cancer* 2007; 97: 1005–1008.

[54] Calle EE, Rodriguez C, Walker-Thurmond K, et al. Overweight, Obesity, and Mortality from Cancer in a Prospectively Studied Cohort of U.S. Adults. *N Engl J Med* 2003; 348: 1625–1638.

[55] Lagiou P, Kuper H, Stuver SO, et al. Role of diabetes mellitus in the etiology of hepatocellular carcinoma. *J Natl Cancer Inst* 2000; 92: 1096–1099.

[56] Li X, Xu H, Gao Y, et al. Diabetes mellitus increases the risk of hepatocellular carcinoma in treatment-naïve chronic hepatitis C patients in China. *Medicine (Baltimore)* 2017; 96: e6508.

[57] Weng CJ, Hsieh YH, Tsai CM, et al. Relationship of insulin-like growth factors system gene polymorphisms with the susceptibility and pathological development of hepatocellular carcinoma. *Ann Surg Oncol* 2010; 17: 1808–1815.

[58] Park EJ, Lee JH, Yu GY, et al. Dietary and Genetic Obesity Promote Liver Inflammation and Tumorigenesis by Enhancing IL-6 and TNF Expression. *Cell* 2010; 140: 197–208.

[59] Moore M A PCBtH. Implications of the hyperinsulinaemia-diabetes-cancer link for preventive efforts - PubMed, https://pubmed.ncbi.nlm.nih.gov/9818771/ (1988, accessed 3 May 2021).

[60] Hsu H-C, Peng S-Y, Lai P-L, et al. Allelotype and loss of heterozygosity of p53 in primary and recurrent hepatocellular carcinomas. A study of 150 patients. *Cancer* 1994; 73: 42–47.

[61] Chen J, Han Y, Xu C, et al. Effect of type 2 diabetes mellitus on the risk for hepatocellular carcinoma in chronic liver diseases: A meta-analysis of cohort studies. *Eur J Cancer Prev* 2015; 24: 89–99.

[62] Bakir A, Ali-Eldin Z. Is diabetes mellitus a risk factor for hepatocellular carcinoma in Egyptian patients. *undefined*.

[63] Morsy K H, Al-Islam M S, Ibrahi E M. Hepatocellular Carcinoma in Upper Egypt: A Retrospective Study | ARC Journal of Hepatology and Gastroenterology, https://www.arcjournals.org/journal-of-gastroenterology/volume-3-issue-1/3 (2018, accessed 3 May 2021).

[64] HJALGRIM H, FRISCH M, EKBOM A, et al. Cancer and diabetes - a follow-up study of two populationbased cohorts of diabetic patients. *J Intern Med* 2007; 241: 471–475.

[65] Hassan MM, Hwang LY, Hatten CJ, et al. Risk factors for hepatocellular carcinoma: Synergism of alcohol with viral hepatitis and diabetes mellitus. *Hepatology* 2002; 36: 1206–1213.

[66] Adami HO, Chow WH, Nyrén O, et al. Excess risk of primary liver cancer in patients with diabetes mellitus. *J Natl Cancer Inst* 1996; 88: 1472–1477.

[67] Byrne CD, Targher G. NAFLD: A multisystem disease. *Journal of Hepatology* 2015; 62: S47–S64.

[68] Nalbantoglu I, Brunt EM. Role of liver biopsy in nonalcoholic fatty liver disease. *World Journal of Gastroenterology* 2014; 20: 9026–9037.

[69] Neuschwander-Tetri BA, Caldwell SH. Nonalcoholic steatohepatitis: Summary of an AASLD Single Topic Conference. In: *Hepatology*. W.B. Saunders, pp. 1202–1219.

[70] Bugianesi E, Leone N, Vanni E, et al. Expanding the natural history of nonalcoholic steatohepatitis: From cryptogenic cirrhosis to hepatocellular carcinoma. *Gastroenterology* 2002; 123: 134–140.

[71] Michelotti GA, Machado M V., Diehl AM. NAFLD, NASH and liver cancer. *Nature Reviews Gastroenterology and Hepatology* 2013; 10: 656–665.

[72] Ekstedt M, Franzén LE, Mathiesen UL, et al. Long-term follow-up of patients with NAFLD and elevated liver enzymes. *Hepatology* 2006; 44: 865–873.

[73] Yatsuji S, Hashimoto E, Tobari M, et al. Clinical features and outcomes of cirrhosis due to non-alcoholic steatohepatitis compared with cirrhosis caused by chronic hepatitis C. *J Gastroenterol Hepatol* 2009; 24: 248–254.

[74] Saleh S, Elhosary YA, Ezzat W, et al. Hepatocellular Carcinoma and Possible Related Risk Factors. *undefined*.

[75] El-Serag HB, Hampel H, Javadi F. The association between diabetes and hepatocellular carcinoma: A systematic review of epidemiologic evidence. *Clin Gastroenterol Hepatol* 2006; 4: 369–380.

[76] Hashimoto E, Yatsuji S, Tobari M, et al. Hepatocellular carcinoma in patients with nonalcoholic steatohepatitis. *J Gastroenterol* 2009; 44: 89–95.

[77] Mori S, Yamasaki T, Sakaida I, et al. Hepatocellular carcinoma with nonalcoholic steatohepatitis. *J Gastroenterol* 2004; 39: 391–396.

[78] Hai S, Kubo S, Shuto T, et al. Hepatocellular carcinoma arising from nonalcoholic steatohepatitis: Report of two cases. *Surgery Today* 2006; 36: 390–394.

[79] Teufel A, Weinmann A, Centner C, et al. Hepatocellular carcinoma in patients with autoimmune hepatitis. *World J Gastroenterol* 2009; 15: 578–582.

[80] Wong RJ, Gish R, Frederick T, et al. Development of hepatocellular carcinoma in autoimmune hepatitis patients: A case series. *Dig Dis Sci* 2011; 56: 578–585.

[81] Shiani A, Narayanan S, Pena L, et al. The Role of Diagnosis and Treatment of Underlying Liver Disease for the Prognosis of Primary Liver Cancer. *Cancer Control* 2017; 24: 107327481772924.

[82] Propst T, Propst A, Dietze O, et al. Prevalence of hepatocellular carcinoma in alpha-1-antitrypsin deficiency. *J Hepatol* 1994; 21: 1006–1011.

[83] Hazari YM, Bashir A, Habib M, et al. Alpha-1-antitrypsin deficiency: Genetic variations, clinical

manifestations and therapeutic interventions. *Mutation Research - Reviews in Mutation Research* 2017; 773: 14–25.

[84] Carlson JA, Barton Rogers B, Sifers RN, et al. Accumulation of PiZ α1-antitrypsin causes liver damage in transgenic mice. *J Clin Invest* 1989; 83: 1183–1190.

[85] Elzouki A-N, Eriksson S. Risk of hepatobiliary disease in adults with severe ??1-antitrypsin deficiency (PiZZ): is chronic viral hepatitis B or C an additional risk factor for cirrhosis and hepatocellular carcinoma? *Eur J Gastroenterol Hepatol* 1996; 8: 989–994.

[86] Topic A, Ljujic M, Radojkovic D. Alpha-1-antitrypsin in pathogenesis of hepatocellular carcinoma. *Hepat Mon*; 12. Epub ahead of print October 2012. DOI: 10.5812/hepatmon.7042.

[87] Settin A, El-Bendary M, Al-Kassem R, et al. Molecular analysis of A1AT (S and Z) and HFE (C282Y and H63D) gene mutations in Egyptian cases with HCV liver cirrhosis - PubMed, https://pubmed.ncbi.nlm.nih.gov/16802007/ (2006, accessed 3 May 2021).

[88] Kew MC. Hepatic iron overload and hepatocellular carcinoma. *Liver Cancer* 2014; 3: 31–40.

[89] Powell LW, Subramaniam VN, Yapp TR. Haemochromatosis in the new millennium. *J Hepatol* 2000; 32: 48–62.

[90] Kowdley K V. Iron, hemochromatosis, and hepatocellular carcinoma. In: *Gastroenterology*. W.B. Saunders. Epub ahead of print 2004. DOI: 10.1016/j.gastro.2004.09.019.

[91] Elmberg M, Hultcrantz R, Ekbom A, et al. Cancer Risk in Patients with Hereditary Hemochromatosis and in Their First-Degree Relatives. *Gastroenterology* 2003; 125: 1733–1741.

[92] Fracanzani AL, Conte D, Fraquelli M, et al. Increased cancer risk in a cohort of 230 patients with hereditary hemochromatosis in comparison to matched control patients with non-iron-related chronic liver disease. *Hepatology* 2001; 33: 647–651.

[93] Yang Q, McDonnell SM, Khoury MJ, et al. Hemochromatosis-associated mortality in the United States from 1979 to 1992: An analysis of multiple-cause mortality data. *Ann Intern Med* 1998; 129: 946–953.

[94] Omar A, Abou-Alfa GK, Khairy A, et al. Risk factors for developing hepatocellular carcinoma in Egypt. *Chinese Clinical Oncology*; 2. Epub ahead of print 2013. DOI: 10.3978/j.issn.2304-3865.2013.11.07.

[95] Mandishona E, MacPhail AP, Gordeuk VR, et al. Dietary iron overload as a risk factor for hepatocellular carcinoma in Black Africans. *Hepatology* 1998; 27: 1563–1566.

[96] Borgna-Pignatti C, Vergine G, Lombardo T, et al. Hepatocellular carcinoma in the thalassaemia syndromes. *Br J Haematol* 2004; 124: 114–117.

[97] Moyo VM, Makunike R, Gangaidzo IT, et al. African iron overload and hepatocellular carcinoma (HA-7-0-080). *Eur J Haematol* 1998; 60: 28–34.

[98] Shen FM, Lee MK, Gong HM, et al. Complex segregation analysis of primary hepatocellular carcinoma in Chinese families: Interaction of inherited susceptibility and hepatitis B viral infection. *Am J Hum Genet* 1991; 49: 88–93.

[99] Dragani TA. Risk of HCC: Genetic heterogeneity and complex genetics. *Journal of Hepatology*

2010; 52: 252–257.

[100] Shih WL, Yu MW, Chen PJ, et al. Evidence for association with hepatocellular carcinoma at the PAPSS1 locus on chromosome 4q25 in a family-based study. *Eur J Hum Genet* 2009; 17: 1250–1259.

[101] Yang Y, Wu QJ, Xie L, et al. Prospective cohort studies of association between family history of liver cancer and risk of liver cancer. *Int J Cancer* 2014; 135: 1605–1614.

[102] Shih WL, Yu MW, Chen PJ, et al. Localization of a susceptibility locus for hepatocellular carcinoma to chromosome 4q in a hepatitis B hyperendemic area. *Oncogene* 2006; 25: 3219–3224.

[103] Ziada DH, El Sadany S, Soliman H, et al. Prevalence of hepatocellular carcinoma in chronic hepatitis C patients in Mid Delta, Egypt: A single center study. *J Egypt Natl Canc Inst* 2016; 28: 257–262.

[104] McGlynn KA, Petrick JL, London WT. Global Epidemiology of Hepatocellular Carcinoma: An Emphasis on Demographic and Regional Variability. *Clinics in Liver Disease* 2015; 19: 223–238.

[105] Zucman-Rossi J, Villanueva A, Nault JC, et al. Genetic Landscape and Biomarkers of Hepatocellular Carcinoma. *Gastroenterology* 2015; 149: 1226-1239.e4.

[106] Rahman El-Zayadi A, Abaza H, Shawky S, et al. Prevalence and epidemiological features of hepatocellular carcinoma in Egypt - A single center experience. *Hepatol Res* 2001; 19: 170–179.

[107] World Health Organization International Agency For Research On Cancer. Some Traditional Herbal Medicines, Some Mycotoxins, Naphthalene and Styrene - IARC Working Group on the Evaluation of Carcinogenic Risks to Humans, International Agency for Research on Cancer - Google Books, https://books.google.com.eg/books?hl=en&lr=&id=iUXBe9cYzW8C&oi=fnd&pg=PP2&ots=1ogxWne57T&sig=eNoI9GYzeRa3AGra2VTMWhHKCvo&redir_esc=y#v=onepage&q&f=false (accessed 3 May 2021).

[108] Hsia CC, Kleiner DE, Axiotis CA, et al. Mutations of p53 gene in hepatocellular carcinoma: Roles of hepatitis b virus and aflatoxin contamination in the diet. *J Natl Cancer Inst* 1992; 84: 1638–1641.

[109] Wang H, Liao P, Zeng SX, et al. It takes a team: A gain-of-function story of p53-R249S. *Journal of Molecular Cell Biology* 2019; 11: 277–283.

[110] Hosny G, Farahat N, Tayel H, et al. Ser-249 TP53 and CTNNB1 mutations in circulating free DNA of Egyptian patients with hepatocellular carcinoma versus chronic liver diseases. *Cancer Lett* 2008; 264: 201–208.

[111] Jiao J, Niu W, Wang Y, et al. Prevalence of Aflatoxin-Associated TP53R249S Mutation in Hepatocellular Carcinoma in Hispanics in South Texas . *Cancer Prev Res* 2018; 11: 103–112.

[112] Dragani TA. Risk of HCC: Genetic heterogeneity and complex genetics. *Journal of Hepatology* 2010; 52: 252–257.

[113] Pineau P, Marchio A, Battiston C, et al. Chromosome instability in human hepatocellular carcinoma depends on p53 status and aflatoxin exposure. *Mutat Res - Genet Toxicol Environ*

Mutagen 2008; 653: 6–13.

[114] Wu HC, Wang Q, Yang HI, et al. Aflatoxin B1 exposure, hepatitis B virus infection, and hepatocellular carcinoma in Taiwan. *Cancer Epidemiol Biomarkers Prev* 2009; 18: 846–853.

[115] Wu HC, Wang Q, Yang HI, et al. Urinary 15-F2t-isoprostane, aflatoxin B1 exposure and hepatitis B virus infection and hepatocellular carcinoma in Taiwan. *Carcinogenesis* 2008; 29: 971–976.

[116] Gomaa AI, Khan SA, Toledano MB, et al. Hepatocellular carcinoma: Epidemiology, risk factors and pathogenesis. *World J Gastroenterol* 2008; 14: 4300–4308.

[117] Qian G S, Ross R K, Yu M C, et al. A follow-up study of urinary markers of aflatoxin exposure and liver cancer risk in Shanghai, People's Republic of China - PubMed, https://pubmed.ncbi.nlm.nih.gov/8118382/ (1994, accessed 3 May 2021).

[118] Ross RK, Yu MC, Henderson BE, et al. Urinary aflatoxin biomarkers and risk of hepatocellular carcinoma. *Lancet* 1992; 339: 943–946.

[119] Liu Y, Wu F. Global burden of Aflatoxin-induced hepatocellular carcinoma: A risk assessment. *Environ Health Perspect* 2010; 118: 818–824.

[120] Polychronaki N, Wild CP, Mykkänen H, et al. Urinary biomarkers of aflatoxin exposure in young children from Egypt and Guinea. *Food Chem Toxicol* 2008; 46: 519–526.

[121] Turner PC, Loffredo C, Kafrawy S El, et al. Pilot survey of aflatoxin–albumin adducts in sera from Egypt. *Food Addit Contam - Part A Chem Anal Control Expo Risk Assess* 2008; 25: 583–587.

[122] Anwar WA, Khaled HM, Amra HA, et al. Changing pattern of hepatocellular carcinoma (HCC) and its risk factors in Egypt: Possibilities for prevention. *Mutation Research - Reviews in Mutation Research* 2008; 659: 176–184.

[123] Villanueva A, Minguez B, Forner A, et al. Hepatocellular carcinoma: Novel molecular approaches for diagnosis, prognosis, and therapy. *Annual Review of Medicine* 2010; 61: 317–328.

[124] Nordenstedt H, White DL, El-Serag HB. The changing pattern of epidemiology in hepatocellular carcinoma. *Dig Liver Dis* 2010; 42: S206–S214.

[125] Fiorino S, Bacchi-Reggiani ML, Visani M, et al. MicroRNAs as possible biomarkers for diagnosis and prognosis of hepatitis b-and c-related-hepatocellularcarcinoma. *World J Gastroenterol* 2016; 22: 3907–3936.

[126] Ghanaati H, Alavian SM, Jafarian A, et al. Imaging and imaging-guided interventions in the diagnosis and management of hepatocellular carcinoma (HCC)-review of evidence. *Iranian Journal of Radiology* 2012; 9: 167–177.

[127] Ayuso C, Rimola J, Vilana R, et al. Diagnosis and staging of hepatocellular carcinoma (HCC): current guidelines. *Eur J Radiol* 2018; 101: 72–81.

[128] El-Serag HB, Marrero JA, Rudolph L, et al. Diagnosis and Treatment of Hepatocellular Carcinoma. *Gastroenterology* 2008; 134: 1752–1763.

[129] Johnson PJ. Role of alpha-fetoprotein in the diagnosis and management of hepatocellular carcinoma. *J Gastroenterol Hepatol*; 14. Epub ahead of print 1999. DOI: 10.1046/j.1440-1746.1999.01873.x.

[130] Trevisani F, D'Intino PE, Morselli-Labate AM, et al. Serum α-fetoprotein for diagnosis of hepatocellular carcinoma in patients with chronic liver disease: Influence of HBsAg and anti-HCV status. *J Hepatol* 2001; 34: 570–575.

[131] Stefaniuk P, Cianciara J, Wiercinska-Drapalo A. Present and future possibilities for early diagnosis of hepatocellular carcinoma. *World Journal of Gastroenterology* 2010; 16: 418–424.

[132] Chen S, Chen H, Gao S, et al. Differential expression of plasma microRNA-125b in hepatitis B virus-related liver diseases and diagnostic potential for hepatitis B virus-induced hepatocellular carcinoma. *Hepatol Res* 2017; 47: 312–320.

[133] Han LL, Lv Y, Guo H, et al. Implications of biomarkers in human hepatocellular carcinoma pathogenesis and therapy. *World J Gastroenterol* 2014; 20: 10249–10261.

[134] Bruix J, Sherman M. Management of hepatocellular carcinoma: An update. *Hepatology* 2011; 53: 1020–1022.

[135] Dimitroulis D, Damaskos C, Valsami S, et al. From diagnosis to treatment of hepatocellular carcinoma: An epidemic problem for both developed and developing world. *World Journal of Gastroenterology* 2017; 23: 5282–5294.

[136] Miller G, Schwartz LH, D'Angelica M. The Use of Imaging in the Diagnosis and Staging of Hepatobiliary Malignancies. *Surgical Oncology Clinics of North America* 2007; 16: 343–368.

[137] Colli A, Fraquelli M, Casazza G, et al. Accuracy of Ultrasonography, Spiral CT, Magnetic Resonance, and Alpha-Fetoprotein in Diagnosing Hepatocellular Carcinoma: A Systematic Review: CME. *American Journal of Gastroenterology* 2006; 101: 513–523.

[138] Durot I, Wilson SR, Willmann JK. Contrast-enhanced ultrasound of malignant liver lesions. *Abdom Radiol* 2018; 43: 819–847.

[139] Wilson SR, Burns PN. An algorithm for the diagnosis of focal liver masses using microbubble contrast-enhanced pulse-inversion sonography. *Am J Roentgenol* 2006; 186: 1401–1412.

[140] Hatanaka K, Kudo M, Minami Y, et al. Differential diagnosis of hepatic tumors: Value of contrast-enhanced harmonic sonography using the newly developed contrast agent, Sonazoid. In: *Intervirology*. Intervirology, pp. 61–69.

[141] Zech CJ, Reiser MF, Herrmann KA. Imaging of hepatocellular carcinoma by computed tomography and magnetic resonance imaging: State of the art. *Digestive Diseases* 2009; 27: 114–124.

[142] Iannaccone R, Laghi A, Catalane C, et al. Hepatocellular carcinoma: Mole of unenhanced and delayed phase multi-detector mew helical CT in patients with cirrhosis. *Radiology* 2005; 234: 460–467.

[143] Sahani D V., Holalkere NS, Mueller PR, et al. Advanced hepatocellular carcinoma: CT perfusion of liver and tumor tissue - Initial experience. *Radiology* 2007; 243: 736–743.

[144] Ariff B, Lloyd CR, Khan S, et al. Imaging of liver cancer. *World Journal of Gastroenterology* 2009; 15: 1289–1300.

[145] Lencioni R, Cioni D, Della Pina C, et al. Imaging diagnosis. *Seminars in Liver Disease* 2005; 25:

162–170.

[146] Marrero JA, Hussain HK, Nghiem H V., et al. Improving the prediction of hepatocellular carcinoma in cirrhotic patients with an arterially-enhancing liver mass. *Liver Transplant* 2005; 11: 281–289.

[147] Young KK, Chong SK, Gyong HC, et al. Comparison of gadobenate dimeglumine-enhanced dynamic MRI and 16-MDCT for the detection of hepatocellular carcinoma. *Am J Roentgenol* 2006; 186: 149–157.

[148] Ebara M, Ohto M, Watanabe Y, et al. Diagnosis of small hepatocellular carcinoma: Correlation of MR imaging and tumor histologic studies. *Radiology* 1986; 159: 371–378.

[149] Willatt JM, Hussain HK, Adusumilli S, et al. MR imaging of hepatocellular carcinoma in the cirrhotic liver: Challenges and controversies. *Radiology* 2008; 247: 311–330.

[150] Li J, Cheng ZJ, Liu Y, et al. Serum thioredoxin is a diagnostic marker for hepatocellular carcinoma. *Oncotarget* 2015; 6: 9551–9563.

[151] Pocha C, Dieperink E, McMaken KA, et al. Surveillance for hepatocellular cancer with ultrasonography vs. computed tomography - A randomised study. *Aliment Pharmacol Ther* 2013; 38: 303–312.

[152] Jang HJ, Tae KK, Burns PN, et al. Enhancement patterns of hepatocellular carcinoma at contrast-enhanced US: Comparison with histologic differentiation. *Radiology* 2007; 244: 898–906.

[153] Lencioni R, Piscaglia F, Bolondi L. Contrast-enhanced ultrasound in the diagnosis of hepatocellular carcinoma. *Journal of Hepatology* 2008; 48: 848–857.

[154] Giorgio A, Montesarchio L, Gatti P, et al. Contrast-enhanced ultrasound: A simple and effective tool in defining a rapid diagnostic work-up for small nodules detected in cirrhotic patients during surveillance. *J Gastrointest Liver Dis* 2016; 25: 205–211.

[155] Galassi M, Iavarone M, Rossi S, et al. Patterns of appearance and risk of misdiagnosis of intrahepatic cholangiocarcinoma in cirrhosis at contrast enhanced ultrasound. *Liver Int* 2013; 33: 771–779.

[156] Vilana R, Forner A, Bianchi L, et al. Intrahepatic peripheral cholangiocarcinoma in cirrhosis patients may display a vascular pattern similar to hepatocellular carcinoma on contrast-enhanced ultrasound. *Hepatology* 2010; 51: 2020–2029.

[157] Kim SH, Choi BI, Lee JY, et al. Diagnostic accuracy of multi-/single-detector row CT and contrast-enhanced MRI in the detection of hepatocellular carcinomas meeting the Milan criteria before liver transplantation. In: *Intervirology*. Intervirology, pp. 52–60.

[158] Brancatelli G, Baron RL, Peterson MS, et al. Helical CT screening for hepatocellular carcinoma in patients with cirrhosis: Frequency and causes of false-positive interpretation. *Am J Roentgenol* 2003; 180: 1007–1014.

[159] Singal AG, Conjeevaram HS, Volk ML, et al. Effectiveness of hepatocellular carcinoma surveillance in patients with cirrhosis. *Cancer Epidemiol Biomarkers Prev* 2012; 21: 793–799.

[160] Luo P, Wu S, Yu Y, et al. Current Status and Perspective Biomarkers in AFP Negative HCC:

Towards Screening for and Diagnosing Hepatocellular Carcinoma at an Earlier Stage. *Pathology and Oncology Research* 2020; 26: 599–603.

[161] Marrero JA, Feng Z, Wang Y, et al. α-Fetoprotein, Des-γ Carboxyprothrombin, and Lectin-Bound α-Fetoprotein in Early Hepatocellular Carcinoma. *Gastroenterology* 2009; 137: 110–118.

[162] Hartke J, Johnson M, Ghabril M. The diagnosis and treatment of hepatocellular carcinoma. *Semin Diagn Pathol* 2017; 34: 153–159.

[163] Marrero JA, Fontana RJ, Barrat A, et al. Prognosis of hepatocellular carcinoma: Comparison of 7 staging systems in an American cohort. *Hepatology* 2005; 41: 707–715.

[164] Bruix J, Sherman M. Management of hepatocellular carcinoma. *Hepatology* 2005; 42: 1208–1236.

[165] Golfieri R, Bargellini I, Spreafico C, et al. Patients with Barcelona Clinic Liver Cancer Stages B and C Hepatocellular Carcinoma: Time for a Subclassification. *Liver Cancer* 2019; 8: 78–91.

[166] Ling Khoo TSW, Rehman A, Olynyk JK. Tyrosine Kinase Inhibitors in the Treatment of Hepatocellular Carcinoma. In: *Hepatocellular Carcinoma*. Codon Publications, pp. 127–139.

[167] Abdelfattah AAM, Rizk F, Hawash N, et al. Randomized trial of preoperative administration of oral pregabalin for postoperative analgesia in patients scheduled for radiofrequency ablation of focal lesions in the liver. *Int J Hyperth* 2018; 34: 1367–1371.

[168] Sheta E, El-Kalla F, El-Gharib M, et al. Comparison of single-session transarterial chemoembolization combined with microwave ablation or radiofrequency ablation in the treatment of hepatocellular carcinoma: A randomized-controlled study. *Eur J Gastroenterol Hepatol* 2016; 28: 1198–1203.

[169] Rashed WM, Kandeil MAM, Mahmoud MO, et al. Hepatocellular Carcinoma (HCC) in Egypt: A comprehensive overview. *Journal of the Egyptian National Cancer Institute* 2020; 32: 1–11.

[170] Llovet JM, Brú C, Bruix J. Prognosis of hepatocellular carcinoma: The BCLC staging classification. *Semin Liver Dis* 1999; 19: 329–337.

[171] Bruix J, Qin S, Merle P, et al. Regorafenib for patients with hepatocellular carcinoma who progressed on sorafenib treatment (RESORCE): a randomised, double-blind, placebo-controlled, phase 3 trial. *Lancet* 2017; 389: 56–66.

[172] Henderson JM, ShermanM., Tavill A, et al. AHPBA/AJCC consensus conference on staging of hepatocellular carcinoma: Consensus statement. In: *HPB*. Martin Dunitz Ltd, pp. 243–250.

[173] Mazzaferro V, Regalia E, Doci R, et al. Liver Transplantation for the Treatment of Small Hepatocellular Carcinomas in Patients with Cirrhosis. *N Engl J Med* 1996; 334: 693–700.

[174] Choi BI, Lee JM. Advancement in HCC imaging: diagnosis, staging and treatment efficacy assessments. *J Hepatobiliary Pancreat Sci* 2010; 17: 369–373.

[175] Tsoris A, Marlar CA. Use Of The Child Pugh Score In Liver Disease. *StatPearls*, http://www.ncbi.nlm.nih.gov/pubmed/31194448 (2019, accessed 3 May 2021).

[176] Peng Y, Qi X, Guo X. Child–Pugh Versus MELD Score for the Assessment of Prognosis in Liver Cirrhosis: A Systematic Review and Meta-Analysis of Observational Studies. *Medicine*

(Baltimore); 95. Epub ahead of print 4 March 2016. DOI: 10.1097/MD.0000000000002877.

[177] BioRender Templates. Barcelona Clinic Liver Cancer (BCLC) Staging System, https://app.biorender.com/biorender-templates/t-5efa6d1fbc0c9f00ab59e095-barcelona-clinic-liver-cancer-bclc-staging-system (2020, accessed 24 May 2021).

[178] Takano S, Yokosuka O, Imazeki F, et al. Incidence of hepatocellular carcinoma in chronic Hepatitis B and C: A prospective study of 251 patients. *Hepatology* 1995; 21: 650–655.

[179] Takayama T, Makuuchi M. Segmental liver resections, present and future - Caudate lobe resection for liver tumors. *Hepato-Gastroenterology* 1998; 45: 20–23.

[180] Cheng AL, Kang YK, Chen Z, et al. Efficacy and safety of sorafenib in patients in the Asia-Pacific region with advanced hepatocellular carcinoma: a phase III randomised, double-blind, placebo-controlled trial. *Lancet Oncol* 2009; 10: 25–34.

[181] Ungtrakul T, Mahidol C, Chun-On P, et al. Hepatocellular carcinoma screening and surveillance in 2293 chronic hepatitis B patients in an endemic area. *World J Gastroenterol* 2016; 22: 7806–7812.

[182] Bruix J, Reig M, Sherman M. Evidence-Based Diagnosis, Staging, and Treatment of Patients with Hepatocellular Carcinoma. *Gastroenterology* 2016; 150: 835–853.

[183] Obi S, Yoshida H, Toune R, et al. Combination therapy of intraarterial 5-fluorouracil and systemic interferon-alpha for advanced hepatocellular carcinoma with portal venous invasion. *Cancer* 2006; 106: 1990–1997.

[184] Marrero JA. Screening tests for hepatocellular carcinoma. In: *Clinics in Liver Disease*. W.B. Saunders, pp. 235–251.

[185] Benson AB, Abrams TA, Ben-Josef E, et al. Hepatobiliary cancers. *JNCCN Journal of the National Comprehensive Cancer Network* 2009; 7: 350–391.

[186] Yang JD, Roberts LR. Hepatocellular carcinoma: A global view. *Nature Reviews Gastroenterology and Hepatology* 2010; 7: 448–458.

[187] Bruix J, Sherman M. Management of hepatocellular carcinoma. *Hepatology* 2005; 42: 1208–1236.

[188] Llovet JM, Ducreux M, Lencioni R, et al. EASL-EORTC Clinical Practice Guidelines: Management of hepatocellular carcinoma. *J Hepatol* 2012; 56: 908–943.

[189] Bialecki ES, Ezenekwe AM, Brunt EM, et al. Comparison of liver biopsy and noninvasive methods for diagnosis of hepatocellular carcinoma. *Clin Gastroenterol Hepatol* 2006; 4: 361–368.

[190] Omata M, Lesmana LA, Tateishi R, et al. Asian pacific association for the study of the liver consensus recommendations on hepatocellular carcinoma. *Hepatology International* 2010; 4: 439–474.

[191] Zając M, Muszalska I, Sobczak A, et al. Hepatitis C – New drugs and treatment prospects. *European Journal of Medicinal Chemistry* 2019; 165: 225–249.

[192] Lemon SM, McGivern DR. Is hepatitis C virus carcinogenic? *Gastroenterology* 2012; 142: 1274–1278.

[193] Hoofnagle JH. Hepatitis C: The clinical spectrum of disease. In: *Hepatology*. John Wiley and Sons Inc. Epub ahead of print 1997. DOI: 10.1002/hep.510260703.

[194] El-Maraghy SA, Adel O, Zayed N, et al. Circulatory miRNA-484, 524, 615 and 628 expression profiling in HCV mediated HCC among Egyptian patients; implications for diagnosis and staging of hepatic cirrhosis and fibrosis. *J Adv Res* 2020; 22: 57–66.

[195] Petruzziello A, Marigliano S, Loquercio G, et al. Global epidemiology of hepatitis C virus infection: An up-date of the distribution and circulation of hepatitis C virus genotypes. *World Journal of Gastroenterology* 2016; 22: 7824–7840.

[196] Estes C, Abdel-Kareem M, Abdel-Razek W, et al. Economic burden of hepatitis C in Egypt: The future impact of highly effective therapies. *Aliment Pharmacol Ther* 2015; 42: 696–706.

[197] Lozano R, Naghavi M, Foreman K, et al. Global and regional mortality from 235 causes of death for 20 age groups in 1990 and 2010: A systematic analysis for the Global Burden of Disease Study 2010. *Lancet* 2012; 380: 2095–2128.

[198] Omran D, Alboraie M, Zayed RA, et al. Towards hepatitis C virus elimination: Egyptian experience, achievements and limitations. *World Journal of Gastroenterology* 2018; 24: 4330–4340.

[199] Mohd Hanafiah K, Groeger J, Flaxman AD, et al. Global epidemiology of hepatitis C virus infection: New estimates of age-specific antibody to HCV seroprevalence. *Hepatology* 2013; 57: 1333–1342.

[200] Messina JP, Humphreys I, Flaxman A, et al. Global distribution and prevalence of hepatitis C virus genotypes. *Hepatology* 2015; 61: 77–87.

[201] Demerdash HM, Hussien HM, Hassouna E, et al. Detection of MicroRNA in Hepatic Cirrhosis and Hepatocellular Carcinoma in Hepatitis C Genotype-4 in Egyptian Patients. *Biomed Res Int*; 2017. Epub ahead of print 2017. DOI: 10.1155/2017/1806069.

[202] of Health M. *Egypt Health Issues Survey 2015 [FR313]*.

[203] Elhendawy M, Abo-Ali L, Abd-Elsalam S, et al. HCV and HEV: two players in an Egyptian village, a study of prevalence, incidence, and co-infection. *Environ Sci Pollut Res* 2020; 27: 33659–33667.

[204] Egyptian Ministry of Health. *Viral Hepatitis Plan of Action*. 2018.

[205] Breban R, Doss W, Esmat G, et al. Towards realistic estimates of HCV incidence in Egypt. *J Viral Hepat* 2013; 20: 294–296.

[206] Frank C, Mohamed MK, Strickland GT, et al. The role of parenteral antischistosomal therapy in the spread of hepatitis C virus in Egypt. *Lancet* 2000; 355: 887–891.

[207] Esmat G, El-Sayed MH, Hassany M, et al. One step closer to elimination of hepatitis C in Egypt. *The Lancet Gastroenterology and Hepatology* 2018; 3: 665.

[208] El Kassas M, Elbaz T, Salaheldin M, et al. Impact of treating chronic hepatitis C infection with direct-acting antivirals on the risk of hepatocellular carcinoma: The debate continues – A mini-review. *Journal of Advanced Research* 2019; 17: 43–48.

[209] Zając M, Muszalska I, Sobczak A, et al. Hepatitis C – New drugs and treatment prospects.

European Journal of Medicinal Chemistry 2019; 165: 225–249.

[210] Neddermann P, Tomei L, Steinkühler C, et al. The nonstructural proteins of the hepatitis C virus: Structure and functions. *Biological Chemistry* 1997; 378: 469–476.

[211] Kato N. Genome of human hepatitis C virus (HCV): Gene organization, sequence diversity, and variation. *Microbial and Comparative Genomics* 2000; 5: 129–151.

[212] Penin F, Dubuisson J, Rey FA, et al. Structural biology of hepatitis C virus. *Hepatology* 2004; 39: 5–19.

[213] Ray RB, Martin Lagging L, Meyer K, et al. Transcriptional regulation of cellular and viral promoters by the hepatitis C virus core protein. *Virus Res* 1995; 37: 209–220.

[214] Gawlik K, Gallay PA. HCV core protein and virus assembly: what we know without structures. *Immunol Res* 2014; 60: 1.

[215] Bartosch B, Dubuisson J, Cosset FL. Infectious hepatitis C virus pseudo-particles containing functional E1-E2 envelope protein complexes. *J Exp Med* 2003; 197: 633–642.

[216] Nielsen SU, Bassendine MF, Burt AD, et al. Characterization of the genome and structural proteins of hepatitis C virus resolved from infected human liver. *J Gen Virol* 2004; 85: 1497–1507.

[217] Carrère-Kremer S, Montpellier-Pala C, Cocquerel L, et al. Subcellular Localization and Topology of the p7 Polypeptide of Hepatitis C Virus. *J Virol* 2002; 76: 3720–3730.

[218] Welbourn S, Pause A. HCV NS2/3 Protease. In: Tan S-L (ed) *Hepatitis C Viruses: Genomes and Molecular Biology*. Norfolk (UK): Horizon Bioscience, pp. 151–162.

[219] Grakoui A, McCourt DW, Wychowski C, et al. A second hepatitis C virus-encoded proteinase. *Proc Natl Acad Sci U S A* 1993; 90: 10583–10587.

[220] Grakoui A, Wychowski C, Lin C, et al. Expression and identification of hepatitis C virus polyprotein cleavage products. *J Virol*; 67.

[221] Foy E, Li K, Wang C, et al. Regulation of interferon regulatory factor-3 by the hepatitis C virus serine protease. *Science (80-)* 2003; 300: 1145–1148.

[222] Egger D, Wölk B, Gosert R, et al. Expression of Hepatitis C Virus Proteins Induces Distinct Membrane Alterations Including a Candidate Viral Replication Complex. *J Virol* 2002; 76: 5974–5984.

[223] Gu M, Rice CM. Structures of hepatitis C virus nonstructural proteins required for replicase assembly and function. *Current Opinion in Virology* 2013; 3: 129–136.

[224] World Health Organization. Guidelines for the screening, care and treatment of persons with hepatitis C infection. 2016; 1–135.

[225] Barbaro G, Lorenzo G Di, Soldini M, et al. Evaluation of long-term efficacy of interferon alpha-2b and ribavirin in combination in naive patients with chronic hepatitis C: An Italian multicenter experience. *J Hepatol* 2000; 33: 448–455.

[226] Poynard T, Marcellin P, Lee SS, et al. Randomised trial of interferon α2b plus ribavirin for 48

weeks or for 24 weeks versus interferon α2b plus placebo for 48 weeks for treatment of chronic infection with hepatitis C virus. *Lancet* 1998; 352: 1426–1432.

[227] Palumbo E. Pegylated interferon and ribavirin treatment for hepatitis C virus infection. *Therapeutic Advances in Chronic Disease* 2011; 2: 39–45.

[228] Huang M, Jiang J-D, Peng Z. Recent advances in the anti-HCV mechanisms of interferon. *Acta Pharm Sin B* 2014; 4: 241–247.

[229] Paul D, Madan V, Bartenschlager R. Hepatitis C virus RNA replication and assembly: Living on the fat of the land. *Cell Host and Microbe* 2014; 16: 569–579.

[230] Zhou S, Liu R, Baroudy BM, et al. The effect of ribavirin and IMPDH inhibitors on hepatitis C virus subgenomic replicon RNA. *Virology* 2003; 310: 333–342.

[231] Tam RC, Lau JYN, Hong Z. Mechanisms of action of ribavirin in antiviral therapies. *Antiviral Chemistry and Chemotherapy* 2001; 12: 261–272.

[232] Te HS, Randall G, Jensen DM. Mechanism of action of ribavirin in the treatment of chronic hepatitis C. *Gastroenterology and Hepatology* 2007; 3: 218–225.

[233] Davis GL, Esteban-Mur R, Rustgi V, et al. Interferon Alfa-2b Alone or in Combination with Ribavirin for the Treatment of Relapse of Chronic Hepatitis C. *N Engl J Med* 1998; 339: 1493–1499.

[234] Fried MW, Shiffman ML, Reddy KR, et al. Peginterferon Alfa-2a plus Ribavirin for Chronic Hepatitis C Virus Infection. *N Engl J Med* 2002; 347: 975–982.

[235] Bodenheimer HC, Lindsay KL, Davis GL, et al. Tolerance and efficacy of oral ribavirin treatment of chronic hepatitis C: A multicenter trial. *Hepatology* 1997; 26: 473–477.

[236] Jain MK, Zoellner C. Role of ribavirin in HCV treatment response: Now and in the future. *Expert Opinion on Pharmacotherapy* 2010; 11: 673–683.

[237] McHutchison JG, Gordon SC, Schiff ER, et al. Interferon Alfa-2b Alone or in Combination with Ribavirin as Initial Treatment for Chronic Hepatitis C. *N Engl J Med* 1998; 339: 1485–1492.

[238] Garrison KL, German P, Mogalian E, et al. The drug-drug interaction potential of antiviral agents for the treatment of chronic hepatitis C infection. *Drug Metabolism and Disposition* 2018; 46: 1212–1225.

[239] McCauley JA, Rudd MT. Hepatitis C virus NS3/4a protease inhibitors. *Current Opinion in Pharmacology* 2016; 30: 84–92.

[240] Izquierdo L, Helle F, François C, et al. Simeprevir for the treatment of hepatitis C virus infection. *Pharmacogenomics and Personalized Medicine* 2014; 7: 241–249.

[241] Ali A, Aydin C, Gildemeister R, et al. Evaluating the role of macrocycles in the susceptibility of hepatitis C virus NS3/4A protease inhibitors to drug resistance. *ACS Chem Biol* 2013; 8: 1469–1478.

[242] Liu D, Ji J, Ndongwe TP, et al. Fast hepatitis C virus RNA elimination and NS5A redistribution by NS5A inhibitors studied by a multiplex assay approach. *Antimicrob Agents Chemother* 2015; 59: 3482–3492.

[243] De Clercq E, Li G. Approved antiviral drugs over the past 50 years. *Clinical Microbiology Reviews* 2016; 29: 695–747.

[244] Manns MP, Buti M, Gane E, et al. Hepatitis C virus infection. *Nat Rev Dis Prim* 2017; 3: 1–19.

[245] Wyles DL. Resistance to DAAs: When to Look and When It Matters. *Current HIV/AIDS Reports* 2017; 14: 229–237.

[246] Li G, De Clercq E. Current therapy for chronic hepatitis C: The role of direct-acting antivirals. *Antiviral Research* 2017; 142: 83–122.

[247] Qian XJ, Zhu YZ, Zhao P, et al. Entry inhibitors: New advances in HCV treatment. *Emerging microbes & infections* 2016; 5: e3.

[248] Helle F, Wychowski C, Vu-Dac N, et al. Cyanovirin-N inhibits hepatitis C virus entry by binding to envelope protein glycans. *J Biol Chem* 2006; 281: 25177–25183.

[249] Barth H, Schnober EK, Zhang F, et al. Viral and Cellular Determinants of the Hepatitis C Virus Envelope-Heparan SulfateInteraction. *J Virol* 2006; 80: 10579–10590.

[250] Brimacombe CL, Grove J, Meredith LW, et al. Neutralizing Antibody-Resistant Hepatitis C Virus Cell-to-Cell Transmission. *J Virol* 2011; 85: 596–605.

[251] Lavillette D, Tarr AW, Voisset C, et al. Characterization of host-range and cell entry properties of the major genotypes and subtypes of hepatitis C virus. *Hepatology* 2005; 41: 265–274.

[252] Gottwein JM, Scheel TKH, Jensen TB, et al. Development and characterization of hepatitis C virus genotype 1-7 cell culture systems: Role of CD81 and scavenger receptor class B type I and effect of antiviral drugs. *Hepatology* 2009; 49: 364–377.

[253] Meuleman P, Hesselgesser J, Paulson M, et al. Anti-CD81 antibodies can prevent a hepatitis C virus infection in vivo. *Hepatology* 2008; 48: 1761–1768.

[254] Ji C, Liu Y, Pamulapati C, et al. Prevention of hepatitis C virus infection and spread in human liver chimeric mice by an anti-CD81 monoclonal antibody. *Hepatology* 2015; 61: 1136–1144.

[255] Meertens L, Bertaux C, Dragic T. Hepatitis C Virus Entry Requires a Critical Postinternalization Step and Delivery to Early Endosomes via Clathrin-Coated Vesicles. *J Virol* 2006; 80: 11571–11578.

[256] Tscherne DM, Jones CT, Evans MJ, et al. Time- and Temperature-Dependent Activation of Hepatitis C Virus for Low-pH-Triggered Entry. *J Virol* 2006; 80: 1734–1741.

[257] Ishizu H, Siomi H, Siomi MC. Biology of Piwi-interacting RNAs: New insights into biogenesis and function inside and outside of germlines. *Genes and Development* 2012; 26: 2361–2373.

[258] Ghildiyal M, Zamore PD. Small silencing RNAs: An expanding universe. *Nature Reviews Genetics* 2009; 10: 94–108.

[259] Lee RC, Feinbaum RL, Ambros V. The C. elegans heterochronic gene lin-4 encodes small RNAs with antisense complementarity to lin-14. *Cell* 1993; 75: 843–854.

[260] Filipowicz W, Bhattacharyya SN, Sonenberg N. Mechanisms of post-transcriptional regulation by microRNAs: Are the answers in sight? *Nature Reviews Genetics* 2008; 9: 102–114.

[261] Lee Y, Kim M, Han J, et al. MicroRNA genes are transcribed by RNA polymerase II. *EMBO J* 2004; 23: 4051–4060.

[262] Gregory RI, Yan KP, Amuthan G, et al. The Microprocessor complex mediates the genesis of microRNAs. *Nature* 2004; 432: 235–240.

[263] Denli AM, Tops BBJ, Plasterk RHA, et al. Processing of primary microRNAs by the Microprocessor complex. *Nature* 2004; 432: 231–235.

[264] Han J, Lee Y, Yeom KH, et al. The Drosha-DGCR8 complex in primary microRNA processing. *Genes Dev* 2004; 18: 3016–3027.

[265] Lee Y, Ahn C, Han J, et al. The nuclear RNase III Drosha initiates microRNA processing. *Nature* 2003; 425: 415–419.

[266] Han J, Lee Y, Yeom KH, et al. Molecular Basis for the Recognition of Primary microRNAs by the Drosha-DGCR8 Complex. *Cell* 2006; 125: 887–901.

[267] Burke JM, Kelenis DP, Kincaid RP, et al. A central role for the primary microRNA stem in guiding the position and efficiency of Drosha processing of a viral pri-miRNA. *RNA* 2014; 20: 1068–1077.

[268] Yi R, Qin Y, Macara IG, et al. Exportin-5 mediates the nuclear export of pre-microRNAs and short hairpin RNAs. *Genes Dev* 2003; 17: 3011–3016.

[269] Lund E, Güttinger S, Calado A, et al. Nuclear Export of MicroRNA Precursors. *Science (80-)* 2004; 303: 95–98.

[270] Bohnsack MT, Czaplinski K, Görlich D. Exportin 5 is a RanGTP-dependent dsRNA-binding protein that mediates nuclear export of pre-miRNAs. *RNA* 2004; 10: 185–191.

[271] Bernstein E, Caudy AA, Hammond SM, et al. Role for a bidentate ribonuclease in the initiation step of RNA interference. *Nature* 2001; 409: 363–366.

[272] Chendrimada TP, Gregory RI, Kumaraswamy E, et al. TRBP recruits the Dicer complex to Ago2 for microRNA processing and gene silencing. *Nature* 2005; 436: 740–744.

[273] Bartel DP. MicroRNAs: Target Recognition and Regulatory Functions. *Cell* 2009; 136: 215–233.

[274] Huntzinger E, Izaurralde E. Gene silencing by microRNAs: Contributions of translational repression and mRNA decay. *Nature Reviews Genetics* 2011; 12: 99–110.

[275] Gregory RI, Chendrimada TP, Cooch N, et al. Human RISC couples microRNA biogenesis and posttranscriptional gene silencing. *Cell* 2005; 123: 631–640.

[276] Friedman RC, Farh KKH, Burge CB, et al. Most mammalian mRNAs are conserved targets of microRNAs. *Genome Res* 2009; 19: 92–105.

[277] Lujambio A, Lowe SW. The microcosmos of cancer. *Nature* 2012; 482: 347–355.

[278] Hajarnis S, Lakhia R, Patel V. MicroRNAs and Polycystic Kidney Disease. In: *Polycystic Kidney Disease*. Codon Publications, 2015, pp. 313–334.

[279] Lin S, Gregory RI. MicroRNA biogenesis pathways in cancer. *Nature Reviews Cancer* 2015; 15: 321–333.

[280] BioRender Templates. microRNA in Cancer, https://app.biorender.com/biorender-templates/t-60087a1abb5c0200a2b0d483-microrna-in-cancer (2021, accessed 24 May 2021).

[281] Murakami Y, Yasuda T, Saigo K, et al. Comprehensive analysis of microRNA expression patterns in hepatocellular carcinoma and non-tumorous tissues. *Oncogene* 2006; 25: 2537–2545.

[282] Jiang J, Gusev Y, Aderca I, et al. Association of microRNA expression in hepatocellular carcinomas with hepatitis infection, cirrhosis, and patient survival. *Clin Cancer Res* 2008; 14: 419–427.

[283] Meng F, Henson R, Wehbe-Janek H, et al. MicroRNA-21 Regulates Expression of the PTEN Tumor Suppressor Gene in Human Hepatocellular Cancer. *Gastroenterology* 2007; 133: 647–658.

[284] Pineau P, Volinia S, McJunkin K, et al. miR-221 overexpression contributes to liver tumorigenesis. *Proc Natl Acad Sci U S A* 2010; 107: 264–269.

[285] Wong QWL, Ching AKK, Chan AWH, et al. MiR-222 overexpression confers cell migratory advantages in hepatocellular carcinoma through enhancing AKT signaling. *Clin Cancer Res* 2010; 16: 867–875.

[286] Liang L, Wong CM, Ying Q, et al. MicroRNA-125b suppressesed human liver cancer cell proliferation and metastasis by directly targeting oncogene LIN28B2. *Hepatology* 2010; 52: 1731–1740.

[287] Su H, Yang JR, Xu T, et al. MicroRNA-101, down-regulated in hepatocellular carcinoma, promotes apoptosis and suppresses tumorigenicity. *Cancer Res* 2009; 69: 1135–1142.

[288] Gramantieri L, Ferracin M, Fornari F, et al. Cyclin G1 is a target of miR-122a, a MicroRNA frequently down-regulated in human hepatocellular carcinoma. *Cancer Res* 2007; 67: 6092–6099.

[289] Wang Y, Lu Y, Toh ST, et al. Lethal-7 is down-regulated by the hepatitis B virus x protein and targets signal transducer and activator of transcription 3. *J Hepatol* 2010; 53: 57–66.

[290] Gao P, Wong CCL, Tung EKK, et al. Deregulation of microRNA expression occurs early and accumulates in early stages of HBV-associated multistep hepatocarcinogenesis. *J Hepatol* 2011; 54: 1177–1184.

[291] Wong CM, Wong CCL, Lee JMF, et al. Sequential alterations of microrna expression in hepatocellular carcinoma development and venous metastasis. *Hepatology* 2012; 55: 1453–1461.

[292] Wong CM, Kai AKL, Tsang FHC, et al. Regulation of hepatocarcinogenesis by MicroRNAs. *Frontiers in Bioscience - Elite* 2013; 5 E: 49–60.

[293] Giordano S, Columbano A. MicroRNAs: New tools for diagnosis, prognosis, and therapy in hepatocellular carcinoma? *Hepatology* 2013; 57: 840–847.

[294] Borel F, Konstantinova P, Jansen PLM. Diagnostic and therapeutic potential of miRNA signatures in patients with hepatocellular carcinoma. *Journal of Hepatology* 2012; 56: 1371–1383.

[295] Mizuguchi Y, Takizawa T, Yoshida H, et al. Dysregulated miRNA in progression of hepatocellular carcinoma: A systematic review. *Hepatology Research* 2016; 46: 391–406.

[296] Wong CM, Tsang FH, Ng IOL. Non-coding RNAs in hepatocellular carcinoma: Molecular functions and pathological implications. *Nature Reviews Gastroenterology and Hepatology* 2018; 15: 137–151.

[297] Zhou J, Yu L, Gao X, et al. Plasma microRNA panel to diagnose hepatitis B virus-related hepatocellular carcinoma. *J Clin Oncol* 2011; 29: 4781–4788.

[298] Li LM, Hu Z Bin, Zhou ZX, et al. Serum microRNA profiles serve as novel biomarkers for HBV infection and diagnosis of HBV-positive hepatocarcinoma. *Cancer Res* 2010; 70: 9798–9807.

[299] Wu J, Wu Y, Luo Y, et al. Circulating miRNA-199a and miRNA-122 Levels as Potential Diagnostic and Prognostic Biomarkers for Hepatocellular Carcinoma. *Annals of clinical and laboratory science* 2020; 50: 219–227.

[300] Fang SS, Guo JC, Zhang JH, et al. A P53-related microRNA model for predicting the prognosis of hepatocellular carcinoma patients. *J Cell Physiol* 2020; 235: 3569–3578.

[301] Wang Y, Zhang C, Zhang P, et al. Serum exosomal microRNAs combined with alpha-fetoprotein as diagnostic markers of hepatocellular carcinoma. *Cancer Med* 2018; 7: 1670–1679.

[302] Pezzuto F, Buonaguro L, Buonaguro FM, et al. The role of circulating free DNA and microRNA in non-invasive diagnosis of HBV- and HCV-related hepatocellular carcinoma. *International Journal of Molecular Sciences*; 19. Epub ahead of print 1 April 2018. DOI: 10.3390/ijms19041007.

[303] Morishita A, Fujita K, Iwama H, et al. Role of microRNA-210-3p in hepatitis B virus-related hepatocellular carcinoma. *Am J Physiol - Gastrointest Liver Physiol* 2020; 318: G401–G409.

[304] Li J, Wang Y, Yu W, et al. Expression of serum miR-221 in human hepatocellular carcinoma and its prognostic significance. *Biochem Biophys Res Commun* 2011; 406: 70–73.

[305] Ura S, Honda M, Yamashita T, et al. Differential microRNA expression between hepatitis B and hepatitis C leading disease progression to hepatocellular carcinoma. *Hepatology* 2009; 49: 1098–1112.

[306] Shimakami T, Yamane D, Jangra RK, et al. Stabilization of hepatitis C virus RNA by an Ago2-miR-122 complex. *Proc Natl Acad Sci U S A* 2012; 109: 941–946.

[307] Li Y, Masaki T, Yamane D, et al. Competing and noncompeting activities of miR-122 and the 5' exonuclease Xrn1 in regulation of hepatitis C virus replication. *Proc Natl Acad Sci U S A* 2013; 110: 1881–1886.

[308] Jopling CL, Yi MK, Lancaster AM, et al. Molecular biology: Modulation of hepatitis C virus RNA abundance by a liver-specific MicroRNA. *Science (80-)* 2005; 309: 1577–1581.

[309] Machlin ES, Sarnow P, Sagan SM. Masking the 5' terminal nucleotides of the hepatitis C virus genome by an unconventional microRNA-target RNA complex. *Proc Natl Acad Sci U S A* 2011; 108: 3193–3198.

[310] García-Sastre A, Evans MJ. miR-122 is more than a shield for the hepatitis C virus genome. *Proceedings of the National Academy of Sciences of the United States of America* 2013; 110: 1571–1572.

[311] Luna JM, Scheel TKH, Danino T, et al. Hepatitis C virus RNA functionally sequesters miR-122. *Cell*

2015; 160: 1099–1110.

[312] Murakami Y, Aly HH, Tajima A, et al. Regulation of the hepatitis C virus genome replication by miR-199a*. *J Hepatol* 2009; 50: 453–460.

[313] Pedersen IM, Cheng G, Wieland S, et al. Interferon modulation of cellular microRNAs as an antiviral mechanism. *Nature* 2007; 449: 919–922.

[314] El-Maraghy SA, Adel O, Zayed N, et al. Circulatory miRNA-484, 524, 615 and 628 expression profiling in HCV mediated HCC among Egyptian patients; implications for diagnosis and staging of hepatic cirrhosis and fibrosis. *J Adv Res* 2020; 22: 57–66.

[315] Hassan SS, El-Khazragy N, Elshimy AA, et al. In vitro knock-out of miR-155 suppresses leukemic and HCV virus loads in pediatric HCV-4–associated acute lymphoid leukemia: A promising target therapy. *J Cell Biochem* 2020; 121: 2811–2817.

[316] Bala S, Tilahun Y, Taha O, et al. Increased microRNA-155 expression in the serum and peripheral monocytes in chronic HCV infection. *J Transl Med*; 10. Epub ahead of print 30 July 2012. DOI: 10.1186/1479-5876-10-151.

[317] Zhang Y, Wei W, Cheng N, et al. Hepatitis C virus-induced up-regulation of microRNA-155 promotes hepatocarcinogenesis by activating Wnt signaling. *Hepatology* 2012; 56: 1631–1640.

[318] Wu XM, Xi ZF, Liao P, et al. Diagnostic and prognostic potential of serum microRNA-4651 for patients with hepatocellular carcinoma related to aflatoxin B1. *Oncotarget* 2017; 8: 81235–81249.

[319] Guo X, Lv X, Lv X, et al. Circulating miR-21 serves as a serum biomarker for hepatocellular carcinoma and correlated with distant metastasis. *Oncotarget* 2017; 8: 44050–44058.

[320] Zuo D, Chen L, Liu X, et al. Combination of miR-125b and miR-27a enhances sensitivity and specificity of AFP-based diagnosis of hepatocellular carcinoma. *Tumor Biol* 2016; 37: 6539–6549.

[321] Liu AM, Yao TJ, Wang W, et al. Circulating miR-15b and miR-130b in serum as potential markers for detecting hepatocellular carcinoma: A retrospective cohort study. *BMJ Open*; 2. Epub ahead of print 2012. DOI: 10.1136/bmjopen-2012-000825.

[322] Zheng F, Liao YJ, Cai MY, et al. The putative tumour suppressor microRNA-124 modulates hepatocellular carcinoma cell aggressiveness by repressing ROCK2 and EZH2. *Gut* 2012; 61: 278–289.

[323] Wong CC, Wong C, Tung EK, et al. The MicroRNA miR-139 suppresses metastasis and progression of hepatocellular carcinoma by down-regulating rho-kinase 2. *Gastroenterology* 2011; 140: 322–331.

[324] Ding J, Huang S, Wu S, et al. Gain of miR-151 on chromosome 8q24.3 facilitates tumour cell migration and spreading through downregulating RhoGDIA. *Nat Cell Biol* 2010; 12: 390–399.

[325] Wong CM, Wei L, Au SLK, et al. MiR-200b/200c/429 subfamily negatively regulates Rho/ ROCK signaling pathway to suppress hepatocellular carcinoma metastasis. *Oncotarget* 2015; 6: 13658–13670.

[326] Lin YH, Liao CJ, Huang YH, et al. Thyroid hormone receptor represses miR-17 expression to

enhance tumor metastasis in human hepatoma cells. *Oncogene* 2013; 32: 4509–4518.

[327] Fang JH, Zhou HC, Zeng C, et al. MicroRNA-29b suppresses tumor angiogenesis, invasion, and metastasis by regulating matrix metalloproteinase 2 expression. *Hepatology* 2011; 54: 1729–1740.

[328] Tao ZH, Wan JL, Zeng LY, et al. MiR-612 suppresses the invasive-metastatic cascade in hepatocellular carcinoma. *J Exp Med* 2013; 210: 789–803.

[329] Zhang JP, Zeng C, Xu L, et al. MicroRNA-148a suppresses the epithelial-mesenchymal transition and metastasis of hepatoma cells by targeting Met/Snail signaling. *Oncogene* 2014; 33: 4069–4076.

[330] Brockhausen J, Tay SS, Grzelak CA, et al. miR-181a mediates TGF-β-induced hepatocyte EMT and is dysregulated in cirrhosis and hepatocellular cancer. *Liver Int* 2015; 35: 240–253.

[331] Xia H, Ooi LLPJ, Hui KM. MicroRNA-216a/217-induced epithelial-mesenchymal transition targets PTEN and SMAD7 to promote drug resistance and recurrence of liver cancer. *Hepatology* 2013; 58: 629–641.

[332] Park SM, Gaur AB, Lengyel E, et al. The miR-200 family determines the epithelial phenotype of cancer cells by targeting the E-cadherin repressors ZEB1 and ZEB2. *Genes Dev* 2008; 22: 894–907.

[333] Burk U, Schubert J, Wellner U, et al. A reciprocal repression between ZEB1 and members of the miR-200 family promotes EMT and invasion in cancer cells. *EMBO Rep* 2008; 9: 582–589.

[334] Yang P, Li QJ, Feng Y, et al. TGF-β-miR-34a-CCL22 Signaling-Induced Treg Cell Recruitment Promotes Venous Metastases of HBV-Positive Hepatocellular Carcinoma. *Cancer Cell* 2012; 22: 291–303.

[335] Zhou SL, Hu ZQ, Zhou ZJ, et al. miR-28-5p-IL-34-macrophage feedback loop modulates hepatocellular carcinoma metastasis. *Hepatology* 2016; 63: 1560–1575.

[336] Sehgal A, Vaishnaw A, Fitzgerald K. Liver as a target for oligonucleotide therapeutics. *Journal of Hepatology* 2013; 59: 1354–1359.

[337] Callegari E, Elamin BK, Giannone F, et al. Liver tumorigenicity promoted by microRNA-221 in a mouse transgenic model. *Hepatology* 2012; 56: 1025–1033.

[338] Park JK, Kogure T, Nuovo GJ, et al. miR-221 silencing blocks hepatocellular carcinoma and promotes survival. *Cancer Res* 2011; 71: 7608–7616.

[339] Lanford RE, Hildebrandt-Eriksen ES, Petri A, et al. Therapeutic silencing of microRNA-122 in primates with chronic hepatitis C virus infection. *Science (80-)* 2010; 327: 198–201.

[340] Janssen HLA, Reesink HW, Lawitz EJ, et al. Treatment of HCV Infection by Targeting MicroRNA. *N Engl J Med* 2013; 368: 1685–1694.

[341] Fornari F, Pollutri D, Patrizi C, et al. In hepatocellular carcinoma miR-221 modulates sorafenib resistance through inhibition of caspase-3–mediated apoptosis. *Clin Cancer Res* 2017; 23: 3953–3965.

[342] Kota J, Chivukula RR, O'Donnell KA, et al. Therapeutic microRNA Delivery Suppresses

Tumorigenesis in a Murine Liver Cancer Model. *Cell* 2009; 137: 1005–1017.

[343] Zheng F, Liao YJ, Cai MY, et al. Systemic Delivery of MicroRNA-101 Potently Inhibits Hepatocellular Carcinoma In Vivo by Repressing Multiple Targets. *PLoS Genet* 2015; 11: 1–21.

[344] Li C, Deng M, Hu J, et al. Chronic inflammation contributes to the development of hepatocellular carcinoma by decreasing miR-122 levels. *Oncotarget* 2016; 7: 17021–17034.

[345] National Center of Biotechnology Information Gene Expression Omnibus. GEO Accession viewer, https://www.ncbi.nlm.nih.gov/geo/query/acc.cgi?acc=GSE40744 (accessed 3 May 2021).

[346] Diaz G, Melis M, Tice A, et al. Identification of microRNAs specifically expressed in hepatitis C virus-associated hepatocellular carcinoma. *Int J Cancer* 2013; 133: 816–824.

[347] The Cancer Genome Atlas. The Cancer Genome Atlas - Hepatocellular Carcinoma Study - National Cancer Institute, https://www.cancer.gov/about-nci/organization/ccg/research/structural-genomics/tcga/studied-cancers/liver (accessed 3 May 2021).

[348] Wai CT, Greenson JK, Fontana RJ, et al. A simple noninvasive index can predict both significant fibrosis and cirrhosis in patients with chronic hepatitis C. *Hepatology* 2003; 38: 518–526.

[349] Sterling RK, Lissen E, Clumeck N, et al. Development of a simple noninvasive index to predict significant fibrosis in patients with HIV/HCV coinfection. *Hepatology* 2006; 43: 1317–1325.

[350] Li Y, Chen Y, Zhao Y. The Diagnostic Value of the FIB-4 Index for Staging Hepatitis B-Related Fibrosis: A Meta-Analysis. *PLoS One* 2014; 9: e105728.

[351] Yen Y-H, Kuo F-Y, Kee K-M, et al. APRI and FIB-4 in the evaluation of liver fibrosis in chronic hepatitis C patients stratified by AST level. *PLoS One* 2018; 13: e0199760.

[352] MDCalc. MDCalc - Medical calculators, equations, scores, and guidelines, https://www.mdcalc.com/ (2020, accessed 3 May 2021).

[353] Bedossa P, Poynard T. An algorithm for the grading of activity in chronic hepatitis C. *Hepatology* 1996; 24: 289–293.

[354] Singal AG, Parikh ND, Rich NE, et al. Hepatocellular Carcinoma Surveillance and Staging. Humana, Cham, pp. 27–51.

[355] Li Q, Ren X, Lu C, et al. Evaluation of APRI and FIB-4 for noninvasive assessment of significant fibrosis and cirrhosis in HBeAg-negative CHB patients with ALT≤2 ULN A retrospective cohort study. *Med (United States)* 2017; 96: 12.

[356] Karić U, Pešić-Pavlović I, Stevanović G, et al. FIB-4 and APRI scores for predicting severe fibrosis in chronic hepatitis C - A developing country's perspective in DAA era. *J Infect Dev Ctries* 2018; 12: 178–182.

[357] Nyblom H, Nordlinder H, Olsson R. High aspartate to alanine aminotransferase ratio is an indicator of cirrhosis and poor outcome in patients with primary sclerosing cholangitis. *Liver Int* 2007; 27: 694–699.

[358] Tsoris A, Marlar CA. *Use Of The Child Pugh Score In Liver Disease*. StatPearls Publishing, http://www.ncbi.nlm.nih.gov/pubmed/31194448 (2019, accessed 23 May 2021).

[359] Kim JN, Sohn KM, Kim MY, et al. Relationship between the hepatic venous pressure gradient and first variceal hemorrhage in patients with cirrhosis: a multicenter retrospective study in Korea. *Clin Mol Hepatol* 2012; 18: 391–396.

[360] SPINREACT. Quantitative determination of alanine aminotransferase GPT (ALT), https://www.spinreact.com/files/Inserts/inserts_portugues/BEIS11-P_GPT_ALT_2016.pdf (accessed 3 May 2021).

[361] SPINREACT. Quantitative determination of aspartate aminotransferase GOT (AST), https://www.spinreact.com/files/Inserts/MD/BIOQUIMICA/MDBEIS46_GOT(AST)-LQ_2017.pdf (accessed 3 May 2021).

[362] SPINREACT. Quantitative determination of albumin, http://www.spinreact.com/files/Inserts/SERIE_SPINTECH_(TKB)/Bioquimica/TKBSIS02_ALBUMINA_2019.pdf (accessed 3 May 2021).

[363] RANDOX. Quantitative determination of bilirubin, https://www.betalab-eg.com/wp-content/uploads/2020/06/Br411.pdf (accessed 3 May 2021).

[364] Elecsys Cobas. Modular Analytics E170 Alpha-fetoprotein, http://labogids.sintmaria.be/sites/default/files/files/afp_2018-10_v14.pdf (accessed 3 May 2021).

[365] Livak KJ, Schmittgen TD. Analysis of relative gene expression data using real-time quantitative PCR and the 2-ΔΔCT method. *Methods* 2001; 25: 402–408.

[366] McCall MN, McMurray HR, Land H, et al. On non-detects in qPCR data. *Bioinformatics* 2014; 30: 2310–2316.

[367] Sherina V, McMurray HR, Powers W, et al. Multiple imputation and direct estimation for qPCR data with non-detects. *BMC Bioinformatics*; 21. Epub ahead of print 1 December 2020. DOI: 10.1186/s12859-020-03807-9.

[368] Gevaert AB, Witvrouwen I, Vrints CJ, et al. MicroRNA profiling in plasma samples using qPCR arrays: Recommendations for correct analysis and interpretation. *PLoS One*; 13. Epub ahead of print 1 February 2018. DOI: 10.1371/journal.pone.0193173.

[369] El-Garem H, Ammer A, Shehab H, et al. Circulating microRNA, miR-122 and miR-221 signature in Egyptian patients with chronic hepatitis C related hepatocellular carcinoma. *World J Hepatol* 2014; 6: 818–824.

[370] El-Nady GM, Ling R, Harrison TJ. Gene expression in HCV-associated hepatocellular carcinoma - Upregulation of a gene encoding a protein related to the ubiquitin-conjugating enzyme. *Liver Int* 2003; 23: 329–337.

[371] Alter MJ. Epidemiology of hepatitis C virus infection. *World J Gastroenterol* 2007; 13: 2436–2441.

[372] Lopez PM, Villanueva A, Llovet JM. Systematic review: Evidence-based management of hepatocellular carcinoma - An updated analysis of randomized controlled trials. *Alimentary Pharmacology and Therapeutics* 2006; 23: 1535–1547.

[373] Iwasaki Y, Takaguchi K, Ikeda H, et al. Risk factors for hepatocellular carcinoma in hepatitis C

patients with sustained virologic response to interferon therapy. *Liver Int* 2004; 24: 603–610.

[374] Aleman S, Rahbin N, Weiland O, et al. A risk for hepatocellular carcinoma persists long-term after sustained virologic response in patients with hepatitis C-associated liver cirrhosis. *Clin Infect Dis* 2013; 57: 230–236.

[375] Toyoda H, Kumada T, Tada T, et al. Risk factors of hepatocellular carcinoma development in non-cirrhotic patients with sustained virologic response for chronic hepatitis C virus infection. *J Gastroenterol Hepatol* 2015; 30: 1183–1189.

[376] Makiyama A, Itoh Y, Kasahara A, et al. Characteristics of patients with chronic hepatitis C who develop hepatocellular carcinoma after a sustained response to interferon therapy. *Cancer* 2004; 101: 1616–1622.

[377] Giannitrapani L, Soresi M, La Spada E, et al. Sex hormones and risk of liver tumor. In: *Annals of the New York Academy of Sciences*. Blackwell Publishing Inc., pp. 228–236.

[378] Yi SW, Choi JS, Yi JJ, et al. Risk factors for hepatocellular carcinoma by age, sex, and liver disorder status: A prospective cohort study in Korea. *Cancer* 2018; 124: 2748–2757.

[379] Shi KQ, Lin Z, Chen XJ, et al. Hepatocellular carcinoma associated microRNA expression signature: Integrated bioinformatics analysis, experimental validation and clinical significance. *Oncotarget* 2015; 6: 25093–25108.

[380] Shen J, Siegel AB, Remotti H, et al. Identifying microRNA panels specifically associated with hepatocellular carcinoma and its different etiologies. *Hepatoma Res* 2016; 2: 151.

[381] Wu L, Cai C, Wang X, et al. MicroRNA-142-3p, a new regulator of RAC1, suppresses the migration and invasion of hepatocellular carcinoma cells. *FEBS Lett* 2011; 585: 1322–1330.

[382] Lyu P, Zhai Z, Hao Z, et al. CircWHSC1 serves as an oncogene to promote hepatocellular carcinoma progression. *Eur J Clin Invest*. Epub ahead of print 27 April 2021. DOI: 10.1111/eci.13487.

[383] Shi KQ, Lin Z, Chen XJ, et al. Hepatocellular carcinoma associated microRNA expression signature: Integrated bioinformatics analysis, experimental validation and clinical significance. *Oncotarget* 2015; 6: 25093–25108.

[384] Sun W, Zhang Z, Wang J, et al. MicroRNA-150 suppresses cell proliferation and metastasis in hepatocellular carcinoma by inhibiting the GAB1-ERK axis. *Oncotarget* 2016; 7: 11595–11608.

[385] Murakami Y, Yasuda T, Saigo K, et al. Comprehensive analysis of microRNA expression patterns in hepatocellular carcinoma and non-tumorous tissues. *Oncogene* 2006; 25: 2537–2545.

[386] Ashmawy AM, Elgeshy KM, Abdel Salam EST, et al. Crosstalk between liver-related microRNAs and Wnt/β-catenin pathway in hepatocellular carcinoma patients. *Arab J Gastroenterol* 2017; 18: 144–150.

[387] Yu L, Ding GF, He C, et al. MicroRNA-424 is down-regulated in hepatocellular carcinoma and suppresses cell migration and invasion through c-Myb. *PLoS One*; 9. Epub ahead of print 27 March 2014. DOI: 10.1371/journal.pone.0091661.

[388] Hu WY, Wei HY, Liu LY, et al. miR-3607, a biomarker of hepatocellular carcinoma invasion and

aggressiveness: Its relationship with epithelial-mesenchymal transition process. *IUBMB Life* 2020; 72: 1686–1697.

[389] Fu Y, Sun L-Q, Huang Y, et al. miR-142-3p Inhibits the Metastasis of Hepatocellular Carcinoma Cells by Regulating HMGB1 Gene Expression. *Curr Mol Med* 2018; 18: 135–141.

[390] Tsang FHC, Au SLK, Wei L, et al. MicroRNA-142-3p and microRNA-142-5p are downregulated in hepatocellular carcinoma and exhibit synergistic effects on cell motility. *Front Med* 2015; 9: 331–343.

[391] He C, Liu Z, Jin L, et al. LncRNA TUG1-Mediated miR-142-3p Downregulation Contributes to Metastasis and the Epithelial-to-Mesenchymal Transition of Hepatocellular Carcinoma by Targeting ZEB1. *Cell Physiol Biochem* 2018; 48: 1928–1941.

[392] Li T, Xie J, Shen C, et al. miR-150-5p inhibits hepatoma cell migration and invasion by targeting MMP14. *PLoS One*; 9. Epub ahead of print 30 December 2014. DOI: 10.1371/journal.pone.0115577.

[393] Cui X, Jiang X, Wei C, et al. Astragaloside IV suppresses development of hepatocellular carcinoma by regulating miR-150-5p/β-catenin axis. *Environ Toxicol Pharmacol*; 78. Epub ahead of print 1 August 2020. DOI: 10.1016/j.etap.2020.103397.

[394] Hou J, Lin L, Zhou W, et al. Identification of miRNomes in Human Liver and Hepatocellular Carcinoma Reveals miR-199a/b-3p as Therapeutic Target for Hepatocellular Carcinoma. *Cancer Cell* 2011; 19: 232–243.

[395] Giovannini C, Fornari F, Dallo R, et al. MiR-199-3p replacement affects E-cadherin expression through Notch1 targeting in hepatocellular carcinoma. *Acta Histochem* 2018; 120: 95–102.

[396] Zhan Y, Zheng N, Teng F, et al. MiR-199a/b-5p inhibits hepatocellular carcinoma progression by post-transcriptionally suppressing ROCK1. *Oncotarget* 2017; 8: 67169–67180.

[397] Yao J, Fu J, Liu Y, et al. LncRNA CASC9 promotes proliferation, migration and inhibits apoptosis of hepatocellular carcinoma cells by down-regulating miR-424-5p. *Ann Hepatol*; 23. Epub ahead of print 1 July 2021. DOI: 10.1016/j.aohep.2020.100297.

[398] Shen X, Li Y, He F, et al. LncRNA CDKN2B-AS1 promotes cell viability, migration, and invasion of hepatocellular carcinoma via sponging mir-424-5p. *Cancer Manag Res* 2020; 12: 6807–6819.

[399] Du H, Xu Q, Xiao S, et al. MicroRNA-424-5p acts as a potential biomarker and inhibits proliferation and invasion in hepatocellular carcinoma by targeting TRIM29. *Life Sci* 2019; 224: 1–11.

[400] Dou W, Yang M, Su Y, et al. Dysregulation of miR-3607 predicts prognosis of hepatocellular carcinoma and regulates tumor cell proliferation, migration and invasion. *Diagn Pathol*; 15. Epub ahead of print 13 May 2020. DOI: 10.1186/s13000-020-00973-5.

[401] Lou W, Chen J, Ding B, et al. XIAP, commonly targeted by tumor suppressive miR-3607-5p and miR-3607-3p, promotes proliferation and inhibits apoptosis in hepatocellular carcinoma. *Genomics* 2021; 113: 933–945.

[402] Zhang J, Luo N, Luo Y, et al. MicroRNA-150 inhibits human CD133-positive liver cancer stem cells through negative regulation of the transcription factor c-Myb. *Int J Oncol* 2012; 40: 747–756.

[403] Xu H, Huang J, Hua S, et al. Interactome analysis of gene expression profiles identifies CDC6 as a potential therapeutic target modified by miR-215-5p in hepatocellular carcinoma. *Int J Med Sci* 2020; 17: 2926–2940.

[404] Zhao Y, Zhu C, Chang Q, et al. MiR-424-5p regulates cell cycle and inhibits proliferation of hepatocellular carcinoma cells by targeting E2F7. *PLoS One* 2020; 15: e0242179.

[405] Yang H, Zheng W, Shuai X, et al. MicroRNA-424 inhibits Akt3/E2F3 axis and tumor growth in hepatocellular carcinoma. *Oncotarget* 2015; 6: 27736–27750.

[406] Wu L, Yang F, Lin B, et al. MicroRNA-424 expression predicts tumor recurrence in patients with hepatocellular carcinoma following liver transplantation. *Oncol Lett* 2018; 15: 9126–9132.

[407] Wang J, Zhang Y, Lu L, et al. Insight into the molecular mechanism of LINC00152/miR-215/CDK13 axis in hepatocellular carcinoma progression. *J Cell Biochem* 2019; 120: 18816–18825.

[408] Hua S, Liu C, Liu L, et al. miR-142-3p inhibits aerobic glycolysis and cell proliferation in hepatocellular carcinoma via targeting LDHA. *Biochem Biophys Res Commun* 2018; 496: 947–954.

[409] Liang Z, Gao Y, Shi W, et al. Expression and significance of MicroRNA-183 in hepatocellular carcinoma. *Sci World J*; 2013. Epub ahead of print 2013. DOI: 10.1155/2013/381874.

[410] Wang W, Zhao LJ, Tan YX, et al. Identification of deregulated miRNAs and their targets in hepatitis B virus-associated hepatocellular carcinoma. *World J Gastroenterol* 2012; 18: 5442–5453.

[411] Ladeiro Y, Couchy G, Balabaud C, et al. MicroRNA profiling in hepatocellular tumors is associated with clinical features and oncogene/tumor suppressor gene mutations. *Hepatology* 2008; 47: 1955–1963.

[412] Li J, Fu H, Xu C, et al. MiR-183 inhibits TGF-β1-induced apoptosis by downregulation of PDCD4 expression in human hepatocellular carcinoma cells. *BMC Cancer*; 10. Epub ahead of print 6 July 2010. DOI: 10.1186/1471-2407-10-354.

[413] Duan X, Li W, Hu P, et al. MicroRNA-183-5p contributes to malignant progression through targeting PDCD4 in human hepatocellular carcinoma. *Biosci Rep*; 40. Epub ahead of print 30 October 2020. DOI: 10.1042/BSR20201761.

[414] Goeppert B, Schmezer P, Dutruel C, et al. Down-regulation of tumor suppressor a kinase anchor protein 12 in human hepatocarcinogenesis by epigenetic mechanisms. *Hepatology* 2010; 52: 2023–2033.

[415] Leung WKC, He M, Chan AWH, et al. Wnt/β-Catenin activates MiR-183/96/182 expression in hepatocellular carcinoma that promotes cell invasion. *Cancer Lett* 2015; 362: 97–105.

[416] Sun J, Liu L, Zou H, et al. The long non-coding rna casc2 suppresses cell viability, migration, and invasion in hepatocellular carcinoma cells by directly downregulating mir-183. *Yonsei Med J* 2019; 60: 905–913.

[417] Jiang C, Yu M, Xie X, et al. MiR-217 targeting DKK1 promotes cancer stem cell properties via activation of the Wnt signaling pathway in hepatocellular carcinoma. *Oncol Rep* 2017; 38: 2351–2359.

[418] Xia H, Ooi LLPJ, Hui KM. MicroRNA-216a/217-induced epithelial-mesenchymal transition targets PTEN and SMAD7 to promote drug resistance and recurrence of liver cancer. *Hepatology* 2013; 58: 629–641.

[419] Yu L, Zhang J, Guo X, et al. MicroRNA-224 upregulation and AKT activation synergistically predict poor prognosis in patients with hepatocellular carcinoma. *Cancer Epidemiol* 2014; 38: 408–413.

[420] Liu M, Liu J, Wang L, et al. Association of serum microRNA expression in hepatocellular carcinomas treated with transarterial chemoembolization and patient survival. *PLoS One*; 9. Epub ahead of print 2 October 2014. DOI: 10.1371/journal.pone.0109347.

[421] Ma D, Tao X, Gao F, et al. miR-224 functions as an onco-miRNA in hepatocellular carcinoma cells by activating AKT signaling. *Oncol Lett* 2012; 4: 483–488.

[422] Miao K, Liu S Da, Huang WX, et al. Mir-224 executes a tumor accelerative role during hepatocellular carcinoma malignancy by targeting cytoplasmic polyadenylation element-binding protein 3. *Pharmacology* 2020; 105: 477–487.

[423] El-Guendy NM, Helwa R, El-Halawany MS, et al. The liver microRNA expression profiles associated with chronic hepatitis C virus (HCV) genotype-4 infection: A preliminary study. *Hepat Mon* 2016; 16: 33881.

[424] Wang Y, Liang Z, Gao Y, et al. Factors influencing circulating microRNA level in the studies of hepatocellular carcinoma biomarker. *Neoplasma* 2015; 62: 798–804.

[425] Bharali D, Jebur HB, Baishya D, et al. Expression analysis of serum microRNA-34a and microRNA-183 in hepatocellular carcinoma. *Asian Pacific J Cancer Prev* 2018; 19: 2561–2568.

[426] Gui J, Tian Y, Wen X, et al. Serum microRNA characterization identifies miR-885-5p as a potential marker for detecting liver pathologies. *Clin Sci* 2011; 120: 183–193.

[427] Li J, Jin B, Wang T, et al. Serum microRNA expression profiling identifies serum biomarkers for HCV-related hepatocellular carcinoma. *Cancer Biomarkers* 2019; 26: 501–512.

[428] Yoon EL, Yeon JE, Ko E, et al. An explorative analysis for the role of serum mir-10b-3p levels in predicting response to sorafenib in patients with advanced hepatocellular carcinoma. *J Korean Med Sci* 2017; 32: 212–220.

[429] Zhuang LP, Meng ZQ. Serum miR-224 reflects stage of hepatocellular carcinoma and predicts survival. *Biomed Res Int*; 2015. Epub ahead of print 22 January 2015. DOI: 10.1155/2015/731781.

[430] Yang L, Wei C, Li Y, et al. MiR-224 is an early-stage biomarker of hepatocellular carcinoma with miR-224 and miR-125b as prognostic biomarkers. *Biomarkers in Medicine* 2020; 14: 1485–1500.

[431] Ali LH, Higazi AM, Moness HM, et al. Clinical significances and diagnostic utilities of both miR-215 and squamous cell carcinoma antigen-IgM versus alpha-fetoprotein in egyptian patients with hepatitis C virus-induced hepatocellular carcinoma. *Clin Exp Gastroenterol* 2019; 12: 51–66.

[432] Mamdouh S, Khorshed F, Aboushousha T, et al. Evaluation of Mir-224, Mir-215 and Mir-143 as Serum biomarkers for HCV associated Hepatocellular carcinoma. *Asian Pacific J Cancer Prev* 2017; 18: 3167–3171.

[433] Zhang Z qing, Meng H, Wang N, et al. Serum microRNA 143 and microRNA 215 as potential biomarkers for the diagnosis of chronic hepatitis and hepatocellular carcinoma. *Diagn Pathol* 2014; 9: 135.

[434] Ali S, Alahmady Z, Yamany H, et al. Serum Expression Levels of miR-141 and miR-215 for Differentiation between Liver Cirrhosis, Chronic Hepatitis C and Hepatocellular Carcinoma Patients. *Microbiol Res J Int* 2017; 20: 1–12.

[435] Cabral BCA, Hoffmann L, Bottaro T, et al. Circulating microRNAs associated with liver fibrosis in chronic hepatitis C patients. *Biochem Biophys Reports*; 24. Epub ahead of print 1 December 2020. DOI: 10.1016/j.bbrep.2020.100814.

[436] Wang Y, Zhang C, Zhang P, et al. Serum exosomal microRNAs combined with alpha-fetoprotein as diagnostic markers of hepatocellular carcinoma. *Cancer Med* 2018; 7: 1670–1679.

[437] Devhare PB, Steele R, Bisceglie AMD, et al. Differential expression of MicroRNAs in hepatitis C virus-mediated liver disease between African Americans and Caucasians: Implications for racial health disparities. *Gene Expr* 2017; 17: 89–98.

[438] Shaheen NMH, Zayed N, Riad NM, et al. Role of circulating miR-182 and miR-150 as biomarkers for cirrhosis and hepatocellular carcinoma post HCV infection in Egyptian patients. *Virus Res* 2018; 255: 77–84.

[439] Zhang S, Ouyang X, Jiang X, et al. Dysregulated serum microRNA expression profile and potential biomarkers in hepatitis C virus-infected patients. *Int J Med Sci* 2015; 12: 590–598.

[440] Yao H, Liu X, Chen S, et al. Decreased expression of serum miR-424 correlates with poor prognosis of patients with hepatocellular carcinoma. *Int J Clin Exp Pathol* 2015; 8: 14830–14835.

[441] B Y, E G, D T, et al. Role of mir-33a, mir-203b, mir-361-3p, mir-424 in hepatocellular carcinoma. *TURKISH J Med Sci*; 51. Epub ahead of print 2021. DOI: 10.3906/sag-2004-214.

[442] Khairy RMM, Hmmad SS, Sayed M, et al. Serum MicroRNAs as predictors for fibrosis progression and response to direct-acting antivirals treatment in hepatitis C virus genotype-4 Egyptian patients. *Int J Clin Pract*; 75. Epub ahead of print 1 April 2021. DOI: 10.1111/ijcp.13954.

[443] Kamel RR, Amr KS, Afify M, et al. Relation between microRNAs and apoptosis in hepatocellular carcinoma. *Open Access Maced J Med Sci* 2016; 4: 31–37.

[444] Murakami Y, Aly HH, Tajima A, et al. Regulation of the hepatitis C virus genome replication by miR-199a*. *J Hepatol* 2009; 50: 453–460.

[445] Murakami Y, Yasuda T, Saigo K, et al. Comprehensive analysis of microRNA expression patterns in hepatocellular carcinoma and non-tumorous tissues. *Oncogene* 2006; 25: 2537–2545.

[446] Jia XQ, Cheng HQ, Qian X, et al. Lentivirus-Mediated Overexpression of MicroRNA-199a Inhibits Cell Proliferation of Human Hepatocellular Carcinoma. *Cell Biochem Biophys* 2012; 62: 237–244.

[447] Wu X, Xia M, Chen D, et al. Profiling of downregulated blood-circulating miR-150-5p as a novel tumor marker for cholangiocarcinoma. *Tumor Biol* 2016; 37: 15019–15029.

[448] Wang S, Yin J, Li T, et al. Upregulated circulating miR-150 is associated with the risk of intrahepatic cholangiocarcinoma. *Oncol Rep* 2015; 33: 819–825.

[449] Gao W, Pang D, Yu S. Serum level of miR-142-3p predicts prognostic outcome for colorectal cancer following curative resection. *J Int Med Res* 2019; 47: 2116–2125.

[450] Lin X, Zhang S, Huo Z. Serum circulating miR-150 is a predictor of post-acute myocardial infarction heart failure. *Int Heart J* 2019; 60: 280–286.

[451] Zhao YJ, Song X, Niu L, et al. Circulating exosomal mir-150-5p and mir-99b-5p as diagnostic biomarkers for colorectal cancer. *Front Oncol*; 9. Epub ahead of print 2019. DOI: 10.3389/fonc.2019.01129.

[452] Yilmaz N, Yilmaz U, Tanbek K, et al. The role of miRNAs targeting K-ras and APC genes in colorectal cancer. *Bratislava Med J* 2020; 121: 554–557.

[453] Yu B, Du Q, Li H, et al. Diagnostic potential of serum exosomal colorectal neoplasia differentially expressed long non-coding RNA (CRNDE-p) and microRNA-217 expression in colorectal carcinoma. *Oncotarget* 2017; 8: 83745–83753.

[454] Lei L, Zhao X, Liu S, et al. MicroRNA-3607 inhibits the tumorigenesis of colorectal cancer by targeting DDI2 and regulating the DNA damage repair pathway. *Apoptosis* 2019; 24: 662–672.

[455] Sun H, Shi K, Qi K, et al. Corrigendum: Natural Killer Cell-Derived Exosomal miR-3607-3p Inhibits Pancreatic Cancer Progression by Targeting IL-26 (Frontiers in Immunology, (2019), 10,(2819), 10.3389/fimmu.2019.02819). *Frontiers in Immunology*; 11. Epub ahead of print 21 February 2020. DOI: 10.3389/fimmu.2020.00277.

[456] Qu K, Zhang X, Lin T, et al. Circulating miRNA-21-5p as a diagnostic biomarker for pancreatic cancer: Evidence from comprehensive miRNA expression profiling analysis and clinical validation. *Sci Rep*; 7. Epub ahead of print 1 December 2017. DOI: 10.1038/s41598-017-01904-z.

[457] Liu R, Zheng S, Yu K, et al. Prognostic value of miR-142 in solid tumors: a meta-analysis. *Biosci Rep* 2021; 41: 20204043.

[458] Li N, Zhang QY, Zou JL, et al. miR-215 promotes malignant progression of gastric cancer by targeting RUNX1. *Oncotarget* 2016; 7: 4817–4828.

[459] Liu Y-P, Sun X-H, Cao X-L, et al. *MicroRNA-217suppressed EMT in gastric cancer metastasis*.

[460] Ozawa PMM, Vieira E, Lemos DS, et al. Identification of miRNAs enriched in extracellular vesicles derived from serum samples of breast cancer patients. *Biomolecules*; 10. Epub ahead of print 1 January 2020. DOI: 10.3390/biom10010150.

[461] Zhou S-W, Su B-B, Zhou Y, et al. Aberrant miR-215 expression is associated with clinical outcome in breast cancer patients. DOI: 10.1007/s12032-014-0259-2.

[462] van Schooneveld E, Wouters MCA, Van der Auwera I, et al. Expression profiling of cancerous and normal breast tissues identifies microRNAs that are differentially expressed in serum from patients with (metastatic) breast cancer and healthy volunteers. *Breast Cancer Res* 2012; 14: R34.

[463] Wu J, Jiang Z, Chen C, et al. CircIRAK3 sponges miR-3607 to facilitate breast cancer metastasis. *Cancer Lett* 2018; 430: 179–192.

[464] Zhang K, Liu H, Song Z, et al. The UPR Transducer IRE1 Promotes Breast Cancer Malignancy by

Degrading Tumor Suppressor microRNAs. *iScience*; 23. Epub ahead of print 25 September 2020. DOI: 10.1016/j.isci.2020.101503.

[465] El-Tawdi AHF, Matboli M, Shehata HH, et al. Evaluation of Circulatory RNA-Based Biomarker Panel in Hepatocellular Carcinoma. *Mol Diagnosis Ther* 2016; 20: 265–277.

[466] Ghosh A, Ghosh A, Datta S, et al. Hepatic miR-126 is a potential plasma biomarker for detection of hepatitis B virus infected hepatocellular carcinoma. *Int J Cancer* 2016; 138: 2732–2744.

[467] Chai S, Tong M, Ng KY, et al. Regulatory role of miR-142-3p on the functional hepatic cancer stem cell marker CD133. *Oncotarget* 2014; 5: 5725–5735.

[468] Shi KQ, Lin Z, Chen XJ, et al. Hepatocellular carcinoma associated microRNA expression signature: Integrated bioinformatics analysis, experimental validation and clinical significance. *Oncotarget* 2015; 6: 25093–25108.

[469] Xu Y, Luo X, He W, et al. Long Non-Coding RNA PVT1/miR-150/HIG2 Axis Regulates the Proliferation, Invasion and the Balance of Iron Metabolism of Hepatocellular Carcinoma. *Cell Physiol Biochem* 2018; 49: 1403–1419.

[470] Yu F, Lu Z, Chen B, et al. microRNA-150: A promising novel biomarker for hepatitis B virus-related hepatocellular carcinoma. *Diagn Pathol*; 10. Epub ahead of print 28 July 2015. DOI: 10.1186/s13000-015-0369-y.

[471] Li T, Xie J, Shen C, et al. Amplification of long noncoding RNA ZFAS1 promotes metastasis in hepatocellular carcinoma. *Cancer Res* 2015; 75: 3181–3191.

[472] Ji J, Zheng X, Forgues M, et al. Identification of microRNAs specific for epithelial cell adhesion molecule-positive tumor cells in hepatocellular carcinoma. *Hepatology* 2015; 62: 829–840.

[473] Bian W, Zhang H, Tang M, et al. Potential Role of microRNA-183 as a tumor suppressor in hepatocellular carcinoma. *Cell Physiol Biochem* 2018; 51: 2065–2072.

[474] Mariotti A, Perotti A, Sessa C, et al. N-cadherin as a therapeutic target in cancer. *Expert Opin Investig Drugs* 2007; 16: 451–465.

[475] Xu C, Luo L, Yu Y, et al. Screening therapeutic targets of ribavirin in hepatocellular carcinoma. *Oncol Lett* 2018; 15: 9625–9632.

[476] Murakami Y, Toyoda H, Tanaka M, et al. The progression of liver fibrosis is related with overexpression of the miR-199 and 200 families. *PLoS One*; 6. Epub ahead of print 2011. DOI: 10.1371/journal.pone.0016081.

[477] Hou J, Lin L, Zhou W, et al. Identification of miRNomes in Human Liver and Hepatocellular Carcinoma Reveals miR-199a/b-3p as Therapeutic Target for Hepatocellular Carcinoma. *Cancer Cell* 2011; 19: 232–243.

[478] Qu KZ, Zhang K, Li H, et al. Circulating MicroRNAs as biomarkers for hepatocellular carcinoma. *J Clin Gastroenterol* 2011; 45: 355–360.

[479] Lou Z, Gong YQ, Zhou X, et al. Low expression of miR-199 in hepatocellular carcinoma contributes to tumor cell hyper-proliferation by negatively suppressing XBP1. *Oncol Lett* 2018; 16: 6531–6539.

[480] El-Halawany MS, Ismail HM, Zeeneldin AA, et al. Investigating the pretreatment miRNA expression patterns of advanced hepatocellular carcinoma patients in association with response to TACE treatment. *Biomed Res Int*; 2015. Epub ahead of print 25 February 2015. DOI: 10.1155/2015/649750.

[481] Ogawa T, Enomoto M, Fujii H, et al. MicroRNA-221/222 upregulation indicates the activation of stellate cells and the progression of liver fibrosis. *Gut* 2012; 61: 1600–1609.

[482] Amr KS, Ezzat WM, Elhosary YA, et al. The potential role of miRNAs 21 and 199-a in early diagnosis of hepatocellular carcinoma. *Gene* 2016; 575: 66–70.

[483] Yin J, Hou P, Wu Z, et al. Circulating miR-375 and miR-199a-3p as potential biomarkers for the diagnosis of hepatocellular carcinoma. *Tumor Biol* 2015; 36: 4501–4507.

[484] Zekri ARN, Youssef ASED, El-Desouky ED, et al. Serum microRNA panels as potential biomarkers for early detection of hepatocellular carcinoma on top of HCV infection. *Tumor Biol* 2016; 37: 12273–12286.

[485] El Mahdy HA, Abdelhamid IA, Amen AI, et al. MicroRNA-215 as a diagnostic marker in Egyptian patients with hepatocellular carcinoma. *Asian Pacific J Cancer Prev* 2019; 20: 2723–2731.

[486] Zhang M, Li M, Li N, et al. MiR-217 suppresses proliferation, migration, and invasion promoting apoptosis via targeting MTDH in hepatocellular carcinoma. *Oncol Rep* 2017; 37: 1772–1778.

[487] Su J, Wang Q, Liu Y, et al. miR-217 inhibits invasion of hepatocellular carcinoma cells through direct suppression of E2F3. *Mol Cell Biochem* 2014; 392: 289–296.

[488] Tian YW, Shen Q, Jiang QF, et al. Decreased levels of MIR-34a and MIR-217 act as predictor biomarkers of aggressive progression and poor prognosis in hepatocellular carcinoma. *Minerva Med* 2017; 108: 108–113.

[489] Wang W, Zhao LJ, Tan YX, et al. MiR-138 induces cell cycle arrest by targeting cyclin D3 in hepatocellular carcinoma. *Carcinogenesis* 2012; 33: 1113–1120.

[490] Fu X, Zhang J, He X, et al. Circular RNA MAN2B2 promotes cell proliferation of hepatocellular carcinoma cells via the miRNA-217/ MAPK1 axis. *J Cancer* 2020; 11: 3318–3326.

[491] Amr KS, Elmawgoud Atia HA, Elazeem Elbnhawy RA, et al. Early diagnostic evaluation of miR-122 and miR-224 as biomarkers for hepatocellular carcinoma. *Genes Dis* 2017; 4: 215–221.

[492] Liu HN, Wu H, Chen YJ, et al. Serum microRNA signatures and metabolomics have high diagnostic value in hepatocellular carcinoma. *Oncotarget* 2017; 8: 108810–108824.

[493] Shen J, Siegel AB, Remotti H, et al. Identifying microRNA panels specifically associated with hepatocellular carcinoma and its different etiologies. *Hepatoma Res* 2016; 2: 151.

[494] Zhang Y, Li T, Guo P, et al. MiR-424-5p reversed epithelial-mesenchymal transition of anchorage-independent HCC cells by directly targeting ICAT and suppressed HCC progression. *Sci Rep*; 4. Epub ahead of print 1 September 2014. DOI: 10.1038/srep06248.

[495] Shang A, Gu C, Wang W, et al. Exosomal circPACRGL promotes progression of colorectal cancer via the miR-142-3p/miR-506-3p-TGF-β1 axis. *Mol Cancer*; 19. Epub ahead of print 27 July 2020. DOI: 10.1186/s12943-020-01235-0.

[496] Troschel FM, Böhly N, Borrmann K, et al. miR-142-3p attenuates breast cancer stem cell characteristics and decreases radioresistance in vitro. *Tumor Biol*; 40. Epub ahead of print 1 August 2018. DOI: 10.1177/1010428318791887.

[497] Fan H, Liu X, Zheng WW, et al. Retraction: MiR-150 alleviates EMT and cell invasion of colorectal cancer through targeting Gli1 (European review for medical and pharmacological sciences (2017) 21 21 (4853-4859) PII: 22181). *European review for medical and pharmacological sciences* 2020; 24: 7544.

[498] Chen X, Xu X, Pan B, et al. miR-150-5p suppresses tumor progression by targeting VEGFA in colorectal cancer. *Aging (Albany NY)* 2018; 10: 3421–3437.

[499] Shang A, Wang X, Gu C, et al. Exosomal miR-183-5p promotes angiogenesis in colorectal cancer by regulation of FOXO1. *Aging (Albany NY)* 2020; 12: 8352–8371.

[500] Afshar S, Najafi R, Sedighi Pashaki A, et al. MiR-185 enhances radiosensitivity of colorectal cancer cells by targeting IGF1R and IGF2. *Biomed Pharmacother* 2018; 106: 763–769.

[501] Zhu L, Zhou X, Li S, et al. miR-183-5p attenuates cerebral ischemia injury by negatively regulating PTEN. *Mol Med Rep* 2020; 22: 3944–3954.

[502] Liu T, Zhang X, Wang Y. MiR-183-3p suppresses proliferation and migration of keratinocyte in psoriasis by inhibiting GAB1. *Hereditas*; 157. Epub ahead of print 10 July 2020. DOI: 10.1186/s41065-020-00138-w.

[503] Zhou J, Zhang C, Zhou B, et al. MiR-183 modulated cell proliferation and apoptosis in ovarian cancer through the TGF-β/Smad4 signaling pathway. *Int J Mol Med* 2019; 43: 1734–1746.

[504] Ahmadi A, Khansarinejad B, Hosseinkhani S, et al. miR-199a-5p and miR-495 target GRP78 within UPR pathway of lung cancer. *Gene* 2017; 620: 15–22.

[505] Hua Q, Jin M, Mi B, et al. LINC01123, a c-Myc-activated long non-coding RNA, promotes proliferation and aerobic glycolysis of non-small cell lung cancer through miR-199a-5p/c-Myc axis. *J Hematol Oncol*; 12. Epub ahead of print 5 September 2019. DOI: 10.1186/s13045-019-0773-y.

[506] Liao K, Lin Y, Gao W, et al. Blocking lncRNA MALAT1/miR-199a/ZHX1 Axis Inhibits Glioblastoma Proliferation and Progression. *Mol Ther - Nucleic Acids* 2019; 18: 388–399.

[507] Yang X, Ma L, Wei R, et al. Twist1-induced miR-199a-3p promotes liver fibrosis by suppressing caveolin-2 and activating TGF-β pathway. *Signal Transduct Target Ther*; 5. Epub ahead of print 1 December 2020. DOI: 10.1038/s41392-020-0169-z.

[508] Li DJ, Wang X, Yin WH, et al. MiR-199a-5p suppresses proliferation and invasion of human laryngeal cancer cells. *Eur Rev Med Pharmacol Sci* 2020; 24: 12200–12207.

[509] Ma C, Wang X, Yang F, et al. Circular RNA hsa_circ_0004872 inhibits gastric cancer progression via the miR-224/Smad4/ADAR1 successive regulatory circuit. *Mol Cancer*; 19. Epub ahead of print 1 December 2020. DOI: 10.1186/s12943-020-01268-5.

[510] Yang C, Yuan W, Yang X, et al. Circular RNA circ-ITCH inhibits bladder cancer progression by sponging miR-17/miR-224 and regulating p21, PTEN expression. *Mol Cancer*; 17. Epub ahead of print 31 January 2018. DOI: 10.1186/s12943-018-0771-7.

[511] Chen X, Lou N, Ruan A, et al. miR-224/miR-141 ratio as a novel diagnostic biomarker in renal cell carcinoma. *Oncol Lett* 2018; 16: 1666–1674.

[512] Gan BL, Zhang LJ, Gao L, et al. Downregulation of miR-224-5p in prostate cancer and its relevant molecular mechanism via TCGA, GEO database and in silico analyses. *Oncol Rep* 2018; 40: 3171–3188.

[513] Li J, Liu X, Li C, et al. miR-224-5p inhibits proliferation, migration, and invasion by targeting PIK3R3/AKT3 in uveal melanoma. *J Cell Biochem* 2019; 120: 12412–12421.

[514] Li Y, Liu J, Hu W, et al. miR-424-5p promotes proliferation, migration and invasion of laryngeal squamous cell carcinoma. *Onco Targets Ther* 2019; 12: 10441–10453.

[515] Zhang J, Liu H, Hou L, et al. Circular RNA_LARP4 inhibits cell proliferation and invasion of gastric cancer by sponging miR-424-5p and regulating LATS1 expression. *Mol Cancer* 2017; 16: 151.

[516] Ma LL, Liang L, Zhou D, et al. Tumor suppressor miR-424-5p abrogates ferroptosis in ovarian cancer through targeting ACSL4. *Neoplasma* 2021; 68: 165–173.

[517] Wu J, Yang B, Zhang Y, et al. mir-424-5p represses the metastasis and invasion of intrahepatic cholangiocarcinoma by targeting ARK5. *Int J Biol Sci* 2019; 15: 1591–1599.

[518] Shekhar R, Priyanka P, Kumar P, et al. The microRNAs miR-449a and miR-424 suppress osteosarcoma by targeting cyclin A2 expression. *J Biol Chem* 2019; 294: 4381–4400.

[519] Xu SJ, Xu WJ, Zeng Z, et al. MiR-424 functions as potential diagnostic and prognostic biomarker in Melanoma. *Clin Lab* 2020; 66: 1207–1213.

APPENDIX 1

Bioinformatics R codes

1. Microarray bioinformatics analysis R code

```
if (!requireNamespace("BiocManager", quietly = TRUE))
  install.packages("BiocManager")
BiocManager::install("GOstats")
BiocManager::install(c("Biobase", "GEOquery", " limma ", "mclust", "devtools",
"GOstats","gplots","networkD3","miRNAtap","miRNAtap.db",
                 "visNetwork","SpidermiR"))
################################################################################
########################
#get_data
library("GEOquery")
gset_hcc_hcv <-
getGEO("GSE40744",GSEMatrix=TRUE,AnnotGPL=FALSE,GSElimits=c(1,7))
if(length(gset_hcc_hcv)>1) idx <- grep("GPL14613",attr(gset_hcc_hcv,"names")) else idx <- 1
gset_hcc_hcv <- gset_hcc_hcv[[idx]]
##filter_For_HCCHCV_and_normal
filter <-
colnames(gset_hcc_hcv)[gset_hcc_hcv@phenoData@data$"source_name_ch1"=="specimen
obtained from explanted liver, NL" |
gset_hcc_hcv@phenoData@data$"source_name_ch1"=="specimen obtained from explanted
liver, HCC"]
length(filter)
gset_hcc_hcv$source_name_ch1
gset.filt <- gset_hcc_hcv[,filter]
gset.filt
#data_preprocessing
head(exprs(gset.filt))
dim(exprs(gset.filt))
colnames(gset.filt) <-
c("CTRL1","CTRL2","CTRL3","CTRL4","CTRL5","CTRL6","CTRL7","HCC1","HCC2","H
CC3","HCC4","HCC5","HCC6","HCC7","HCC8","HCC9")
gsms <-"0000000111111111" #Grouping names
sml <- c()
for(i in 1:nchar(gsms)) {sml[i] <- substr(gsms,i,i)}
head(exprs(gset.filt))
ex <- exprs(gset.filt)
boxplot(ex, ylab="Intensities", xlab="Array names")
################################################################################
#####
#data_normalizing
library("limma")
```

```
ex_norm <- normalizeBetweenArrays(ex)
qu <- as.numeric(quantile(ex,c(0.,0.25,0.5,0.75,0.99,1.0),na.rm=T))
filt <- ( qu[5]>100 || (qu[6]-qu[1]>50 && qu[2]>0) || (qu[2]>0 && qu[2]<1 && qu[4]>1 &&
qu[4]<2))
if(filt){ex_norm[which(ex<=0)] <- NaN; exprs(gset.filt) <- log2(ex_norm)}
boxplot(ex_norm, ylab="Intensities", xlab="Array names")
#####################################################################
##differential_expression
sml <- paste("G",sml,sep="")
fl <- as.factor(sml)
head(fl)
View(fl)
gset.filt$description <- fl
design <-model.matrix(~ description + 0, gset.filt)
colnames(design) <- levels(fl)
fit <- lmFit(gset.filt,design)
cont.matrix <- makeContrasts(G1-G0,levels=design)
fit2 <- contrasts.fit(fit,cont.matrix)
fit2 <- eBayes(fit2,0.01)
tT <- topTable(fit2,adjust="fdr",sort.by="B",number=1000)
volcanoplot(fit2,coef=1,highlight=10)
lod <- -log10(tT$adj.P.Val)
head(lod)
plot(tT$logFC,lod,xlab="log-ratio",ylab=expression(-log[10]~p))
abline(h=1.5,col="red")
selected <- which(tT$adj.P.Val<0.01)
length(selected)
esetSel <- ex[selected,]
talsel<-tT[selected,]
heatmap(esetSel)
head(talsel)
write.table(talsel,"DEmiRNAs_2A.txt")
#############################################################################
##
#filter for normal and cirhosis
#get_data
library("GEOquery")
gset_hcc_hcv <-
getGEO("GSE40744",GSEMatrix=TRUE,AnnotGPL=FALSE,GSElimits=c(1,7))
if(length(gset_hcc_hcv)>1) idx <- grep("GPL14613",attr(gset_hcc_hcv,"names")) else idx <- 1
gset_hcc_hcv <- gset_hcc_hcv[[idx]]
##filter_For_HCCHCV_and_normal
filterN <-
colnames(gset_hcc_hcv)[gset_hcc_hcv@phenoData@data$"source_name_ch1"=="specimen
obtained from explanted liver, NL" |
```

```
gset_hcc_hcv@phenoData@data$"source_name_ch1"=="specimen obtained from explanted
liver, CIR"]
length(filterN)
gset_hcc_hcv$source_name_ch1
gset.filtN <- gset_hcc_hcv[,filterN]
gset.filtN
#data_preprocessing
head(exprs(gset.filtN))
dim(exprs(gset.filtN))
colnames(gset.filtN) <-
c("CTRL1","CTRL2","CTRL3","CTRL4","CTRL5","CTRL6","CTRL7","CIR1","CIR2","CIR
3","CIR4","CIR5","CIR6","CIR7","CIR8","CIR9","CIR10","CIR11","CIR12","CIR13","CIR14
","CIR15","CIR16","CIR17","CIR18")
gsmsN <-"00000001111111111111111111" #Grouping names
smlN <- c()
for(i in 1:nchar(gsmsN)) {smlN[i] <- substr(gsmsN,i,i)}
head(exprs(gset.filtN))
exN <- exprs(gset.filtN)
boxplot(exN, ylab="Intensities", xlab="Array names")
################################################################################
#####
#data_normalizing
library("limma")
ex_normN <- normalizeBetweenArrays(exN)
quN <- as.numeric(quantile(exN,c(0.,0.25,0.5,0.75,0.99,1.0),na.rm=T))
filtN <- ( quN[5]>100 || (quN[6]-quN[1]>50 && quN[2]>0) || (quN[2]>0 && quN[2]<1 &&
quN[4]>1 && quN[4]<2))
if(filtN){ex_normN[which(exN<=0)] <- NaN; exprs(gset.filtN) <- log2(ex_normN)}
boxplot(ex_normN, ylab="Intensities", xlab="Array names")
#####################################################################
##differential_expression
smlN<-paste("G",smlN,sep="")
flN <- as.factor(smlN)
head(flN)
View(flN)
gset.filtN$description <- flN
designN <-model.matrix(~ description + 0, gset.filtN)
colnames(designN) <- levels(flN)
fitN <- lmFit(gset.filtN,designN)
cont.matrixN <- makeContrasts(G1-G0,levels=designN)
fit2N <- contrasts.fit(fitN,cont.matrixN)
fit2N <- eBayes(fit2N,0.01)
tTN <- topTable(fit2N,adjust="fdr",sort.by="B",number=1000)
volcanoplot(fit2N,coef=1,highlight=10)
lodN <- -log10(tTN$adj.P.Val)
head(lodN)
```

```
plot(tTN$logFC,lodN,xlab="log-ratio",ylab=expression(-log[10]~p))
abline(h=1.5,col="red")
selectedN <- which(tTN$adj.P.Val<0.01)
length(selectedN)
esetSelN <- exN[selectedN,]
talselN<-tTN[selectedN,]
heatmap(esetSelN)
head(talselN)
write.table(talselN,"DEmiRNAs_2C.txt")
##############################################################################
###
##filter_For_HCC_and_CirNoHCC
filter2 <-
colnames(gset_hcc_hcv)[gset_hcc_hcv@phenoData@data$"source_name_ch1"=="specimen
obtained from explanted liver, CIR" |
gset_hcc_hcv@phenoData@data$"source_name_ch1"=="specimen obtained from explanted
liver, HCC"]
length(filter2)
gset_hcc_hcv$source_name_ch1
gset.filt2 <- gset_hcc_hcv[,filter2]
gset.filt2
#data_preprocessing
head(exprs(gset.filt2))
dim(exprs(gset.filt2))
colnames(gset.filt2) <-
c("CIR1","CIR2","CIR3","CIR4","CIR5","CIR6","CIR7","CIR8","CIR9","CIR10","CIR11","C
IR12","CIR13","CIR14","CIR15","CIR16","CIR17","CIR18","HCC1","HCC2","HCC3","HCC
4","HCC5","HCC6","HCC7","HCC8","HCC9")
gsms2 <-"00000000000000000000111111111" #Grouping names
sml2 <- c()
for(i in 1:nchar(gsms2)) {sml2[i] <- substr(gsms2,i,i)}
head(exprs(gset.filt2))
ex2 <- exprs(gset.filt2)
boxplot(ex2, ylab="Intensities", xlab="Array names")
##############################################################################
#####
#data_normalizing
library("limma")
ex_norm2 <- normalizeBetweenArrays(ex2)
qu2 <- as.numeric(quantile(ex2,c(0.,0.25,0.5,0.75,0.99,1.0),na.rm=T))
filt2 <- ( qu2[5]>100 || (qu2[6]-qu2[1]>50 && qu2[2]>0) || (qu2[2]>0 && qu2[2]<1 &&
qu2[4]>1 && qu2[4]<2))
if(filt2){ex_norm2[which(ex2<=0)] <- NaN; exprs(gset.filt2) <- log2(ex_norm2)}
boxplot(ex_norm2, ylab="Intensities", xlab="Array names")
#####################################################################
##differential_expression
```

```
sml2 <- paste("G",sml2,sep="")
fl2 <- as.factor(sml2)
head(fl2)
View(fl2)
gset.filt2$description <- fl2
design2 <-model.matrix(~ description + 0, gset.filt2)
colnames(design2) <- levels(fl2)
fit100 <- lmFit(gset.filt2,design2)
cont.matrix2 <- makeContrasts(G1-G0,levels=design2)
fit300 <- contrasts.fit(fit100,cont.matrix2)
fit300 <- eBayes(fit300,0.01)
tT2 <- topTable(fit300,adjust="fdr",sort.by="B",number=1000)
volcanoplot(fit300,coef=1,highlight=10)
lod2 <- -log10(tT2$adj.P.Val)
head(lod2)
plot(tT2$logFC,lod,xlab="log-ratio",ylab=expression(-log[10]~p))
abline(h=1.5,col="red")
selected2 <- tT[tT2$adj.P.Val<0.01,]
length(selected2)
esetSel2 <- ex2[row.names(ex2) %in% selected2$ID,]
talsel2<-tT2[selected2,]
heatmap(esetSel2)
head(talsel2)
write.table(talsel2,"DEmiRNAs_2B.txt")
##########################################################################
#######
##########################################################################
#######
#COMMON_miRNAs
common=intersect(talsel[,1],talsel2[,1])
length(common)
head(common)
common1=subset(talsel, ID %in% common )
common2=subset(talsel2, ID%in% common)
common_table=cbind(common1,common2)
common_table=common_table[,c(1,12,29)]
write.table(talsel2,"DEmiRNAs_common.txt")
#################################################
####ANOVA_analysis
filter3 <-
colnames(gset_hcc_hcv)[gset_hcc_hcv@phenoData@data$"source_name_ch1"=="specimen
obtained from explanted liver, NL" |
gset_hcc_hcv@phenoData@data$"source_name_ch1"=="specimen obtained from explanted
liver, CIR" | gset_hcc_hcv@phenoData@data$"source_name_ch1"=="specimen obtained from
explanted liver, HCC"]
length(filter3)
```

```
gset_hcc_hcv$source_name_ch1
gset.filt3 <- gset_hcc_hcv[,filter3]
gset.filt3
#data_preprocessing
head(exprs(gset.filt3))
dim(exprs(gset.filt3))
colnames(gset.filt3) <-
c("CTRL1","CTRL2","CTRL3","CTRL4","CTRL5","CTRL6","CTRL7","CIR1","CIR2","CIR
3","CIR4","CIR5","CIR6","CIR7","CIR8","CIR9","CIR10","CIR11","CIR12","CIR13","CIR14
","CIR15","CIR16","CIR17","CIR18","HCC1","HCC2","HCC3","HCC4","HCC5","HCC6","H
CC7","HCC8","HCC9")
gsms3 <-"000000011111111111111111111222222222" #Grouping names
sml3 <- c()
for(i in 1:nchar(gsms3)) {sml3[i] <- substr(gsms3,i,i)}
head(exprs(gset.filt3))
ex3 <- exprs(gset.filt3)
boxplot(ex3, ylab="Intensities", xlab="Array names")
################################################################################
#####
#data_normalizing
library("limma")
ex_norm3 <- normalizeBetweenArrays(ex3)
qu3 <- as.numeric(quantile(ex3,c(0.,0.25,0.5,0.75,0.99,1.0),na.rm=T))
filt3 <- ( qu3[5]>100 || (qu3[6]-qu3[1]>50 && qu3[2]>0) || (qu3[2]>0 && qu3[2]<1 &&
qu3[4]>1 && qu3[4]<2))
if(filt3){ex_norm3[which(ex3<=0)] <- NaN; exprs(gset.filt3) <- log2(ex_norm3)}
boxplot(ex_norm3, ylab="Intensities", xlab="Array names")
################################################################
##differential_expression
sml3 <- paste("G",sml3,sep="")
fl3 <- as.factor(sml3)
head(fl3)
View(fl3)
gset.filt3$description <- fl3
design3 <-model.matrix(~ description + 0, gset.filt3)
colnames(design3) <- levels(fl3)
fit4 <- lmFit(gset.filt3,design3)
cont.matrix3 <- makeContrasts(G2-G0,G1-G0,G2-G1,levels=design3)
fit6 <- contrasts.fit(fit4,cont.matrix3)
fit6 <- eBayes(fit6,0.01)
tT3 <- topTable(fit6, coef=1, adjust="BH",sort.by="B",number=1000)
results <- decideTests(fit6)
vennDiagram(results)
anova=topTableF(fit6,number = 1000)
volcanoplot(fit6,coef=1,highlight=10)
lod3 <- -log10(anova$adj.P.Val)
```

```
head(lod3)
selected3 <- which(anova$adj.P.Val<0.01)
length(selected3)
esetSel3 <- ex3[selected3,]
talsel3<-anova[selected3,]
heatmap(esetSel3)
head(talsel3)
write.table(talsel3,"DEmiRNAs_2D.txt")
##############################################################################
#######
#####common between anova and  the rest!
common_anova_and_normal=intersect(talsel[,1],talsel3[,1])
common_anova_and_cirh=intersect(talsel2[,1],talsel3[,1])
common_anova_and_cirN=intersect(talselN[,1],talsel3[,1])
common_HCC_path=intersect(talselN[,1],talsel2[,1])
common_CirhorHCC=intersect(talsel[,1],talselN[,1])

commonall=intersect(intersect(talsel[,1],talsel2[,1]),intersect(talsel3[,1],talselN[,1]))
diff=setdiff(talsel2[,1],talsel3[,1])
writeLines(common_anova_and_normal,"common_anova_normal.txt")
writeLines(common_anova_and_cirh,"common_anova_cirhosis.txt")
writeLines(commonall,"common_all.txt")
writeLines(common_anova_and_cirN,"common_anova_normalvscirhosis.txt")
writeLines(common_HCC_path,"common_HCC_path.txt")
writeLines(common_CirhorHCC,"common_CirhorHCC.txt")

#########################################################################
##target_identification
library("SpidermiR")
mirna=tT[selected,]$miRNA_LIST[1:49]
mirna <- c('hsa-miR-4429','hsa-miR-1827','hsa-miR-5002-5p','hsa-miR-5187-3p','hsa-miR-
4455')

mirnaTar <- SpidermiRdownload_miRNAprediction(mirna_list=mirna)
head(mirnaTar)
#####################################################################
###gene_enrichment
library("org.Hs.eg.db")
library("GSEABase")
library("GOstats")
mirTarget <- mirnaTar$V2
View(mirTarget)
goAnn <- get("org.Hs.egGO")
universe <- Lkeys(goAnn)
entrezIDs <- mget(mirTarget, org.Hs.egSYMBOL2EG)
mirTarget <- as.character(mirTarget)
```

```
params <- new("GOHyperGParams", geneIds=entrezIDs, universeGeneIds=universe,
annotation="org.Hs.eg.db",
ontology="BP",pvalueCutoff=0.01,conditional=FALSE,testDirection="over")
goET <- hyperGTest(params)
library(Category)
genelist <- geneIdsByCategory(goET)
genelist <- sapply(genelist, function(.ids) {.sym &lt;- mget(.ids, envir=org.Hs.egSYMBOL,
ifnotfound=NA),.sym[is.na(.sym)] &lt;- .ids[is.na(.sym)],paste(.sym, collapse=";") })
GObp <- summary(goET)
GObp$Symbols <- genelist[as.character(GObp$GOBPID)]
head(GObp)
```

2. RNA sequencing bioinformatic analysis R code

```
if (!requireNamespace("BiocManager", quietly = TRUE))
  install.packages("BiocManager")

BiocManager::install("TCGAbiolinks")
BiocManager::install("visNetwork")
library(TCGAbiolinks)
library(dplyr)
library(DT)
library(TCGAbiolinks)
##downlaod miRNA gene expression HCC samples from TCGA
HCC <- GDCquery(project = "TCGA-LIHC",
                data.category = "Transcriptome Profiling",
                experimental.strategy = "miRNA-Seq",
                data.type = "miRNA Expression Quantification",
                workflow.type = "BCGSC miRNA Profiling")

GDCdownload(HCC)
data <- GDCprepare(HCC)
##download clinical data for HCC samples
clinic=GDCquery_clinic("TCGA-LIHC", type = "Clinical", save.csv = TRUE)
HCC_clinic <- GDCquery(project = "TCGA-LIHC",
                  data.category = "Clinical",
                  data.type = "Clinical Supplement",
                  legacy = TRUE)
GDCdownload(HCC_clinic)
clinic<-GDCprepare_clinic(HCC_clinic, clinical.info="patient",directory = "GDCdata")
#############################################################################
##
## extract etilogy specific hcc samples
HCV=clinic %>% filter(history_hepato_carcinoma_risk_factors=="Hepatitis C")
HBV=clinic %>% filter(history_hepato_carcinoma_risk_factors=="Hepatitis B")
```

```
Alcohol=clinic %>% filter(history_hepato_carcinoma_risk_factors=="Alcohol consumption")
NAFLD=clinic %>% filter(history_hepato_carcinoma_risk_factors=="Non-Alcoholic Fatty
Liver Disease")
##############################################################################
##DE for miRNA of different etiological groups
miRNA_HCV=GDCquery(project = "TCGA-LIHC",
              data.category = "Transcriptome Profiling",
              experimental.strategy = "miRNA-Seq",
              data.type = "miRNA Expression Quantification",workflow.type = "BCGSC miRNA
Profiling",
              barcode =HCV[,1])

GDCdownload(miRNA_HCV)
miRNA_HCV_data<- GDCprepare(miRNA_HCV)
miRNA_HCV_data1<-miRNA_HCV_data %>% select(starts_with("reads_per_million"))
row.names(miRNA_HCV_data1)=miRNA_HCV_data[,1]
miRNA_HCV_data=miRNA_HCV_data[,c(2:94)]
##############################################
#dataFilt <- TCGAanalyze_Filtering(tabDF = dataFilt, method = "quantile", qnt.cut = 0.25)
dataFilt <- miRNA_HCV_data1[!(rowSums(miRNA_HCV_data1 >10) < 15),]
samplesNT <- TCGAquery_SampleTypes(colnames(dataFilt), typesample = c("NT"))
samplesTP <- TCGAquery_SampleTypes(colnames(dataFilt), typesample = c("TP"))
dataDEGs <- TCGAanalyze_DEA(dataFilt[,samplesNT],
                    dataFilt[,samplesTP],
                    Cond1type = "Normal",
                    Cond2type = "Tumor", paired = FALSE, log.trans = TRUE,fdr.cut = 0.05)
dataDEGsFilt <- dataDEGs[abs(dataDEGs$logFC) >= 1,]
dataTP <- dataFilt[,samplesTP]
dataTN <- dataFilt[,samplesNT]
dataDEGsFiltLevel <- TCGAanalyze_LevelTab(dataDEGsFilt,"Tumor","Normal",
                              dataTP,dataTN)
##############################################################################
#######
##HBV
miRNA_HBV=GDCquery(project = "TCGA-LIHC",
              data.category = "Transcriptome Profiling",
              experimental.strategy = "miRNA-Seq",
              data.type = "miRNA Expression Quantification",
              workflow.type = "BCGSC miRNA Profiling",
              barcode =HBV[,1])

GDCdownload(miRNA_HBV)

miRNA_HBV_data<- GDCprepare(miRNA_HBV)
miRNA_HBV_data1<-miRNA_HBV_data %>% select(starts_with("reads_per_million"))
row.names(miRNA_HBV_data1)=miRNA_HBV_data[,1]
```

```
##########################################
dataFilt1 <- miRNA_HBV_data1[!(rowSums(miRNA_HBV_data1 >10) < 42),]

#dataFilt1 <- TCGAanalyze_Filtering(tabDF = dataFilt1, method = "quantile", qnt.cut =
0.25,var.cutoff = 0.75, eta = 0.05, foldChange = )
samplesNT1 <- TCGAquery_SampleTypes(colnames(dataFilt1), typesample = c("NT"))
samplesTP1 <- TCGAquery_SampleTypes(colnames(dataFilt1), typesample = c("TP"))
dataDEGs1 <- TCGAanalyze_DEA(dataFilt1[,samplesNT1],
                    dataFilt1[,samplesTP1],
                    Cond1type = "Normal",
                    Cond2type = "Tumor",paired = FALSE, log.trans = TRUE,fdr.cut = 0.05)
dataDEGsFilt1 <- dataDEGs1[abs(dataDEGs1$logFC) >= 1,]
dataTP1 <- dataFilt1[,samplesTP1]
dataTN1 <- dataFilt1[,samplesNT1]
dataDEGsFiltLevel1 <- TCGAanalyze_LevelTab(dataDEGsFilt1,"Tumor","Normal",
                              dataTP1,dataTN1)
##########################################################################
########
##Alcohol
miRNA_Alcohol=GDCquery(project = "TCGA-LIHC",
              data.category = "Transcriptome Profiling",
              experimental.strategy = "miRNA-Seq",
              data.type = "miRNA Expression Quantification",
              workflow.type = "BCGSC miRNA Profiling",
              barcode =Alcohol[,1])

GDCdownload(miRNA_Alcohol)

miRNA_Alcohol_data<- GDCprepare(miRNA_Alcohol)
miRNA_Alcohol_data1<-miRNA_Alcohol_data %>% select(starts_with("reads_per_million"))
row.names(miRNA_Alcohol_data1)=miRNA_Alcohol_data[,1]
##########################################
#dataNorm2 <- TCGAbiolinks::TCGAanalyze_Normalization(miRNA_Alcohol_data1,
geneInfo,method = "geneLength")

#dataFilt2 <- TCGAanalyze_Filtering(tabDF = miRNA_Alcohol_data1, method = "quantile",
qnt.cut = 0.9,var.cutoff = 0.75, eta = 0.05, foldChange = )
dataFilt2 <- miRNA_Alcohol_data1[!(rowSums(miRNA_Alcohol_data1 >10) < 36),]

samplesNT2 <- TCGAquery_SampleTypes(colnames(dataFilt2), typesample = c("NT"))
samplesTP2 <- TCGAquery_SampleTypes(colnames(dataFilt2), typesample = c("TP"))
dataDEGs2 <- TCGAanalyze_DEA(dataFilt2[,samplesNT2],
                    dataFilt2[,samplesTP2],
                    Cond1type = "Normal",
                    Cond2type = "Tumor",paired = FALSE, log.trans = TRUE,fdr.cut = 0.05)
dataDEGsFilt2 <- dataDEGs2[abs(dataDEGs2$logFC) >= 1,]
```

```
dataTP2 <- dataFilt2[,samplesTP2]
dataTN2 <- dataFilt2[,samplesNT2]
dataDEGsFiltLevel2 <- TCGAanalyze_LevelTab(dataDEGsFilt2,"Tumor","Normal",
                                dataTP2,dataTN2)
#####NAFLD
miRNA_NAFLD=GDCquery(project = "TCGA-LIHC",
                     data.category = "Transcriptome Profiling",
                     experimental.strategy = "miRNA-Seq",
                     data.type = "miRNA Expression Quantification",
                     workflow.type = "BCGSC miRNA Profiling",
                     barcode =NAFLD[,1])

GDCdownload(miRNA_NAFLD)

miRNA_NAFLD_data<- GDCprepare(miRNA_NAFLD)
miRNA_NAFLD_data1<-miRNA_NAFLD_data %>% select(starts_with("reads_per_million"))
row.names(miRNA_NAFLD_data1)=miRNA_NAFLD_data[,1]
############################################
dataFilt3 <- TCGAanalyze_Filtering(tabDF = miRNA_NAFLD_data1, method = "quantile",
qnt.cut = 0.9,var.cutoff = 0.75, eta = 0.05, foldChange = )
dataFilt3 <- miRNA_NAFLD_data1[!(rowSums(miRNA_NAFLD_data1 >10) < 6),]

samplesNT3 <- TCGAquery_SampleTypes(colnames(dataFilt3), typesample = c("NT"))
samplesTP3 <- TCGAquery_SampleTypes(colnames(dataFilt3), typesample = c("TP"))
dataDEGs3 <- TCGAanalyze_DEA(dataFilt3[,samplesNT3],
                     dataFilt3[,samplesTP3],
                     Cond1type = "Normal",
                     Cond2type = "Tumor",paired = FALSE, log.trans = FALSE,fdr.cut = 0.05)
dataDEGsFilt3 <- dataDEGs3[abs(dataDEGs3$logFC) >= 1,]
dataTP3 <- dataFilt3[,samplesTP3]
dataTN3 <- dataFilt3[,samplesNT3]
dataDEGsFiltLevel3 <- TCGAanalyze_LevelTab(dataDEGsFilt3,"Tumor","Normal",
                                dataTP3,dataTN3)
######
All=setdiff(dataDEGsFiltLevel[,1],union(dataDEGsFiltLevel1[,1],dataDEGsFiltLevel2[,1]))
All
```

APPENDIX 2

Informed consent form: English version

THE AMERICAN UNIVERSITY IN CAIRO
INSTITUTIONAL REVIEW BOARD

Documentation of Informed Consent for Participation in Research Study

Project Title: *Identifying microRNAs panel associated with hepatocellular carcinoma in patients with chronic hepatitis C in serum and urine*

Principal Investigator: Areeg Mohammad Medhat Dabbish, research assistant and graduate student in the master's program at School of science and engineering at the American University in Cairo.

*You are being asked to participate in a research study. The purpose of the research is to identify a novel biomarker for early detection of liver cancer through detecting circulating specific micro RNAs (miRNAs) in serum and urine, and the findings may be presented and/or published in a scientific proceeding.

The expected duration of your participation is around 15 minutes once for blood and urine sampling.

***The procedures of the research will be as follows**: The study will include 100 patients (with hepatitis C and liver cancer) and 50 healthy individuals. With all the listed high precautions, a trained nurse will take two blood samples and one urine sample from you. The nurse would be following all the safety hygienic practices and would place the blood and urine samples in special glass closed containers separately and these samples will be subjected to further analysis.

***There will be certain risks or discomforts associated with this research**: A simple blood clot from the site where the blood sample is withdrawn, and you may feel a drop-in blood pressure. If there are any harms due to participation in the research, you will be given urgent medical care.

***There will be benefits to you from this research**, as we will gain a self-satisfaction by the potentiality of helping sufferers of this life threating disease.

*The information you provide for purposes of this research is anonymous and confidential.

*Questions about the research, my rights, or research-related injuries should be directed to the PI: Dr. Anwar Abdelnaser at (01009813624) / Ms. Areeg Mohammad (tel. 01090027177).

*Participation in this study is voluntary. Refusal to participate will involve no penalty or loss of benefits to which you are otherwise entitled. You may discontinue participation at any time without penalty or the loss of benefits to which you are otherwise entitled.

Signature _____

Printed Name _____

Date _____

APPENDIX 3

Informed consent form: Arabic version

استمارة موافقة مسبقة للمشاركة في دراسة بحثية

عنوان البحث : تحديد الاحماض النووية الميكروية microRNAs المصاحبة للسرطان الكبدي لمرضى التهاب الكبد الفيروسى المزمن (ج) في مصل الدم والبول

الباحث الرئيسي: أريج محمد مدحت ضبيش ، مساعد باحث و طالبة دراسات عليا ببرنامج الماجستير بكلية العلوم و الهندسة بالجامعة الأمريكية بالقاهرة
البريد الالكتروني: adabbish@aucegypt.edu
الهاتف: +201090027177

أنت مدعو للمشاركة فى دراسة بحثية عن تحديد الاحماض النووية الميكروية (miRNAs) لمرض السرطان الكبدى الناتج عن الألتهاب الكبدى الفيروسى (ج) للمساعدة فى التشخيص المبكر للمرض و ايجاد طرق جديده، دقيقه، غير مكلفه و غير مؤلمة لتشخيص السرطان الكبدي

هدف الدراسة هو التعرف على طريقة جديدة للكشف المبكر عن سرطان الكبد من خلال الكشف عن الاحماض النووية الميكروية (miRNAs) في سوائل بيولوجية مختلفة كمصل الدم و البول

نتائج البحث ستنشر فى دورية متخصصة أو مؤتمر علمي أو ربما كليهما.

المدة المتوقعة للمشاركة فى هذا البحث: 15 دقيقة مرة واحدة لسحب عينات الدم و البول.
اجراءات الدراسة تشتمل على 100مريضا و 50 أصحاء. إيجابية فيروس الكبدي (ج) في الدم, او سرطان كبدى فى مرحلة مبكرة. سيتم سحب عينات دم و بول ثم استخدام عينات الدم و البول لاستخلاص الحمض النووى الميكروي ككل من عينات الدم و البول للمرضى و الأصحاء.

المخاطر المتوقعة من المشاركة فى هذه الدراسة تجمع دموي بسيط من مكان اخذ عينة الدم , وربما تشعر بهبوط. عند حدوث أي أضرار بسبب المشاركة بالبحث فسيتم إعطاؤك الرعاية الطبية العاجلة اللازمة .

الاستفادة المتوقعة من المشاركة في البحث: الرضا الذاتى من خلال المشاركة فى احتمالية مساعدة المصابين بهذا المرض المزمن الذي يهدد حياتهم.

السرية واحترام الخصوصية: المعلومات التى ستدلى بها فى هذا البحث سوف تكون (سرية و ستكون هويتك غير محددة).

- اذا زادت المخاطر المتوقعة نتيجة هذا البحث عن الحد الادنى المقبول أذكر باختصار ما اذا كان هناك تعويضات أو خدمات طبية فى حالة حدوث أى اصابة. كذلك أذكر نوعية الدعم المقدم وكيفية الحصول على معلومات اضافية عنه.

" أي أسئلة متعلقة بهذه الدراسة أو حقوق المشاركين فيها أوعند حدوث أى اصابات ناتجة عن هذه المشاركة يجب ان توجه الى : د. أنور عبد الناصر تليفون 01009813624 / أستاذة أريج محمد 01090027177

إن المشاركة فى هذه الدراسة ماهى إلا عمل تطوعى، حيث أن الامتناع عن المشاركة لايتضمن أى عقوبات أو فقدان أى مزايا تحق لك. ويمكنك أيضا التوقف عن المشاركة فى أى وقت من دون عقوبة أو فقدان لهذه المزايا.

الامضاء: .....

اسم المشارك : .....

التاريخ : ...../...../.....

APPENDIX 4

AUC IRB approval form

CASE #2018-2019-060

THE AMERICAN UNIVERSITY IN CAIRO
INSTITUTIONAL REVIEW BOARD

To: Areeg Dabbish

Cc: Hind Al Helaly

From: Atta Gebril, Chair of the IRB

Date: Feb 6, 2019

Re: Approval of study

This is to inform you that I reviewed your revised research proposal entitled "**Identifying microRNAs panel associated with hepatocellular carcinoma in patients with chronic hepatitis C in serum and urine**" and determined that it required consultation with the IRB under the "expedited" category. As you are aware, the members of the IRB suggested certain revisions to the original proposal, but your new version addresses these concerns successfully. The revised proposal used appropriate procedures to minimize risks to human subjects and that adequate provision was made for confidentiality and data anonymity of participants in any published record. I believe you will also make adequate provision for obtaining informed consent of the participants.

This approval letter was issued under the assumption that you have not started data collection for your research project. Any data collected before receiving this letter could not be used since this is a violation of the IRB policy.

Please note that IRB approval does not automatically ensure approval by CAPMAS, an Egyptian government agency responsible for approving some types of off-campus research. CAPMAS issues are handled at AUC by the office of the University Counsellor, Dr. Ashraf Hatem. The IRB is not in a position to offer any opinion on CAPMAS issues, and takes no responsibility for obtaining CAPMAS approval.

This approval is valid for only one year. In case you have not finished data collection within a year, you need to apply for an extension.

Thank you and good luck.

Dr. Atta Gebril
IRB chair, The American University in Cairo
2046 HUSS Building
T: 02-26151919
Email: agebril@aucegypt.edu

Institutional Review Board
The American University in Cairo
AUC Avenue, P.O. Box 74
New Cairo 11835, Egypt
tel 20.2.2615.1000
fax 20.2.27957565
Email: aucirb@aucegypt.edu

APPENDIX 5

NHTMRI IRB approval form

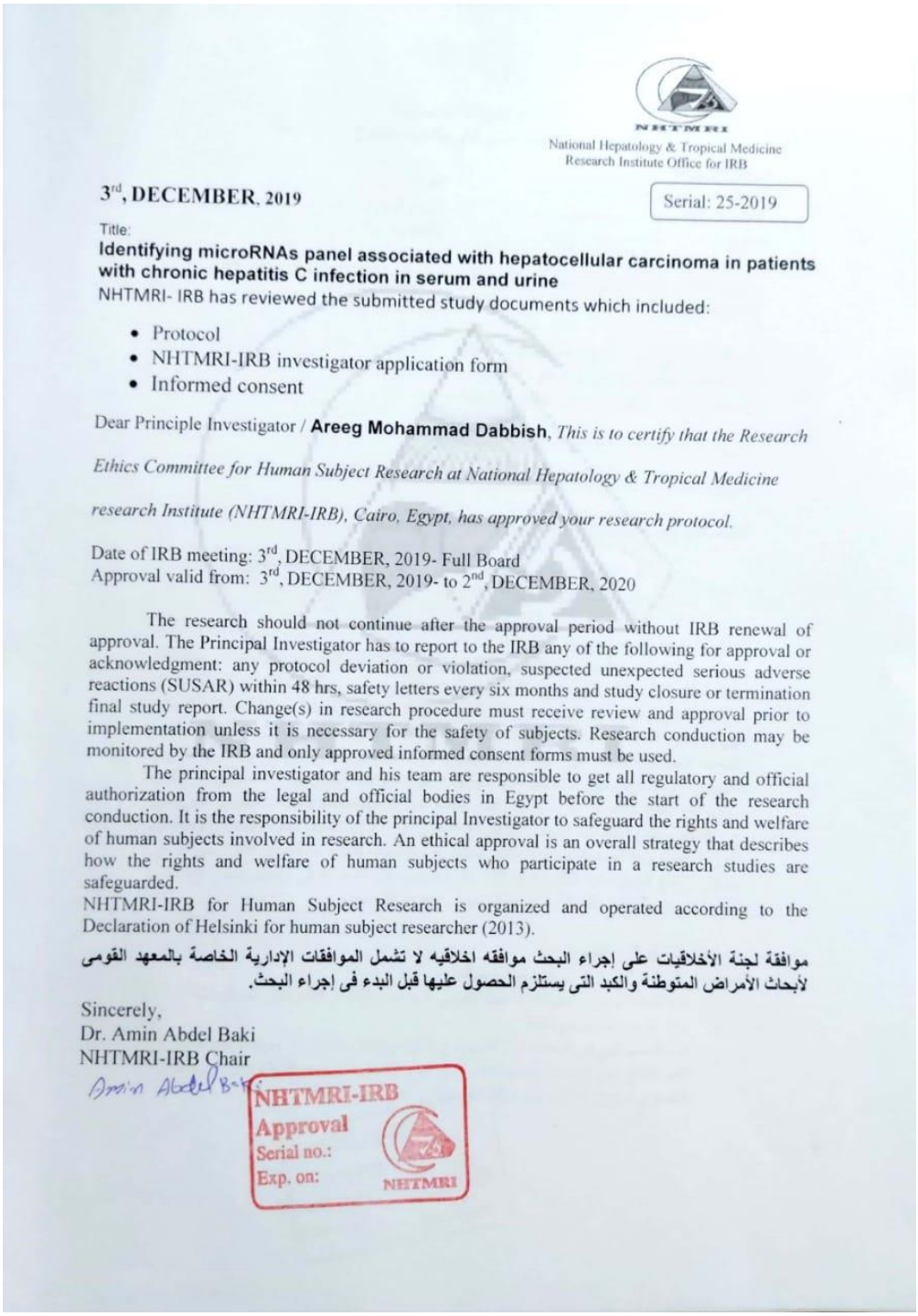

National Hepatology & Tropical Medicine
Research Institute Office for IRB

3rd, DECEMBER, 2019

Serial: 25-2019

Title:
Identifying microRNAs panel associated with hepatocellular carcinoma in patients with chronic hepatitis C infection in serum and urine

NHTMRI- IRB has reviewed the submitted study documents which included:

- Protocol
- NHTMRI-IRB investigator application form
- Informed consent

Dear Principle Investigator / **Areeg Mohammad Dabbish**, *This is to certify that the Research Ethics Committee for Human Subject Research at National Hepatology & Tropical Medicine research Institute (NHTMRI-IRB), Cairo, Egypt, has approved your research protocol.*

Date of IRB meeting: 3rd, DECEMBER, 2019- Full Board
Approval valid from: 3rd, DECEMBER, 2019- to 2nd, DECEMBER, 2020

The research should not continue after the approval period without IRB renewal of approval. The Principal Investigator has to report to the IRB any of the following for approval or acknowledgment: any protocol deviation or violation, suspected unexpected serious adverse reactions (SUSAR) within 48 hrs, safety letters every six months and study closure or termination final study report. Change(s) in research procedure must receive review and approval prior to implementation unless it is necessary for the safety of subjects. Research conduction may be monitored by the IRB and only approved informed consent forms must be used.

The principal investigator and his team are responsible to get all regulatory and official authorization from the legal and official bodies in Egypt before the start of the research conduction. It is the responsibility of the principal Investigator to safeguard the rights and welfare of human subjects involved in research. An ethical approval is an overall strategy that describes how the rights and welfare of human subjects who participate in a research studies are safeguarded.

NHTMRI-IRB for Human Subject Research is organized and operated according to the Declaration of Helsinki for human subject researcher (2013).

موافقة لجنة الأخلاقيات على إجراء البحث موافقه اخلاقيه لا تشمل الموافقات الإدارية الخاصة بالمعهد القومى لأبحاث الأمراض المتوطنة والكبد التى يستلزم الحصول عليها قبل البدء فى إجراء البحث.

Sincerely,
Dr. Amin Abdel Baki
NHTMRI-IRB Chair

Amin Abdel Baki

NHTMRI-IRB
Approval
Serial no.:
Exp. on:
NHTMRI